



# **IMMUNE MONITORING IN THE CONTEXT OF HEMATOPOIETIC CELL TRANSPLANTATION IN CHILDREN**

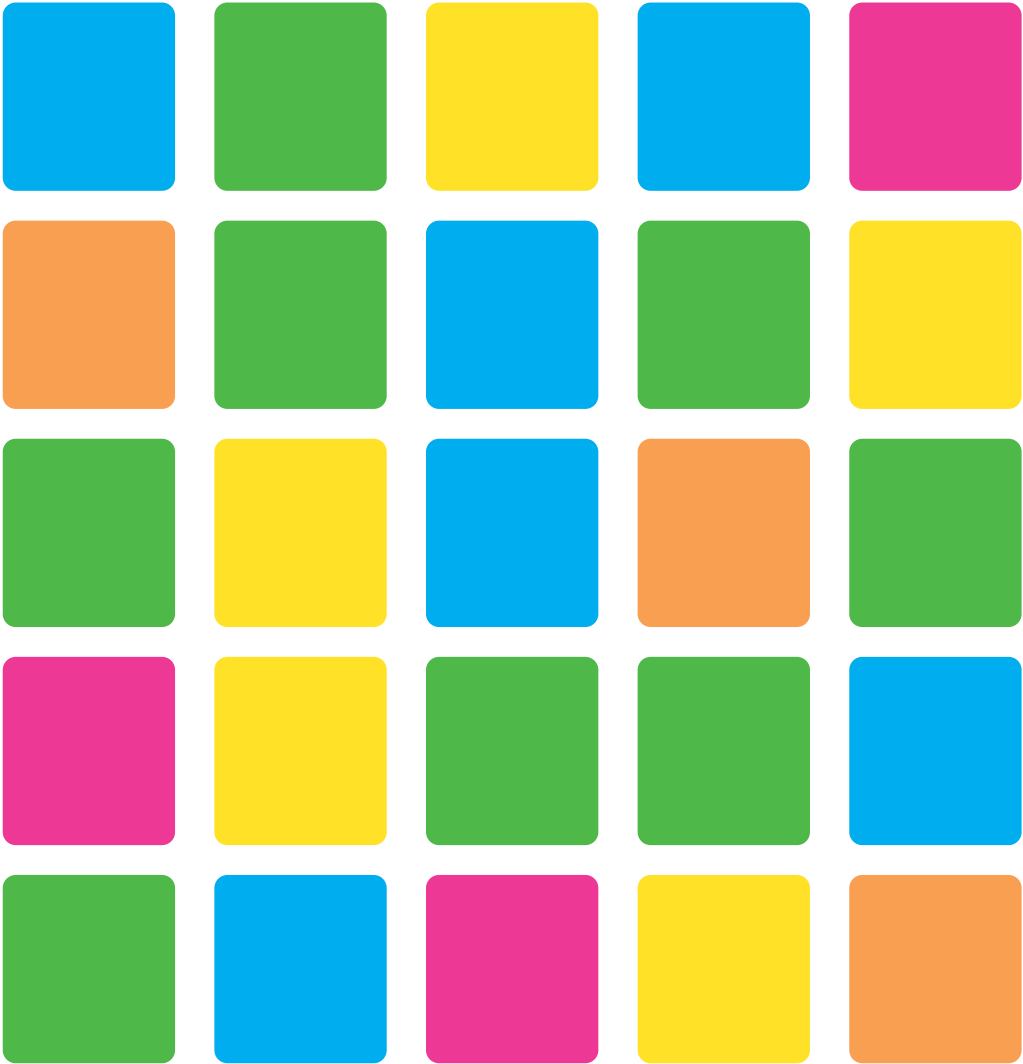


**Celina Szanto**



**Immune monitoring in the context of  
hematopoietic cell transplantation in children**

Celina Livia Szanto



Thesis University Medical Center Utrecht, Utrecht University, Infection and Immunity, Center of Translational Immunology

The research in this thesis was financially supported by the Villa Joep foundation

ISBN: 978-94-6375-918-2

Copyright © 2020 Celina Szanto

No part of this thesis may be reproduced or transmitted in any form or by any means without written permission from the author and publisher holding the copyright of the published articles.

Cover Design and Lay-out: Jules Verkade, [persoonlijkproefschrift.nl](http://persoonlijkproefschrift.nl)

Printing: Ridderprint | [www.ridderprint.nl](http://www.ridderprint.nl)

# **Immune monitoring in the context of hematopoietic cell transplantation in children**

**Immuunmonitoring in de context van hematopoietische  
stamceltransplantatie in kinderen**  
(met een samenvatting in het Nederlands)

## **Proefschrift**

ter verkrijging van de graad van doctor aan de  
Universiteit Utrecht  
op gezag van de  
rector magnificus, prof.dr. H.R.B.M. Kummeling,  
ingevolge het besluit van het college voor promoties  
in het openbaar te verdedigen op

dinsdag 15 december 2020 des middags te 2.30 uur

door

**Celina Livia Szanto**

**Promotoren:**

Prof. dr. A.D.R. Huitema

Prof. dr. J.J. Boelens

**Copromotoren:**

Dr. S. Nierkens

**Beoordelingscommissie:**

Prof. dr. C.T.W. Moonen

Prof. dr. L. Koenderman

Prof. dr. M.C. Minnema

Dr. S. Roberts

Prof. dr. C.M. Zwaan

**Paranimfen:**

Vania Lo Presti

Ester Dünnebach



# Contents

<b>Chapter 1</b>	<b>General introduction and outline of the thesis</b>	8
<b>Part 1 – Immune monitoring in high-risk neuroblastoma patients</b>		19
Chapter 2	Monitoring immune responses in neuroblastoma patients during therapy ( <i>Cancers</i> 2020)	20
Chapter 3	Functional immune monitoring in patients with high-risk neuroblastoma during chemo- and immunotherapy reveals T-cell unresponsiveness	52
Chapter 4	Quantification of Total Dinutuximab Concentrations in Neuroblastoma patients with Liquid ChromatographyTandem Mass-spectrometry ( <i>Anal. Bioanal. Chem.</i> 2018)	74
Chapter 5	A ‘no-touch’ antibody-staining method of adherent cells for high-throughput flow cytometry in 384-well microplate formatfor cell-based drug library screening ( <i>Cytometry A.</i> 2019)	94
<b>Part 2 – Immune monitoring in pediatric patients receiving allogeneic HCT</b>		115
Chapter 6	Adequate CD4+ T-cell reconstitution enhances Survival probability after acute Graft-versus-Host-Disease	116
Chapter 7	Predictors for Autoimmune Cytopenias after Allogeneic Hematopoietic Cell Transplantation in Children ( <i>BBMT</i> 2020)	130
Chapter 8	Relating Alloimmune-Mediated Lung Complications after Hematopoietic Cell Transplantation (HCT) to Immune Reconstitution after HCT to Identify Early Predictors	152
<b>Chapter 9</b>	<b>General discussion</b>	166
<b>Appendices</b>		175
	Nederlandse samenvatting	176
	Dankwoord	182
	Curriculum Vitae	190
	List of publications	191



# Chapter 1

## **General introduction and outline of the thesis**

---

Hematopoietic cell transplantation (HCT) is a potentially curative treatment strategy for various malignant and non-malignant diseases. However, many risk factors such as acute and chronic graft-versus-host disease (GvHD), infections and non-infectious complications, relapse and transplant related mortality result in high morbidity and mortality after HCT. In addition, with the rise of immunotherapy, HCT is more and more combined with other immunotherapeutic approaches. The number of active immuno-oncology drugs in development increased by 91% last 2 years<sup>1</sup>. Despite, the large increase of immune-oncology drugs in development, data of immune response and predictors for complications are lacking. Therefore, there is a strong need to monitor patients' immune response when evaluating these treatments, to better understand the effect of immunotherapies in the clinical setting.

Immune monitoring can provide crucial insights into immune cell behavior at different stages during therapy. Monitoring at diagnosis (but also during therapy) can provide new insights in the mechanism of disease and identify better correlates/risk factors of disease status. In addition, immune monitoring can facilitate the design of new therapeutic strategies by monitoring response to therapy, preventing toxicities, predicting combination treatment strategies and assigning individualized therapies. However, the small treatment groups and lack of harmonized immune monitoring protocols complicate the design of new therapeutic strategies. Harmonizing the design of immune monitoring protocols within clinical trials will enable comparison between trials and increase patient numbers. As each patient is unique, immune monitoring can facilitate future personalized treatment. These efforts may maximize clinical efficacy and minimizing toxicities.

In this thesis, two complex entities are studied and monitored in detail (Figure 1). Part 1 focusses on immune monitoring in high-risk neuroblastoma patients. Part 2 describes the effects of immune modulation of malignant and non-malignant pediatric patients receiving an allogeneic HCT.

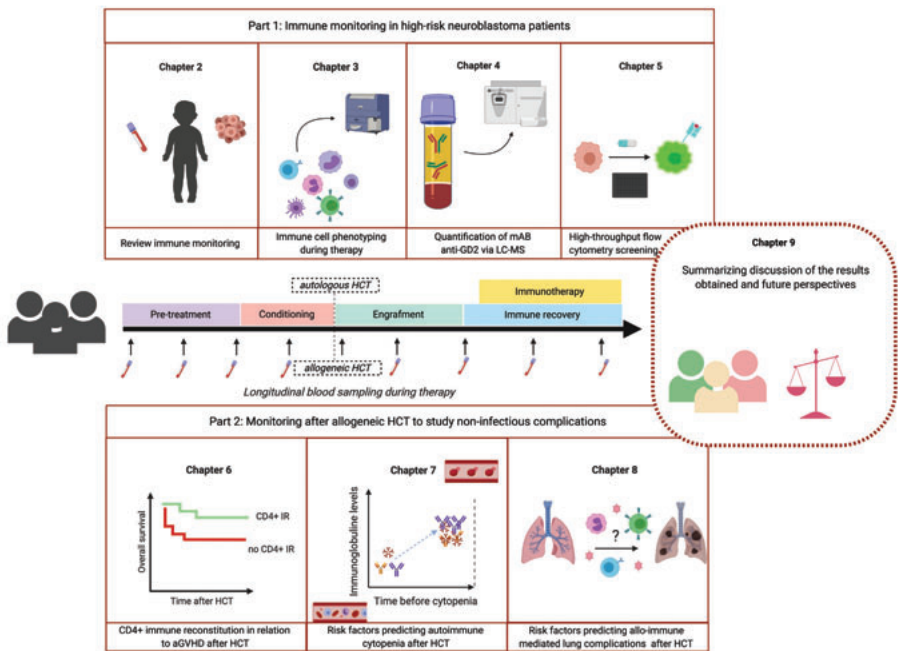


**Figure 1: Outline of the thesis**

Immune monitoring literature was reviewed (chapter 2) in neuroblastoma patients and an extensive immune monitoring protocol was performed in Dutch and German neuroblastoma patients (chapter 3). Chapter 4 and chapter 5 describe two new methods for antibody quantification and high-throughput flow cytometry screening respectively. Chapter 6 shows that CD4+ immune reconstitution is related to aGVHD status and outcome. This is followed by the analysis of immune profiles before the development of autoimmune cytopenia (chapter 6) and allo-immune mediated lung syndromes (chapter 7). This thesis finishes with a summarizing discussion (chapter 9), in which the obtained results and future perspectives are discussed. *Created with BioRender.com*

## Part 1 – Immune monitoring in high-risk neuroblastoma patients

Neuroblastoma is the most common extracranial solid tumor in children. It represents 7% of all solid childhood tumors and 15% of childhood cancer related deaths<sup>2</sup>. The mean age of diagnosis is 17 months, and 90% of cases are diagnosed under the age of 6 years<sup>3</sup>. Depending on various parameters patients are stratified into 4 risk groups: very low, low, intermediate and high risk. Neuroblastoma is an extremely heterogeneous disease, with 5-year survival rates varying from 40-50% (for high-risk neuroblastoma) to 90-95% (for very low, low and intermediate risk patients). This implies that the already small patient group is divided into even smaller subgroups, following different treatment protocols.

Treatment of high-risk neuroblastoma is divided into three phases: induction, consolidation and maintenance therapy. The induction phase consists of chemotherapy, stem cell collection and

surgical resection of the primary tumor. In the consolidation phase high dose chemotherapy is administered to the patient followed by an autologous HCT and radiotherapy. Despite intensive induction and consolidation treatment regimens, still around 50% of patients relapse. The maintenance phase was introduced to target eventual residual disease. This phase consists of immunotherapy with an anti-ganglioside 2 (GD2) in conjunction with the cytokine GM-CSF, isotretinoin, and until recently, IL-2. Patients treated with this immunotherapy schedule showed improved survival compared to isotretinoin alone (two-year event free survival 66% vs. 46%, and two-year overall survival 86% vs 75%)<sup>4,5</sup>.

Despite introduction of immunotherapy as maintenance phase, the actual 5- year survival rate is still around 50%. Response to immunotherapy varies widely, and often therapy is stopped due to severe toxicity. Monitoring the immune system of these patients, may be a suitable strategy to identify responders to therapy, prevent potential side effects and develop new treatment strategies. However, the small patient groups complicate the analysis of immune monitoring results and the design of clinical trials guided by immune monitoring. Literature on immune monitoring, these difficulties and other immunotherapeutic approaches are reviewed in **chapter 2**.

In **chapter 3**, immune subsets in blood of high-risk neuroblastoma patients were monitored longitudinally during treatment. In this study, peripheral blood mononuclear cells (PBMCs) were isolated and stained with markers for flow cytometry analysis. Besides phenotyping, proliferation assays and suppression assays were performed and cytokine production was measured to confirm functionality.

Anti-GD2 targets the disialoganglioside GD2, which is highly expressed in most neuroblastoma tumors. Unfortunately, a major toxicity of anti-GD2 antibody infusions, is neuropathic pain. Quantification of anti-GD2 levels in plasma could potentially lead to personalized dosing regimens, limiting toxicities and increasing efficacy of treatment. However, techniques to quantify the chimeric monoclonal antibody anti-GD2 are limited to antibody-based binding assays which are time consuming and difficult to implement in a harmonized setting<sup>6,7,8</sup>. Therefore, **chapter 4** describes a faster method, with a wider linear dynamic range and higher selectivity than antibody-based binding assays. This method is based on liquid chromatography tandem mass spectrometry to quantify anti-GD2 levels in plasma of treated patients.

Besides monitoring of immune status or antibodies in patients, there is a strong need for new therapeutic strategies. Previous studies have shown that neuroblastoma can evade recognition by cytotoxic T cells via downregulation of major histocompatibility complex (MHC) class

<sup>19,10</sup>. Down regulation of MHC-1 can be reversed through IFN $\gamma$  stimulation by restoring the immunogenicity of neuroblastoma and enabling killing by tumor associated antigen specific cytotoxic T cells<sup>11</sup>. Identifying compounds that can upregulate MHC-1, can potentially improve treatment strategies when combining these compounds with current treatment options. To identify new compounds, high-throughput screening techniques need to be developed for adherent neuroblastoma cell lines. In **chapter 5**, a 'no touch' high-throughput flow cytometry antibody staining protocol was developed for 384-well microplate screening that can be used for adherent neuroblastoma cell lines.

## Part 2 – Immune monitoring in pediatric patients receiving allogeneic HCT

Allogeneic HCT is a potentially curative procedure for malignant (leukemia, lymphoma, plasma cell disorders and myelodysplastic syndrome) and non-malignant (bone marrow failures, immune deficiencies and inborn errors of metabolism) diseases<sup>12</sup>. During allogeneic HCT, hematopoietic (stem) cells from a matched related or unrelated donor are transferred to the patient. The donor hematopoietic cells can be derived from bone marrow, peripheral blood (PBSCs) or umbilical cord blood. Donor selection is based on the match between donor and recipient human leukocyte antigen (HLA) in the MHC on chromosome 6.

Despite the success in treating fatal diseases, survival rates after allogeneic HCT vary from 30-70%, depending on HCT indication, treatment regimen and treating physician/center. HCT is associated with multiple posttransplant complications that influence morbidity, mortality and quality of life, especially when long-term immunosuppressive therapy is required to control these complications. Complications such as GvHD, graft failure, viral reactivations, relapse of disease and toxicities from conditioning are serious and frequent complications after allogeneic HCT<sup>13</sup>. To get a better understanding which immune mechanisms underly these complications, it is important to study the immune status prior and during these complications. A better understanding can explain why certain patients suffer from these complications, and what tools can be applied to improve survival and limit side effects. The most difficult to treat complications occurring after HCT are studied in part 2 of this thesis.

As the immune system has a major role in the development of acute GvHD, multiple studies have related immune reconstitution to acute GvHD. However, studies evaluating the relationship between CD4+ immune reconstitution, aGvHD and survival are lacking. In **chapter 6** CD4+ immune reconstitution prior to aGvHD was studied and related to survival probability after GvHD. In **chapter 7** risk factors predicting autoimmune cytopenia after HCT were studied in a retrospective cohort analysis of 380 pediatric patients. Incidence of the complication, outcomes and

various related variables, including immune reconstitution markers were evaluated. In the same cohort, risk factors for idiopathic pneumonia syndrome (IPS) and bronchiolitis obliterans (BO), associated with high rates of morbidity and mortality, were studied prior to development of these non-infectious pulmonary complications. The main outcome of interest was the development of IPS and BO in relationship to immune reconstitution. Early immune predictors to detect these alloimmune mediated lung syndromes are described in **chapter 8**.

**Chapter 9** summarizes the obtained results in this thesis and discusses them in relation to future perspectives.

Overall this thesis aims to provide a basis for the design of new harmonized immune monitoring protocols during clinical trials.

1. Xin Yu J, Hubbard-Lucey VM, Tang J, Immuno-oncology drug development goes global. *Nat Rev Drug Discov*. 2019 Nov; 18(12):899-900.
2. Maris. MJ. Recent Advances in Neuroblastoma. *N Engl J Med*. 2010;362(23):2202–11. Available from: <http://dx.doi.org/10.1056/NEJMra0804577>
3. London WB, Castleberry RP, Matthay KK, Look AT, Seeger RC, Shimada H, et al. Evidence for an age cutoff greater than 365 days for neuroblastoma risk group stratification in the Children's Oncology Group. *J Clin Oncol*. 2005; 23(27):6459-65.
4. Yu AL, Gilman AL, Ozkaynak MF, London WB, Kreissman SG, Chen HX, et al. Anti-GD2 Antibody with GM-CSF, Interleukin-2, and Isotretinoin for Neuroblastoma. *N Engl J Med*. 2010;363(14):1324–34.
5. Cheung NK V, Cheung IY, Kushner BH, Ostrovnaya I, Chamberlain E, Kramer K, et al. Murine anti-GD2 monoclonal antibody 3F8 combined with granulocyte- macrophage colony-stimulating factor and 13-cis-retinoic acid in high-risk patients with stage 4 neuroblastoma in first remission. *J Clin Oncol*. 2012;30(26):3264-70.
6. Siebert N, Seidel D, Eger C, Brackrock D, Reker D, Schmidt M, et al. Validated detection of anti-GD2 antibody ch14.18/CHO in serum of neuroblastoma patients using anti-idiotypic antibody ganglidiomab. *J. Immunol Methods*. 2013;398-399:51-9.
7. Soman G, Yang X, Jiang H, Giardina S, Mitra G. Comparison of GD2 binding capture ELISA assays for anti-GD2 antibodies using GD2-coated plates and a GD2-expressing cell-based ELISA. *J. Immunol Methods*. 2011;373(1-2):181-91.
8. Desai AV, Fox E, Smith LM, Lim AP, Maris JM, Balis FM. Pharmacokinetics of the chimeric anti-GD2 antibody, ch14.18, in children with high-risk neuroblastoma. *Cancer Chemother Pharmacol*. 2014;74(5):1047-55.
9. Bao L, Dunham K, Lucas K. MAGE-A1, MAGE-A3, and NY-ESO-1 can be upregulated on neuroblastoma cells to facilitate cytotoxic T lymphocyte-mediated tumor cell killing. *Cancer Immunol Immunother*. 2011;60(9):1299-307.
10. Wölfl M, Jungbluth AA, Garrido F, Cabrera T, Meyen-Southard S, Spitz R, et al. Expression of MHC class I, MHC class II, and cancer germline antigens in neuroblastoma. *Cancer Immunol Immunother*. 2005;54(4):400-6.
11. Spel L, Boelens J-J, van der Steen DM, Blokland NJG, van Noesel MM, Molenaar JJ, et al. Natural killer cells facilitate PRAME-specific T-cell reactivity against neuroblastoma. *Oncotarget*. 2015;6(34):35770–81.

12. Majhail NS, Farnia SH, Carpenter PA, Champlin RE, Crawford S, Marks DI, et al. Indications for Autologous and Allogeneic Hematopoietic Cell Transplantation: Guidelines from the American Society for Blood and Marrow Transplantation. *Biol Blood Marrow Transplant*. 2015;21(11):1863-1869.
13. Munchel A, Chen A, Symons H. Emergent Complications in the Pediatric Hematopoietic Stem Cell Transplant Patient. *Clin Pediatr Emerg Med*. 2011 Sep;12(3):233-44.





# Part 1

## **Immune monitoring in high-risk neuroblastoma patients**

---



# Chapter 2

# Monitoring immune responses in neuroblastoma patients during therapy

---

Celina L. Szanto<sup>1†</sup>, Annelisa M. Cornel<sup>1†</sup>, Saskia V. Vijver<sup>1</sup> and Stefan Nierkens<sup>1,2</sup>

<sup>1</sup> Center for Translational Immunology, University Medical Center Utrecht, Utrecht University, Utrecht, The Netherlands

<sup>2</sup> Princess Máxima Center for Pediatric Oncology, Utrecht University, Utrecht, The Netherlands

<sup>†</sup> These authors contributed equally to this work.

*Cancers* 2020 Feb 24; 12(2), 519.

## **Abstract**

Neuroblastoma (NBL) is the most common extracranial solid tumor in childhood. Despite intense treatment, children with this high-risk disease have a poor prognosis. Immunotherapy showed a significant improvement in event-free survival in high-risk NBL patients receiving chimeric anti-GD2 in combination with cytokines and isotretinoin after myeloablative consolidation therapy. However, response to immunotherapy varies widely, and often therapy is stopped due to severe toxicities. Objective markers that help to predict which patients will respond or develop toxicity to a certain treatment are lacking. Immunotherapy guided via immune monitoring protocols will help to identify responders as early as possible, to decipher the immune response at play, and to adjust or develop new treatment strategies. In this review, we summarize recent studies investigating frequency and phenotype of immune cells in NBL patients prior and during current treatment protocols and highlight how these findings are related to clinical outcome. In addition, we discuss potential targets to improve immunogenicity and strategies that may help to improve therapy efficacy. We conclude that immune monitoring during therapy of NBL patients is essential to identify predictive biomarkers to guide patients towards effective treatment, with limited toxicities and optimal quality of life.

## 1. Introduction

Neuroblastoma (NBL) is a tumor derived from sympathoadrenal progenitor cells of the developing sympathetic nervous system. It occurs most often in the adrenal medulla or sympathetic ganglia [1–3]. NBL is the most commonly diagnosed solid tumor during the first year of life and is responsible for approximately 15% of pediatric cancer deaths [2–4]. Risk classification of patients is based on different clinical factors, such as patients' age and International Neuroblastoma Risk Group (INRG) tumor stage, as well as biologic factors, such as histopathologic classification, DNA ploidy, MYCN status, and copy-number of chromosome 11q [3]. Outcome dramatically differs between patients with different tumor stages.

The high-risk NBL tumor environment is often referred to as 'cold' or 'immune-deserted', characterized by presence of very few immune cells in the tumor microenvironment (TME) [5]. However, the probability for a cold tumor to respond to immune therapy depends on strategies to transform it to 'hot' tumors [6]. The cold phenotype is likely caused by the development of multiple immunomodulatory mechanisms by the tumor and its environment, including major histocompatibility complex I (MHC-I) downregulation, regulatory T cell (Treg) and myeloid-derived suppressor cell (MDSC) accumulation, and decreased T cell cytotoxicity [7]. Infiltrating immune cells are observed especially in low-risk NBL. The presence of tumor-infiltrating lymphocytes (TILs) was found to be correlated with favorable clinical outcome [8]. This suggests a role of immune infiltration in regression of NBL, which is supported by increased serum levels of granulysin, an effector molecule of cytotoxic T cells, observed in a case study of spontaneous NBL regression [9]. Therapeutic interference to increase immune infiltration and recognition might therefore be key to increase therapy efficiency against NBL.

High-risk NBL is currently treated with surgery, radiotherapy, 5–8 cycles of intensive chemotherapy, including platinum-, alkylating-, and topoisomerase agents—which is often followed by autologous stem cell transplantation (ASCT)—and immunotherapy [1–4,10]. High expression of GD2 (a disialoganglioside) across NBLs and low expression levels in healthy tissue has led to the rationale of GD2 targeting immunotherapy [11]. Administration of the chimeric monoclonal antibody (mAb) anti-GD2 (ch14.18), combined with the cytokines IL-2 and granulocyte macrophage-colony stimulation factor (GM-CSF), and isotretinoin in patients with high-risk NBL resulted in a significant increase 2-year event-free (EFS) and overall survival (OS) [10]. The observation of this effect, despite the harsh immunomodulatory immune environment of NBL, shows the potential of immune interference in NBL. However, as about 40% relapse is still observed in these patients, there is a clear medical need to optimize (immuno)therapeutic strategies. The current immunotherapy protocol is particularly ineffective for high-burden

disease. In addition, osteomedullary metastatic disease occurs in most patients with high-risk neuroblastoma [12]. Elucidating the mechanisms of effective anti-tumor responses is key to find out, and act upon, what discriminates responders from non-responders.

Several studies in multiple types of cancer report increased tumor infiltration of immune cells upon (chemo)therapy [13–15], which could potentially predict overall therapy response and prognosis in an early stage. Immune monitoring during therapy provides the opportunity to study biological mechanisms of response and resistance [16]. This enables identification of biomarkers to monitor therapy response, potentially aiding to early stratification of responders and non-responders. In the 1960s, it was reported that the correlation between prognosis and degree of lymphocyte infiltration is also observed in NBL [17–19]. It is now known that NBL tumors are intermixed with different immune cells, recently identified to include CD4- and CD8-T cells, natural killer (NK) cells, and gd-T cells [20]. Interestingly, Mina et al. showed that the prognostic value of TIL levels at diagnosis is even better than criteria currently used to stage NBL, such as MYCN amplification [8]. This illustrates the potential role of immune cells in influencing the clinical outcome and emphasizes the need for standardized immune monitoring during therapy in this patient group.

This review provides an overview of predictive immune biomarkers of clinical response to treatment, emphasizes the importance of immune monitoring during NBL treatment, and describes its relevance for evaluation of the immune response and patient stratification by developing new biomarkers.

## **2. Immune Monitoring at Diagnosis: Correlates of Outcome?**

### **2.1. Immune Markers at the Tumor Site**

Histological analysis of human tumor types, including melanoma, ovarian-, head- and neck, breast-, urothelial-, colorectal-, lung- hepatocellular-, and esophageal cancer showed the presence of tumor infiltrating immune cells, such as macrophages, dendritic cells (DCs), polymorphonuclear cells, NK cells, B cells, and T cells. Although these studies revealed a broad interpatient variability, a high density of CD3 T cells, CD8 T cells, and CD45RO+ memory T cells was generally associated with improved EFS and OS [21,22]. In addition, for NBL, multiple studies show that increased CD3 T cell infiltration and proliferation is associated with favorable clinical outcome [8,23]. These data correspond with the findings that high-risk MYCN-amplified primary metastatic NBL tumors show lower levels of infiltrated lymphocytes, monocytes, and

macrophages, and exhibit lower interferon pathway activity and chemokine expression [23]. T cell proliferation is most likely impaired by high arginase activity in the TME [24], resulting in low arginine levels (an essential molecule for T cell proliferation).

CD4 T cell infiltration is associated with better survival, regardless of MYCN amplification [23]. However, extensive phenotyping of these CD4 T cells, with markers such as CD25, CD127, and FoxP3 to distinguish regulatory T cells (Treg), is lacking. Based on gene set enrichment analyses, gene expression of IL-4 (indicative for Th2) was elevated and associated with better prognosis in tumors with high CD4 T cells infiltration whereas no association was observed with interferon  $\gamma$  (IFN $\gamma$ ), IL-2 and tumor necrosis factor  $\alpha$  (TNF $\alpha$ ) (indicative for Th1) [25]. In addition, NKT cell infiltration has been reported to be favorable for outcome, possibly by inhibition of suppressive monocytes in the TME [26].

Presence of immune cell populations with presumed regulatory properties, including tumor associated monocytes, macrophages (TAMs), and Tregs, predict poor outcome [8,27]. Tumor infiltrating macrophages often display an immunosuppressive M2-phenotype supporting T cell suppression, tumor cell migration, and treatment evasion [28]. High expression of TAM-associated genes CD14, CD16, IL-6, IL-6R, and transforming growth factor (TGF $\beta$ 1) is associated with decreased 5-year EFS [26]. Additionally, monocytes isolated from the TME are able to suppress T cell proliferation in vitro [24] and excrete multiple soluble T cell inhibitory factors, such as TGF $\beta$  and IL-10 [29,30]. Although Tregs and MDSCs are well known for their suppressive effects on the immune system, associations of these subsets with clinical outcome remain limited to studies investigating bone marrow (BM) or peripheral blood (PB). One study showed that tumor-induced overexpression of high-mobility group box 1 (HMBG1) induces a Treg phenotype. Patients with overexpression of this protein were at higher risk for progression of disease, relapse, and death [7].

Despite these correlations in retrospective analyses, there are no prognostic markers in the TME to steer clinical decision making. Inclusion of markers of cell differentiation, function, activation, and exhaustion in multiple parameter analysis may help determine which factors have the strongest associations with, and prognostic value for patient outcome. Advanced techniques, such as tissue cytometry by time-of-flight (CyTOF), can overcome the limitations of measuring only a few markers in common practice immune histology.

## 2.2. Circulatory Immune Markers

Despite advances in immune profiling and the easy accessibility of, PB; no validated circulatory immune biomarkers exist for patients with NBL. Surprisingly, studies implementing immune monitoring in NBL patients are limited.

### 2.2.1. Cytokines and Soluble Molecules in Plasma/Serum

Cytokines and chemokines are components of a complex network promoting angiogenesis and metastasis, diminishing adaptive immunity, and changing responses to hormones and therapeutic agents. As such, cytokines involved in cancer-related inflammation are easy to monitor and relate to patient outcome and could be a target for therapeutic strategies.

Oliveira and colleagues reported an increase of IL-2, IL-4, IL-5, IL-6, IL-9, IL-10, IL-13, IL-17A, IL-17F, IL-21, IL-22, interferon  $\gamma$  (IFN $\gamma$ ), and tumor necrosis factor  $\alpha$  (TNF $\alpha$ ) in plasma of NBL patients compared to age matched controls. One of these cytokines, IL-6, is a key growth-promoting and anti-apoptotic inflammatory cytokine, which correlated with poor prognosis and high-risk disease [31]. When integrating levels of IL-6 with other candidate biomarkers (serum amyloid A (SAA), apolipoprotein (APOA1), epidermal growth factor (EGF), macrophage derived chemokine (MDC), sCD40L, and Eotaxin), the multivariate classifier predicted active disease with a sensitivity of 81% and specificity of 90% [32]. These data are encouraging and are awaiting validation in other patient cohorts.

Even though mRNA levels of IL-10 (a product of Tregs, NK cells and macrophages) in BM and, PB; as well as IL-10 plasma concentrations were higher in metastatic NBL patients compared to healthy controls, a prognostic role of IL-10 alone could not be demonstrated [29]. Low levels of soluble proteins other than cytokines, such as human leukocyte antigens HLA-E and HLA-F, were associated with worse prognosis [33]. In contrast to this, several other studies were not able to correlate markers measured in plasma/serum to outcome.

In other cancers, the analyses of cytokine profiles rather than single markers has shown positive prediction values at diagnosis [34–37]. The studies summarized above hopefully initiate validation studies in NBL patients with multiparameter analyses in different patient cohorts.

### 2.2.2. Immune Cells in Peripheral Blood

Leukocyte counts have found to be significantly higher in NBL patients compared to controls [38]. Although no difference is observed in total lymphocyte count between healthy controls, localized, and metastatic patients, relative numbers of multiple lymphocyte subsets do vary [31].

Semeraro et al. measured a significant increase in the percentage of CD3-CD56+ NK cells in PB of metastatic NBL patients compared to patients with localized tumors, which was associated with a minor response to induction chemotherapy. The percentage of cytotoxic (CD16+) NK cells positively correlated with clinical response to therapy [39]. These correlations could potentially be explained by NK cell mediated cytotoxic effects on MHC-I lacking tumor cells. Activated NK cells may also upregulate MHC-I expression on NBL cells, thereby circumventing further NK cell mediated cytotoxicity, while at the same time increasing their susceptibility to T cell mediated cytotoxicity [40].

Morandi and colleagues found that Treg (CD4+CD25hiCD127-) and Tr1 (CD4+CD45R0+CD49b+LAG3+) subsets are decreased in NBL patients compared to controls, but no correlation was found with prognostic factors, such as age and stage. MYCN amplification was the only prognostic factor associated with higher levels of Treg numbers in BM and Tr1 levels in PB [41]. In addition, CD4+ and CD8+ T cells show increased surface expression levels of the checkpoint inhibitor CTLA-4, and PD-1 on CD4 T cells. In contrast, Semeraro et al. found increased CD4+FoxP3+ T cells in metastatic NBL patients compared to localized tumors. The differences in the markers used to identify specific cell subsets (in this case Treg) in different studies complicates a valid comparison between the data from these studies and indicates the need for harmonization of immune phenotyping protocols.

When comparing the myeloid compartment, NBL patients with localized tumors showed higher monocyte, neutrophil and erythrocyte counts as compared to patients with metastatic disease. When zooming in on the phenotype of myeloid cells, increased levels of the checkpoint inhibitor programmed death ligand 2 (PD-L2) were observed in transitional (CD14+CD16+) and non-classical monocytes (CD14-CD16+) in patients compared to controls [31]. Furthermore, increased expression of CSF-1R, a regulator inducing MDSC expression, was observed in patients, and correlated with poor clinical outcome [42].

In summary, it is clear that NBL patients show alterations in absolute numbers and subset percentages of immune cells, as well as in immune proteins in the TME and in PB. An overview of the reviewed studies can be found in Table 1. However, so far, no robust prognostic marker correlating with survival has been identified and validated. Such immune signatures at diagnosis could aid in therapy decision making and prognosis prediction.

**Table 1.** Overview of neuroblastoma immune monitoring studies at diagnosis.

Flow Cytometry				
Number of Unique Patient Samples Measured Including Material		Tumor Characteristics	Markers	Reference
8	Primary Tumor PB	I (4x) + II (1x) + III (2x) + IV (1x)	CD3, CD4, CD8, CD25, CD45RA, CCR7	Carlson et al. 2013 [43]
26	Primary Tumor PB	II (2x) + III (2x) + IV (21x) + IVs (1x) 15 MYCN amp, 11 non MYCN amp	GD2 CD15, CD14, CD11b	Mussai et al. 2015 [24]
20	BM	IV (20x)	CD45, CD33, CD14, GD2, CD56	Song et al. 2009 [26]
41	PB	13 MYCN amp, 28 non MYCN amp	CD4, CD25, CD127, CD45RO, CD49b, LAG-3	Morandi et al. 2015 [29]
5	PB	High-Risk Patients	HLA-DR, CD33, CD11b	Gowda et al. 2013 [44]
21	PB	7 MYCN amp, 20 non MYCN amp (14 localized, 13 metastatic)	CD4, CD25, CD127, CD45RO, CD49b, LAG-3	Morandi et al. 2016 [41]
27	BM			
59	PB BM	23 localized, 36 metastatic tumors	CD8, NKp46, CD4, CD16, CD56, NKp30, DNAM-1, CD127, CD25, CD14, CD45, CD15, GD2, CD235a, CD9, CD81, TCRgd, NKp44, NKp80, CD3e, CD158a/h, CD158b, CD158e/k, CD158i, FoxP3	Semeraro et al. 2015 [39]
Immunohistochemistry				
24	Primary	7 MYCN amp, 26 non MYCN amp	CD68	Apps et al. 2013 [45]
21	Tumor		CD3	
19			pSTAT3	
8	Primary Tumor	I (4x) + II (1x) + III (2x) + IV (1x)	Ki67, CD3	Carlson et al. 2013 [43]
15	Primary Tumor	3 low risk, 6 intermediate risk, 6 high risk	CD4, CD45	Zhang et al. 2017 [25]
129	Primary Tumor	IV (129x)	CD1d, Va24-Ja18inv, TCRaβ11	Song et al. 2017 [26]
71	Primary Tumor	stage I–III (n = 29), stage IV (n = 31), stage IVS (n = 11)	CD163, AIF1	Asgharzadeh et al. 2012 [27]
84	Primary Tumor	I (34x) + II (19x) + III (5x) + IV (20x) + IVS (6x)	CD3, CD4, CD8, CD25, FOXP3, Ki67, β2m-free MHC1 heavy chain	Mina et al. 2015 [8]

Elisa				
57	Plasma	IV (49x) + non IV (8x)	IL-10, ARG-1 (57)	Morandi et al. 2015 [29]
53	PB	PB: I (8x) + II (8x) + III (6x) + IV (28x) + IVS (3x)	IL-6	Egler et al. 2008 [46]
18	BM	BM: I (1x) + II (3x) + III (2x) + IV (11x) + IVS (1x)		
35	PB	PB: I (5x) + II (5x) + III (3x) + IV (20x) + IVS (2x)	sIL-6R	
16	BM	BM: I (1x) + II (2x) + III (2x) + IV (10x) + IVS (1x)		
84	Primary Tumor	I (7x) + II (8x) + III (22x) + IV (42x) + 4S (5x) 27 MYCN amp, 57 non MYCN amp	sHLA-F, sB7H3, sHLA-E	Morandi et al. 2013 [33]
Luminex				
55	Plasma	20 low-risk, 35 high-risk In addition, 28 HR blood samples from 7 patients at various timepoints during treatment	GM-CSF, G-CSF, IFN $\gamma$ , IL-1a, IL-1ra, IL-1b, IL-2, IL-3, IL-4, IL-5, IL-6, IL-7, IL-8, IL-9, IL-10, IL-12p70, IL-12p40, IL-13, IL-15, IL-17, MCP-1, MCP-3, MDC, TNF $\alpha$ , TNF $\beta$ , TGF $\alpha$ , Eotaxin, IFN $\alpha$ 2, IP-10, MIP-1a, MIP-1b, EGF, FGF-2, FLT3L, Fractalkine, GRO, VEGF, sCD40L, sIL-2Ra	Egler et al. 2011 [32]

### 3. Immune Monitoring during Therapy

Immune monitoring during therapy is crucial to identify potentially prognostic factors that could be exploited to enhance immunogenicity of the tumor and predict treatment response. This section will start by reviewing studies which monitor the immune response upon standard therapy, including chemotherapy and monoclonal antibody therapy. Subsequently, immune monitoring in more experimental treatment regimens, including vaccination strategies, adoptive cell-, and checkpoint inhibition therapy will be discussed.

#### 3.1. Chemotherapy

In general, high-risk NBL patients receive 5–8 cycles of intensive chemotherapy including platinum, alkylating, and topoisomerase agents. In North-America, induction regimens include vincristine, doxorubicin, cyclophosphamide, cisplatin, and etoposide, while the Society of pediatric oncology Europe NBL group (SIOPEN) used a rapid COJEC regimen that gives eight cycles with combinations of vincristine, carboplatin, etoposide, cyclophosphamide, and cisplatin [47].

A limited number of studies has monitored immune profiles during chemotherapy in cancer patients. Monitoring lymphocyte levels during and after chemotherapy in hematopoietic and solid tumors generally showed increased EFS in patients with higher lymphocyte counts at diagnosis as well as after induction chemotherapy [42,47–49]. In addition, fast monocyte recovery after chemotherapy is predictive for EFS in patients with leukemias and lymphomas [50,51]. In line with these data, an elevated neutrophil to lymphocyte ratio after chemotherapy, but before surgical resection of the NBL tumor, was associated with decreased OS [52].

Upon chemotherapy treatment, Treg counts decreased, possibly due to nonspecific targeting of Tregs by chemotherapeutic agents. More studies are warranted to determine if the effect can be subscribed to chemotherapy-induced decrease in T cells in general, or whether specific subsets, like Tregs, might be more susceptible to chemotherapy-induced cytotoxicity [53]. Chemotherapy generally does not affect NK cells [54], however, the expression levels of NKp30, an NK cell receptor involved in tumor cell killing and DC recognition, positively correlate with survival after chemotherapy [55]. Expression levels of the immunosuppressive isoform NKp30C and the activating isoforms NKp30A and NKp30B affect NK cell function and correlate with EFS of NBL patients after chemotherapy [39].

No studies have monitored immune markers in the TME during chemotherapy in patients. An *in vivo* mouse study showed that depletion of TAMs from NBL tumors is associated with increased chemotherapeutic efficacy without requiring T cell contribution [56]. This observation led to the author's suggestion to combine CSF-1R blockade with chemotherapy to potentially increase treatment efficacy.

To date, too few studies have monitored immune status during chemotherapy to identify markers that could predict response to therapy. It seems that patients with higher numbers or faster recovery of lymphocytes and monocytes have better EFS changes. Whether this is a reflection or a result of the development of a healthier immunological niche should be studied, but the observation could lead to the hypothesis that these patients might also be responding better to immune treatment options.

### **3.2. Monoclonal Antibody Therapy**

A frequent immunotherapy protocol of high-risk NBL consists of anti-GD2 combined with all-trans-retinoic acid (ATRA), IL-2, and GM-CSF. Even though immunotherapy increased 2-year EFS and OS [10], relapse is still observed in 40% of patients. Elucidation of effective anti-tumor responses is key to study what discriminates responders from non-responders.

IL-2 and GM-CSF have been added to the treatment protocol as they were observed to enhance cytotoxicity of anti-GD2 in vitro [10,57–59]. In addition, GM-CSF also increased myeloid cell activation, another important cell type in the anti-tumor response [57,60]. The multi-component nature of the immunotherapy protocol makes that the observed immune effects cannot be ascribed to a specific component of the protocol.

A primary mechanism of action of anti-GD2 is the induction of antibody-dependent cellular cytotoxicity (ADCC), which requires recognition by effector cells (mainly NK cells, monocytes, neutrophils, and macrophages) [11,60]. Cytotoxic activity of NK-cells is mediated by CD16, whereas cytotoxic activity of monocytes, neutrophils, and macrophages is mediated by CD32. Both receptors recognize the Fc fragment of anti-GD2 on opsonized NBL cells and induce cytotoxic effector functions. Complement-dependent cytotoxicity (CDC) is another mechanism of action of anti-GD2, however, most studies focus on its implications regarding pain toxicity rather than on-tumor toxicity.

Nassin et al. monitored immune reconstitution at the start of immunotherapy containing IL-2, GM-CSF, and anti-GD2 [61]. They showed that absolute lymphocyte counts (T cell, B cell and NK cell subsets) are lower in the vast majority of patients as compared to age-matched controls. Patients with disease progression, relapse or residual disease had significantly lower total leukocyte counts, as well as a lower absolute lymphocyte-, neutrophil-, and CD16+ cell counts compared to disease-and progression-free patients observed three months after therapy. Siebert and colleagues found that presence of human anti-chimeric antibodies against chimeric anti-GD2 resulted in significant reduction in peripheral anti-GD2 levels, as well as significant abrogation in ADCC and CDC [62]. However, in this study, it is not clear if such immune responses are a disadvantage for survival of the treated patients. In addition, the induction of the host anti-idiotypic network, measured indirectly by human anti-mouse antibody responses correlated with long term survival [63–65]

The importance of NK cells in ADCC was illustrated by Chowdhury et al.; showing that in vitro anti-GD2 mediated lysis of the LAN1 NBL cell line upon co-culture with peripheral blood mononuclear cells (PBMCs) from a NBL patient abrogated after NK cell depletion [66]. In addition, cell lysis correlated with NK cell expression of CD69, an early activation marker, as well as with the degranulation marker CD107a. Furthermore, variation in ADCC between patients was found to be caused by genetic predispositions resulting in better cytotoxic activity of effector cells and correlations with better survival [59,63,64]. Siebert et al. studied the level of ADCC in vitro in combination with FCGR polymorphisms and killer cell immunoglobulin like receptor

KIR/KIR ligand genotypes of 53 patients. They showed that patients with high affinity FCGRs had higher ADCC levels and better EFS compared to patients with low affinity genotypes. In addition, a correlation was found between the activating KIR 2DS2 genotype on ADCC and EFS. A combination of high-affinity FCGR2A,-3A and stimulating genotypeB/x or the presence of activating KIR 2DS2 resulted in the strongest anti-NBL cellular cytotoxicity mediated by anti-GD2 and improved EFS [67]. In addition, Tarek et al. found that patients treated with monoclonal antibodies (moABs) lacking HLA class I ligands for their inhibitory KIRs have significantly higher survival rates. Unlicensed NK cells mediate tumor control via ADCC [68]. These results show that FCGR polymorphisms and KIR/KIRL genotypes could function as biomarkers in response to immunotherapy.

The importance of NK cell mediated ADCC in anti-GD2 efficacy, together with the observation of relatively fast NK cell recovery early after ASCT was an important rationale for immunotherapy timing early after transplantation [69]. However, more detailed evaluation of NK cell subsets showed that most of these NK cells are immature, cytokine releasing (CD56bright, CD16+/-) rather than the cytotoxic (CD56dim, CD16+) NK cells known to be mainly responsible for anti-GD2 dependent ADCC [61]. This is further substantiated by observed impaired immune recovery of CD16+ NK cells in patients with disease progression or relapse at time of transplantation compared to those without. These studies may suggest suboptimal timing of anti-GD2 immunotherapy early after transplantation. Utilizing haploidentical allogeneic hematopoietic cell sources rather than autologous sources could be explored as a transplantation source regarding NK cell recovery early after transplantation.

In addition to NK cell subset monitoring, Nassin et al. showed increased CD25 expression on CD4 T cells as compared to CD8 T cells at the start of immunotherapy [61]. Even though FoxP3 expression of these cells is unknown, it is hypothesized that these cells could be classified as Tregs [70]. Ladenstein et al. recently concluded from a phase III clinical trial that there is no additive effect of IL-2 administration on outcome of high-risk NBL patients [71]. As (low dose) IL-2 administration to autoimmune patients resulted in preferential expression of Tregs [72], authors hypothesize that adjuvant IL-2 administration could be responsible for Treg expansion during immunotherapy, diminishing the positive effects (e.g., NK expansion) of IL-2. Indeed, we observed a rise in Treg numbers upon every round of IL-2 to NBL patients (unpublished). Furthermore, administration of IL-2 also results in development of eosinophils through stimulating growth factors derived from T cells, such as IL-3, IL-5, and GM-CSF that help to maintain eosinophils in vitro [73]. In addition, an increase in IL-5 levels during immunotherapy with anti-GD2 and cytokines was observed, that could induce and maintain eosinophils [74]. Although their effect

is unknown, suppressive eosinophils have been reported in murine studies and could possibly also be present in IL-2 treated NBL patients [75]. Further studies are required to confirm these effects of IL-2 on levels of Treg and eosinophils, preferably with functional testing of the different cell subsets.

To overcome limitations of the current anti-GD2 monoclonal antibody therapy, including monoclonality of the response, anti-idiotypic responses, and memory induction, Kusher et al. reported a strategy in which patients are vaccinated with GD2 and GD3. This results in an intrinsic, polyclonal, multivalent antibody response through stimulation of B-cells to produce anti-GD2 and -GD3 [76]. As B-cell recovery is key for vaccination efficacy, immunomonitoring of B-cell recovery after ASCT is key for optimal vaccination timing.

To conclude, immune monitoring studies during immunotherapy are largely lacking and studies that are available have only monitored patients at start and end of therapy. All new phase II/III trials and standard treatment protocols should not only assess outcome but also monitor the immune system during therapy to get a better and faster understanding of treatment success.

### 3.3. Adoptive Cell Therapy

The development of adoptive cell therapy (ACT) strategies has taken flight in the last decade. These cell products should ideally possess the capacity to expand, actively migrate through the entire body (including to the solid tumor core and over the blood brain barrier), and induce systemic immune memory to prevent future relapse. ACT products are generated by harvesting, ex vivo expansion, and re-direction of immune cells to target tumor cells. Even though successes have been achieved in several hematological malignancies [77–80], translation of these successes to solid tumors is difficult. Target expression heterogeneity, localization to the tumor site, and overcoming the immunosuppressive, nutrient-, and stimuli- deprived TME are thought to be the main challenges in effective adoptive cell therapy in solid tumors [81].

To date, pre-clinical studies as well as clinical trials are exploiting T-, NK-, and NKT cells in both autologous and allogeneic ACT strategies in NBL. Infused cells can be isolated from PB [82–85], as well as from tumor tissue (e.g., TILs) [8,20]. In addition, isolated cells can be genetically modified to improve recognition of tumor cells, for example through knock-in of a NBL-specific T cell receptor (TCR) [40,86,87], a chimeric antigen receptor (CAR) [20,88–95], or a bispecific antibody [96,97] against tumor specific targets such as GD2, PRAME, NY-ESO-1, L1-CAM, B7-H3, and mutated ALK. Very low or even absent surface expression of major histocompatibility complex I (MHC-I) on NBL cells has led to the focus on MHC-I unrestricted ACT-strategies,

mainly exploiting NK cell- and CAR therapy (or a combination of both). Excellent overviews of clinical trials of (adoptive cell) therapy strategies in NBL are provided by Le and Thai [98] and Zage [99].

Even though multiple recent (pre-clinical) studies have demonstrated efficacy of various forms of ACT in NBL, the observed clinical benefit is limited. Persistence of ACT products in general is a widely discussed topic and is thought to be depending on balanced activation (appropriate co-stimulation, prevention of tonic/chronic receptor signaling, and of activation-induced cell death), tolerance induction (caused by native antigen expression and tumor immunosuppression), the cell phenotype of both the apheresis material and the product itself, as well as by the need of antigen availability for cell persistence [87,100,101]. The extremely immunosuppressive, nutrient- and stimuli deprived TME of solid tumors is thought to be the main factor responsible for the discrepancies in successes with hematological tumors [82,102].

Monitoring the tumor infiltrating cell population, its phenotype, and other related factors will provide the much-needed insight to predict therapy response and to understand what is driving resistance and success and where can be acted upon. Sporadic monitoring after ACT resulted in the observation that the presence of central memory and naïve T cell phenotypes in cell products has a positive effect on persistence of the cell product in several cancer types, including NBL [8,82,103–106]. Hurtado et al. recently showed that the presence of central memory NBL TILs greatly decreases after non-specific ex vivo rapid expansion cycles, stressing the importance of ex vivo expansion protocol evaluation in adoptive cell strategies [20]. Moreover, lymphodepletion before T cell infusion or early T cell infusion after ASCT (day 2) caused significantly improved expansion and persistence of the cell product [82,89]. This indicates that the immunosuppressive status of the immune system of these patients is an important limiting factor in effective ACT and led to the rationale to combine ACT with checkpoint inhibitors [89,107]. Remarkably, combining PD-1 blockade by pembrolizumab with GD2 CAR T cell administration upon lymphodepletion in a phase 1 clinical trial in NBL did not show any beneficial effect of PD-1 blockade on peripheral CAR T cell expansion [89]. A limitation of this study is that the arm studying the effect of PD-1 blockade on non-lymphodepleted GD2 CAR T cell treated patients was missing. Furthermore, T cell expansion and persistence was solely measured in the blood and not at the tumor site. The fact that two out of three treated patients in this arm experienced complete remission is encouraging and warrants more research. Controversially, immune monitoring in the same phase 1 GD2 CAR study showed specific expansion of circulating immunosuppressive M2 macrophage-like myeloid cells (CD45+CD33+CD11b+CD163+) independent of lymphodepletion and PD-1 blockade [89]. Inhibitory myeloid cells are correlated with poor prognosis

in several cancer types, including NBL, even though this study does not provide any data on whether these mobilized cells are attracted to the tumor site. Induction of MDSCs was also reported in GD2-CAR T cell therapy for sarcomas in xenograft mice, which impaired CAR T cell activity [108]. Addition of all-trans retinoic acid (ATRA) destroyed the MDSCs and thereby improved the efficacy of the GD2-CAR T cells [108], suggesting that patients might also benefit from ATRA to eradicate the circulating M2 macrophage-like myeloid cells that are induced by GD2-CAR3. Thirdly, immune monitoring in this phase 1 study indicated a correlation between circulating IL-15 levels and GD2 CAR T cell expansion [89]. Circulating IL-15 levels could not only potentially be used as a biomarker for CAR T cell expansion, but a pre-clinical xenograft mouse model transduced with GD2 CAR T cells overexpressing IL-15 also showed improved expansion, enhanced anti-tumor activity and improved survival [93].

Even though immune monitoring data during ACT in NBL is scarce, the above mentioned studies all resulted in clear rationales for research into new therapeutic strategies or biomarker development. This clearly indicates the need for more elaborate immune monitoring during ACT.

### 3.4. Checkpoint Inhibitors

Another interesting strategy would be to target the immunosuppressive environment of NBL [7]. Checkpoint inhibitors (CPis), blocking CTLA-4, PD-1, PD-L1, or PD-L2, are proven to be effective in a variety of tumors, including solid tumors [109]. The potential of these inhibitors is illustrated by the growing list of FDA-approvals, as reviewed by Hargadon et al. [110]. Currently, most of these approvals are in unresectable metastatic disease settings. Nevertheless, the potency of CPis to induce a more potent anti-tumor immune response, and therefore potential induction of anti-tumor immunological memory, makes checkpoint inhibition a very interesting candidate as an adjuvant therapy in curative treatment settings. The utilization of CPis as a monotherapy in NBL has been investigated in multiple pre-clinical studies [42,111–113]. These studies show no effect of CPI treatment on systemic NBL progression in vivo. This has been supported in a phase I clinical trial in pediatric patients with advanced solid tumors, in which one NBL patient was included [114]. More clinical trials assessing CPis as a monotherapy in refractory NBL are currently running (NCT02304458; NCT02332668; NCT02541604).

Several rationales have been proposed for the ineffectiveness of CPI therapy in high-risk NBL. First of all, evaluation of NBL tumors from patients with different tumor stages does not only, as mentioned before, show inverse correlation between tumor grade and TILs [8], but also between tumor grade and PD-L1 tumor expression [113]. Absence of TILs and PD-L1 tumor expression provides a first rationale to CPI therapy resistance. Secondly, one of the immunomodulatory

mechanisms of NBL is the upregulation of PD-L1 in response to IFN- $\gamma$  [111,113]. This highlights a potential resistance mechanism against CPI therapy, as persistent IFN- $\gamma$  production by activated T cells may lead to a continuous cascade causing even higher upregulation of the immune checkpoints resulting in T cell senescence. Impaired IFN pathway activity in MYCN-amplified tumors [23] may prevent PD-L1 expression upon IFN- $\gamma$  exposure and provides a third rationale for CPI therapy effectiveness in high-risk NBL.

Next to these observations, especially studies investigating CPI-including combination therapies revealed some insights in mechanisms explaining NBL resistance to CPI monotherapy [42,111–113]. Rigo and colleagues showed that combining CPI with temporary CD4 depletion by anti-CD4 monoclonal antibody (mAb) treatment caused a very potent CD8 T cell dependent response causing significantly longer tumor-free survival, complete tumor regression, and durable anti-NBL immunity in vivo [111]. Combining CPI with immune enhancer IL-21, or Treg targeting agents polyoxotungstate (POM-1) and anti-CD25 antibody, revealed no significant effect. This indicates that CD4<sup>+</sup> CD25<sup>high</sup> Tregs, as well as adenosine generation in Tregs are not responsible for CPI resistance in NBL. More specific studies into effects of CD4<sup>+</sup> CD25<sup>-/low</sup> FOXP3<sup>+</sup> Tregs or other CD4<sup>+</sup> Tregs should be performed to further unravel the synergistic effect observed upon CD4 depletion [111].

Mao et al. reported that targeting of CSF-1R<sup>+</sup> suppressive myeloid cells in combination with CPis caused spontaneous control of NBL in vivo [42], a mechanism confirmed in several other types of cancers, as reviewed by Weber et al. [115]. A possible explanation for this is the observation that T cells start to produce M-CSF upon PD-1 blockade, which can bind to CSF-1R on myeloid-derived suppressor cells, thereby enhancing their suppressive phenotype [116]. This causes a further reduction of IFN-regulated chemokine release (e.g., CXCL9, 10, and 11) in the TME, which are important for T cell infiltration and could therefore potentially explain the synergistic effect of targeting CSF-1R<sup>+</sup> suppressive myeloid cells in combination with CPI.

Other combination strategies which seem promising based on preclinical studies include combinations of CPis with whole tumor cell vaccination [113], high intensity ultrasound [117], and anti-GD2 treatment [112]. All mentioned preclinical evidence of effective NBL targeting treatment combinations provides a clear rationale for clinical assessment of CPI therapy as an adjuvant therapy against NBL. Even though data obtained in these induced tumor mouse models should be interpreted with caution, the data should be used as a rationale for focusing on immune monitoring of adjuvant CPI therapy in coming clinical trials.

## 4. Discussion

The present review shows the potential of standardized immune monitoring in NBL. Despite many efforts, high-risk NBL has a poor response to treatment and novel therapies are urgently required. We should therefore better understand the functional kinetics of tumor- and immune cells to guide and modulate immune therapy strategies. As such, immune monitoring may provide evidence-based directions to optimize treatment protocols, e.g., in the recent discussion whether IL-2 should be removed from the current treatment protocol [118].

Studies listed in this review use flow cytometry, CyTOF, immunohistochemistry, as well as functional assays to perform immune monitoring on tissue, PBMCs or plasma/serum from NBL patients. Monitoring PBMCs and plasma/serum cytokines is by far the easiest approach as blood is easily available during treatment. As the immune system is a multifaceted system, it is important to question if findings in the circulatory system are related to the TME. Monitoring peripheral blood subsets currently have insufficient clinical value for clinical decision making. Future studies with paired monitoring of PB, BM, and TME samples will increase our understanding of underlying mechanism and shed light on the use of biomarkers over the treatment course as predictors for efficacy and/or toxicity.

As most studies describe small patient populations, high interpatient variability, and no harmonization of monitoring protocols, it can be difficult to interpret results and relate it to recent literature [119]. The studies used in this review are sometimes limited to results of 3–5 patients. Therefore, we propose to define and implement standardized immune monitoring protocols in the trial- and study design to increase patient numbers and study interpatient variability. An example is proposed in Figure 1. As each patient is unique, immune monitoring can facilitate future personalized treatment in NBL.

Advances in organoid technology is promising in predicting the immunosuppressive capacities as well as the sensitivity to (immune) therapy in a personalized setting. Neuroblastoma tumor models have been developed that represent the tumor better than classical cell lines [120]. This strategy has previously shown to be effective in metastatic gastrointestinal cancers, in which patient derived organoids were instrumental in the prediction of tumor specific responses, stimulating personalized treatment strategies [121]. Single-cell RNA sequencing of NBL tumors can, besides studying tumor heterogeneity and driving factors behind tumor heterogeneity, help to identify new leads for immunotherapeutic strategies [122].

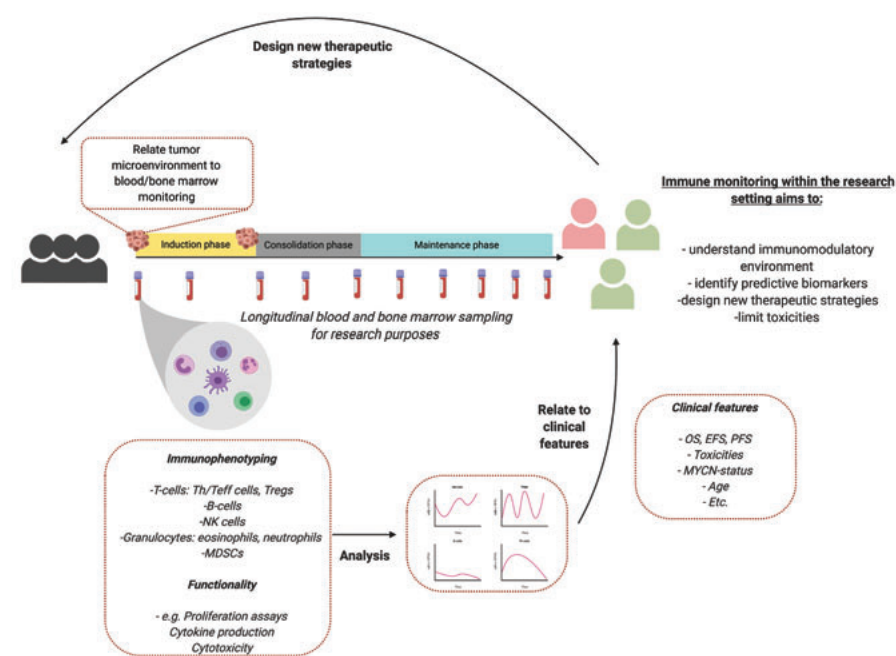


**Figure 1.** Immune monitoring for research purposes. Monitoring peripheral blood subsets currently have insufficient clinical value for clinical decision making. *Created with BioRender.com.*

## 5. Conclusions

In conclusion, immune monitoring before and during therapy of NBL patients could facilitate identification of predictive biomarkers to guide patients towards effective treatment with limited toxicities and optimal quality of life. Furthermore, understanding the immunomodulatory environment of NBL and its response to treatment in responders and non-responders is important to facilitate design of new therapeutic strategies improving outcome of high-risk NBL.

**Funding:** This research was funded by Villa Joep Foundation, Grant number IWOV-Actief.51381.180034.

## References

1. Matthay, K.K.; Maris, J.M.; Schleiermacher, G.; Nakagawara, A.; Mackall, C.L.; Diller, L.; Weiss, W.A. Neuroblastoma. *Nat. Rev. Dis. Prim.* 2016, 2, 16078, doi:10.1038/nrdp.2016.78.
2. Park, J.R.; Eggert, A.; Caron, H. Neuroblastoma: Biology, Prognosis, and Treatment. *Hematol. Oncol. Clin. N. Am.* 2010, 24, 65–86, doi:10.1016/j.hoc.2009.11.011.
3. Maris, J.M. Recent Advances in Neuroblastoma. *N. Engl. J. Med.* 2010, 362, 2202–2211, doi:10.1056/NEJMra0804577.
4. Davidoff, A.M. Neuroblastoma. *Semin. Pediatr. Surg.* 2012, 21, 2–14, doi:10.1053/j.sempedsurg.2011.10.009.
5. Chen, D.S.; Mellman, I. Elements of cancer immunity and the cancer-immune set point. *Nature* 2017, 541, 321–330, doi:10.1038/nature21349.
6. Bonaventura, P.; Shekarian, T.; Alcazer, V.; Valladeau-Guilemond, J.; Valsesia-Wittmann, S.; Amigorena, S.; Caux, C.; Depil, S. Cold Tumors: A Therapeutic Challenge for Immunotherapy. *Front. Immunol.* 2019, 10, 168, doi:10.3389/fimmu.2019.00168.
7. Vanichapol, T.; Chutipongtanate, S.; Anurathapan, U.; Hongeng, S. Immune Escape Mechanisms and Future Prospects for Immunotherapy in Neuroblastoma. *Biomed. Res. Int.* 2018, 2018, 1812535, doi:10.1155/2018/1812535.
8. Mina, M.; Boldrini, R.; Citti, A.; Romania, P.; D'Alicandro, V.; Ioris, M. De; Castellano, A.; Furlanello, C.; Locatelli, F.; Fruci, D. Tumor-infiltrating T lymphocytes improve clinical outcome of therapy-resistant neuroblastoma. *Oncoimmunology* 2015, 4, 1–14, doi:10.1080/2162402X.2015.1019981.
9. Nagasawa, M.; Kawamoto, H.; Tsuji, Y.; Mizutani, S. Transient increase of serum granulysin in a stage IVs neuroblastoma patient during spontaneous regression: Case report. *Int. J. Hematol.* 2005, 82, 456–457, doi:10.1532/IJH97.05091.
10. Yu, A.L.; Gilman, A.L.; Ozkaynak, M.F.; London, W.B.; Kreissman, S.G.; Chen, H.X.; Smith, M.; Anderson, B.; Villablanca, J.G.; Matthay, K.K.; et al. Anti-GD2 Antibody with GM-CSF, Interleukin-2, and Isotretinoin for Neuroblastoma. *N. Engl. J. Med.* 2010, 363, 1324–1334, doi:10.1056/NEJMoa0911123.
11. Zeng, Y.; Fest, S.; Kunert, R.; Katinger, H.; Pistoia, V.; Michon, J.; Lewis, G.; Ladenstein, R.; Lode, H.N. Anti-neuroblastoma effect of ch14.18 antibody produced in CHO cells is mediated by NK-cells in mice. *Mol. Immunol.* 2005, 42, 1311–1319, doi:10.1016/j.molimm.2004.12.018.
12. Modak, S.; Cheung, N.-K. V Neuroblastoma: Therapeutic strategies for a clinical enigma. *Cancer Treat. Rev.* 2010, 36, 307–317, doi:10.1016/j.ctrv.2010.02.006.

13. Kim, R.; Coppola, D.; Wang, E.; Chang, Y.D.; Kim, Y.; Anaya, D.; Kim, D.W. Prognostic value of CD8CD45RO tumor infiltrating lymphocytes in patients with extrahepatic cholangiocarcinoma. *Oncotarget* 2018, 9, 23366–23372, doi:10.18632/oncotarget.25163.
14. Parra, E.R.; Villalobos, P.; Behrens, C.; Jiang, M.; Pataer, A.; Swisher, S.G.; William, W.N.; Zhang, J.; Lee, J.; Cascone, T.; et al. Effect of neoadjuvant chemotherapy on the immune microenvironment in non-small cell lung carcinomas as determined by multiplex immunofluorescence and image analysis approaches. *J. Immunother. Cancer* 2018, 6, 48, doi:10.1186/s40425-018-0368-0.
15. Lo, C.S.; Sanii, S.; Kroeger, D.R.; Milne, K.; Talhouk, A.; Chiu, D.S.; Rahimi, K.; Shaw, P.A.; Clarke, B.A.; Nelson, B.H. Neoadjuvant chemotherapy of ovarian cancer results in three patterns of tumor-infiltrating lymphocyte response with distinct implications for immunotherapy. *Clin. Cancer Res.* 2017, 23, 925–934, doi:10.1158/1078-0432.CCR-16-1433.
16. Hegde, P.S.; Karanikas, V.; Evers, S. The where, the when, and the how of immune monitoring for cancer immunotherapies in the era of checkpoint inhibition. *Clin. Cancer Res.* 2016, 22, 1865–1874, doi:10.1158/1078-0432.CCR-15-1507.
17. Martin, R.F.; Bruce Beckwith, J. Lymphoid infiltrates in neuroblastomas: Their occurrence and prognostic significance. *J. Pediatr. Surg.* 1968, 3, 161–164, doi:10.1016/0022-3468(68)91005-1.
18. Lauder, I. The significance of lymphocytic infiltration in neuroblastoma. *Br. J. Cancer* 1972, 26, 321–330, doi:10.1038/bjc.1972.43.
19. Hellstrom, I.E.; Hellstrom, K.E.; Pierce, G.E.; Bill, A.H. Demonstration of cell-bound and humoral immunity against neuroblastoma cells. *Proc. Natl. Acad. Sci. USA* 1968, 60, 1231–1238, doi:10.1073/pnas.60.4.1231.
20. Ollé Hurtado, M.; Wolbert, J.; Fisher, J.; Flutter, B.; Stafford, S.; Barton, J.; Jain, N.; Barone, G.; Majani, Y.; Anderson, J. Tumor infiltrating lymphocytes expanded from pediatric neuroblastoma display heterogeneity of phenotype and function. *PLoS ONE* 2019, 14, e0216373–e0216373, doi:10.1371/journal.pone.0216373.
21. Fridman, W.H.; Zitvogel, L.; Sautès-Fridman, C.; Kroemer, G. The immune contexture in cancer prognosis and treatment. *Nat. Rev. Clin. Oncol.* 2017, 14, 717–734, doi:10.1038/nrclinonc.2017.101.
22. Berghoff, A.S.; Fuchs, E.; Ricken, G.; Mlecnik, B.; Bindea, G.; Spanberger, T.; Hackl, M.; Widhalm, G.; Dieckmann, K.; Prayer, D.; et al. Density of tumor-infiltrating lymphocytes correlates with extent of brain edema and overall survival time in patients with brain metastases. *Oncoimmunology* 2016, 5, e1057388, doi:10.1080/2162402X.2015.1057388.

23. Layer, J.P.; Kronmüller, M.T.; Quast, T.; Van Den Boorn, D.; Effern, M.; Hinze, D.; Althoff, K.; Westermann, F.; Peifer, M.; Hartmann, G.; et al. Amplification of N-Myc is associated with a T-cell-poor microenvironment in metastatic neuroblastoma restraining interferon pathway activity and chemokine expression. *Oncoimmunology* 2017, 6, 1–13, doi:10.1080/2162402X.2017.1320626.
24. Mussai, F.; Egan, S.; Hunter, S.; Webber, H.; Fisher, J.; Wheat, R.; McConville, C.; Sbirkov, Y.; Wheeler, K.; Bendle, G.; et al. Neuroblastoma arginase activity creates an immunosuppressive microenvironment that impairs autologous and engineered immunity. *Cancer Res.* 2015, 75, 3043–3053, doi:10.1158/0008-5472.CAN-14-3443.
25. Zhang, P.; Wu, X.; Basu, M.; Dong, C.; Zheng, P.; Liu, Y.; Sandler, A.D. MYCN amplification is associated with repressed cellular immunity in neuroblastoma: An in silico immunological analysis of TARGET database. *Front. Immunol.* 2017, 8, 1473, doi:10.3389/fimmu.2017.01473.
26. Song, L.; Asgharzadeh, S.; Salo, J.; Engell, K.; Wu, H.; Sposto, R.; Ara, T.; Silverman, A.M.; Declerck, Y.A.; Seeger, R.C.; et al. V  $\alpha$  24-invariant NKT cells mediate antitumor activity via killing of tumor-associated macrophages. *J. Clin. Invest.* 2009, 119, 1524–1536, doi:10.1172/JCI37869.1524.
27. Asgharzadeh, S.; Salo, J.A.; Ji, L.; Oberthuer, A.; Fischer, M.; Berthold, F.; Hadjidanil, M.; Liu, C.W.Y.; Metelitsa, L.S.; Pique-Regi, R.; et al. Clinical significance of tumor-associated inflammatory cells in metastatic neuroblastoma. *J. Clin. Oncol.* 2012, 30, 3525–3532, doi:10.1200/JCO.2011.40.9169.
28. Qian, B.Z.; Pollard, J.W. Macrophage Diversity Enhances Tumor Progression and Metastasis. *Cell* 2010, 141, 39–51, doi:10.1016/j.cell.2010.03.014.
29. Morandi, F.; Croce, M.; Cangemi, G.; Barco, S.; Rigo, V.; Carlini, B.; Amoroso, L.; Pistoia, V.; Ferrini, S.; Corrias, M.V. IL-10 and ARG-1 concentrations in bone marrow and peripheral blood of metastatic neuroblastoma patients do not associate with clinical outcome. *J. Immunol. Res.* 2015, 2015, 718975, doi:10.1155/2015/718975.
30. Scarpa, S.; Coppa, A.; Ragano-Caracciolo, M.; Mincione, G.; Giuffrida, A.; Modesti, A.; Colletta, G. Transforming growth factor  $\beta$  regulates differentiation and proliferation of human neuroblastoma. *Exp. Cell Res.* 1996, 229, 147–154, doi:10.1006/excr.1996.0352.
31. Oliveira, F.B.; Magalhães, L.M.; Passos, L.S.; Neto, J.C.A.; Dutra, Á.P.; Martins, P.R.; Salles, P.G.O.; Dutra, W.O.; Gollob, K.J. Abstract 707: Circulating immune profile in childhood neuroblastoma displays an activated response with simultaneous expression of checkpoint proteins by T cells and monocytes. In *Proceedings of the AACR Annual Meeting 2018*, Chicago, IL, USA, 14–18 April 2018; p. 707, doi:10.1158/1538-7445.am2018-707.

32. Egler, R.A.; Li, Y.; Dang, T.A.T.; Peters, T.L.; Leung, E.; Huang, S.; Russell, H.V.; Liu, H.; Man, T.K. An integrated proteomic approach to identifying circulating biomarkers in high-risk neuroblastoma and their potential in relapse monitoring. *Proteomics Clin. Appl.* 2011, 5, 532–541, doi:10.1002/prca.201000089.
33. Morandi, F.; Cangemi, G.; Barco, S.; Amoroso, L.; Giuliano, M.; Gigliotti, A.R.; Pistoia, V.; Corrias, M.V. Plasma levels of soluble HLA-E and HLA-F at diagnosis may predict overall survival of neuroblastoma patients. *Biomed Res. Int.* 2013, 2013, 956878, doi:10.1155/2013/956878.
34. Gogali, A.; Charalabopoulos, K.; Zampira, I.; Konstantinidis, A.K.; Tachmazoglou, F.; Daskalopoulos, G.; Constantopoulos, S.H.; Dalavanga, Y. Soluble Adhesion Molecules E-Cadherin, Intercellular Adhesion Molecule-1, and E-Selectin as Lung Cancer Biomarkers. *Chest* 2010, 138, 1173–1179, doi:10.1378/chest.10-0157.
35. Mirabelli, P.; Incoronato, M. Usefulness of traditional serum biomarkers for management of breast cancer patients. *Biomed. Res. Int.* 2013, 2013, 685641, doi:10.1155/2013/685641.
36. Bassani-Sternberg, M.; Barnea, E.; Beer, I.; Avivi, I.; Katz, T.; Admon, A. Soluble plasma HLA peptidome as a potential source for cancer biomarkers. *Proc. Natl. Acad. Sci. USA* 2010, 107, 18769, doi:10.1073/pnas.1008501107.
37. Baron, A.T.; Cora, E.M.; Lafky, J.M.; Boardman, C.H.; Buenafe, M.C.; Rademaker, A.; Liu, D.; Fishman, D.A.; Podratz, K.C.; Maihle, N.J. Soluble Epidermal Growth Factor Receptor (sEGFR/sErbB1) as a Potential Risk, Screening, and Diagnostic Serum Biomarker of Epithelial Ovarian Cancer. *Cancer Epidemiol. Biomarkers Prev.* 2003, 12, 103–113.
38. Morandi, F.; Barco, S.; Stigliani, S.; Croce, M.; Persico, L.; Lagazio, C.; Scuderi, F.; Belli, M.L.; Montera, M.; Cangemi, G.; et al. Altered erythropoiesis and decreased number of erythrocytes in children with neuroblastoma. *Oncotarget* 2017, 8, 53194–53209.
39. Semeraro, M.; Rusakiewicz, S.; Minard-colin, V.; Delahaye, N.F.; Enot, D.; Vély, F.; Marabelle, A.; Papoular, B.; Piperoglou, C.; Ponzoni, M.; et al. Clinical impact of the Nkp30 / B7-H6 axis in high-risk neuroblastoma patients. *Sci. Transl. Med.* 2015, 7, 283ra55.
40. Spel, L.; Boelens, J.-J.; van der Steen, D.M.; Blokland, N.J.G.; van Noesel, M.M.; Molenaar, J.J.; Heemskerk, M.H.M.; Boes, M.; Nierkens, S. Natural killer cells facilitate PRAME-specific T-cell reactivity against neuroblastoma. *Oncotarget* 2015, 6, 35770–35781, doi:10.18632/oncotarget.5657.
41. Morandi, F.; Pozzi, S.; Barco, S.; Cangemi, G.; Amoroso, L.; Carlini, B.; Pistoia, V.; Corrias, M.V. CD4+CD25hiCD127– Treg and CD4+CD45R0+CD49b+LAG3+ Tr1 cells in bone marrow and peripheral blood samples from children with neuroblastoma. *Oncoimmunology* 2016, 5, e1249553, doi:10.1080/2162402X.2016.1249553.

42. Mao, Y.; Eissler, N.; Le Blanc, K.; Johnsen, J.I.; Kogner, P.; Kiessling, R. Targeting suppressive myeloid cells potentiates checkpoint inhibitors to control spontaneous neuroblastoma. *Clin. Cancer Res.* 2016, 22, 3849–3859, doi:10.1158/1078-0432.CCR-15-1912.
43. Carlson, L.-M.; De Geer, A.; Sveinbjörnsson, B.; Orrego, A.; Martinsson, T.; Kogner, P.; Levitskaya, J. The microenvironment of human neuroblastoma supports the activation of tumor-associated T lymphocytes. *Oncoimmunology* 2013, 2, e23618, doi:10.4161/onci.23618.
44. Gowda, M.; Payne, K.; Godder, K.; Manjili, M.H. HLA-DR expression on myeloid cells is a potential prognostic factor in patients with high-risk neuroblastoma. *Oncoimmunology* 2013, 2, e26616, doi:10.4161/onci.26616.
45. Apps, J.R.; Hasan, F.; Campus, O.; Behjati, S.; Jacques, T.S.; J.; Sebire, N.; Anderson, J. The immune environment of paediatric solid malignancies: Evidence from an immunohistochemical study of clinical cases. *Fetal Pediatr. Pathol.* 2013, 32, 298–307, doi:10.3109/15513815.2012.754527.
46. Egler, R.A.; Burlingame, S.M.; Nuchtern, J.G.; Russell, H.V. Interleukin-6 and soluble interleukin-6 receptor levels as markers of disease extent and prognosis in neuroblastoma. *Clin. Cancer Res.* 2008, 14, 7028–7034, doi:10.1158/1078-0432.CCR-07-5017.
47. Smith, V.; Foster, J. High-Risk Neuroblastoma Treatment Review. *Child* 2018, 5, 114, doi:10.3390/children5090114.
48. Behl, D.; Porrata, L.F.; Markovic, S.N.; Letendre, L.; Pruthi, R.K.; Hook, C.C.; Tefferi, A.; Elliot, M.A.; Kaufmann, S.H.; Mesa, R.A.; et al. Absolute lymphocyte count recovery after induction chemotherapy predicts superior survival in acute myelogenous leukemia. *Leukemia* 2006, 20, 29–34, doi:10.1038/sj.leu.2404032.
49. Siddiqui, M.; Ristow, K.; Markovic, S.N.; Witzig, T.E.; Habermann, T.M.; Colgan, J.P.; Inwards, D.J.; White, W.L.; Ansell, S.M.; Micallef, I.N.; et al. Absolute lymphocyte count predicts overall survival in follicular lymphomas. *Br. J. Haematol.* 2006, 134, 596–601, doi:10.1111/j.1365-2141.2006.06232.x.
50. Thoma, M.D.; Huneke, T.J.; DeCook, L.J.; Johnson, N.D.; Wiegand, R.A.; Litzow, M.R.; Hogan, W.J.; Porrata, L.F.; Holtan, S.G. Peripheral blood lymphocyte and monocyte recovery and survival in acute leukemia postmyeloablative allogeneic hematopoietic stem cell transplant. *Biol. Blood Marrow Transplant.* 2012, 18, 600–607, doi:10.1016/j.bbmt.2011.08.007.

51. Galvez-Silva, J.; Maher, O.M.; Park, M.; Liu, D.; Hernandez, F.; Tewari, P.; Nieto, Y. Prognostic Analysis of Absolute Lymphocyte and Monocyte Counts after Autologous Stem Cell Transplantation in Children, Adolescents, and Young Adults with Refractory or Relapsed Hodgkin Lymphoma. *Biol. Blood Marrow Transplant.* 2017, 23, 1276–1281, doi:10.1016/j.bbmt.2017.04.013.
52. Nayak, A.; McDowell, D.T.; Kellie, S.J.; Karpelowsky, J. Elevated Preoperative Neutrophil–Lymphocyte Ratio is Predictive of a Poorer Prognosis for Pediatric Patients with Solid Tumors. *Ann. Surg. Oncol.* 2017, 23, 1276–1281, doi:10.1245/s10434-017-6006-0.
53. Tilak, T.; Sherawat, S.; Agarwala, S.; Gupta, R.; Vishnubhatla, S.; Bakhshi, S. Circulating T-regulatory cells in neuroblastoma: A pilot prospective study. *Pediatr. Hematol. Oncol.* 2014, 31, 717–722, doi:10.3109/08880018.2014.886002.
54. Mackall, C.L.; Fleisher, T.A.; Brown, M.R.; Magrath, I.T.; Shad, A.T.; Horowitz, M.E.; Wexler, L.H.; Adde, M.A.; McClure, L.L.; Gress, R.E. Lymphocyte depletion during treatment with intensive chemotherapy for cancer. *Blood* 1994, 84, 2221–2228.
55. Delahaye, N.F.; Rusakiewicz, S.; Martins, I.; Ménard, C.; Roux, S.; Lyonnet, L.; Paul, P.; Sarabi, M.; Chaput, N.; Semeraro, M.; et al. Alternatively spliced NKp30 isoforms affect the prognosis of gastrointestinal stromal tumors. *Nat. Med.* 2011, 17, 700–707, doi:10.1038/nm.2366.
56. Webb, M.W.; Sun, J.; Sheard, M.A.; Liu, W.-Y.; Wu, H.-W.; Jackson, J.R.; Malvar, J.; Sposto, R.; Daniel, D.; Seeger, R.C. Colony stimulating factor 1 receptor blockade improves the efficacy of chemotherapy against human neuroblastoma in the absence of T lymphocytes. *Int. J. Cancer* 2018, 143, 1483–1493, doi:10.1002/ijc.31532.
57. Cheung, N.-K.V.; Guo, H.; Hu, J.; Tassev, D.V.; Cheung, I.Y. Humanizing murine IgG3 anti-GD2 antibody m3F8 substantially improves antibody-dependent cell-mediated cytotoxicity while retaining targeting in vivo. *Oncoimmunology* 2012, 1, 477–486, doi:10.4161/onci.19864.
58. Shusterman, S.; London, W.B.; Gillies, S.D.; Hank, J.A.; Voss, S.D.; Seeger, R.C.; Reynolds, C.P.; Kimball, J.; Albertini, M.R.; Wagner, B.; et al. Antitumor activity of hu14.18-IL2 in patients with relapsed/refractory neuroblastoma: A Children’s Oncology Group (COG) phase II study. *J. Clin. Oncol.* 2010, 28, 4969–4975, doi:10.1200/JCO.2009.27.8861.
59. Metelitsa, L.S.; Gillies, S.D.; Super, M.; Shimada, H.; Reynolds, C.P.; Seeger, R.C. Antidisialoganglioside/granulocyte macrophage-colony-stimulating factor fusion protein facilitates neutrophil antibody-dependent cellular cytotoxicity and depends on FcγRII (CD32) and Mac-1 (CD11b/CD18) for enhanced effector cell adhesion and azurophi. *Blood* 2002, 99, 4166–4173; doi:10.1182/blood.v99.11.4166.

60. Siebert, N.; Eger, C.; Seidel, D.; Jüttner, M.; Zumpe, M.; Wegner, D.; Kietz, S.; Ehlert, K.; Veal, G.J.; Siegmund, W.; et al. Pharmacokinetics and pharmacodynamics of ch14.18/CHO in relapsed/refractory high-risk neuroblastoma patients treated by long-term infusion in combination with IL-2. *MAbs* 2016, 8, 604–616, doi:10.1080/19420862.2015.1130196.
61. Nassin, M.L.; Nicolaou, E.; Gurbuxani, S.; Cohn, S.L.; Cunningham, J.M.; LaBelle, J.L. Immune Reconstitution Following Autologous Stem Cell Transplantation in Patients with High-Risk Neuroblastoma at the Time of Immunotherapy. *Biol. Blood Marrow Transplant.* 2017, 24, 452–459, doi:10.1016/j.bbmt.2017.11.012.
62. Siebert, N.; Troschke-Meurer, S.; Marx, M.; Zumpe, M.; Ehlert, K.; Gray, J.; Garaventa, A.; Manzitti, C.; Ash, S.; Klingebiel, T.; et al. Impact of HACA on Immunomodulation and Treatment Toxicity Following ch14.18/CHO Long-Term Infusion with Interleukin-2: Results from a SIOPEX Phase 2 Trial. *Cancers* 2018, 10, 387, doi:10.3390/cancers10100387.
63. Cheung, N.-K.V.; Guo, H.; Heller, G.; Cheung, I.Y. Induction of Ab3 and Ab3' Antibody Was Associated with Long-Term Survival after Anti-GD2 Antibody Therapy of Stage 4 Neuroblastoma. *Clin. Cancer Res.* 2000, 6, 2653–2660.
64. Kushner, B.H.; Ostrovskaya, I.; Cheung, I.Y.; Kuk, D.; Kramer, K.; Modak, S.; Yataghene, K.; Cheung, N.K. Prolonged progression-free survival after consolidating second or later remissions of neuroblastoma with Anti-GD2 immunotherapy and isotretinoin: A prospective Phase II study. *Oncoimmunology* 2015, 4, e1016704–e1016704, doi:10.1080/2162402X.2015.1016704.
65. Cheung, N.K.; Kushner, B.H.; Yeh, S.D.; Larson, S.M. 3F8 monoclonal antibody treatment of patients with stage 4 neuroblastoma: A phase II study. *Int. J. Oncol.* 1998, 12, 1299–1306.
66. Chowdhury, F.; Lode, H.N.; Cragg, M.S.; Glennie, M.J.; Gray, J.C. Development of immunomonitoring of antibody-dependent cellular cytotoxicity against neuroblastoma cells using whole blood. *Cancer Immunol. Immunother.* 2014, 63, 559–569, doi:10.1007/s00262-014-1534-y.
67. Siebert, N.; Jensen, C.; Troschke-Meurer, S.; Zumpe, M.; Jüttner, M.; Ehlert, K.; Kietz, S.; Müller, I.; Lode, H.N. Neuroblastoma patients with high-affinity FCGR2A, -3A and stimulatory KIR 2DS2 treated by long-term infusion of anti-GD2 antibody ch14.18/CHO show higher ADCC levels and improved event-free survival. *Oncoimmunology* 2016, 5, e1235108, doi:10.1080/2162402X.2016.1235108.
68. Tarek, N.; Le Luduec, J.-B.; Gallagher, M.M.; Zheng, J.; Venstrom, J.M.; Chamberlain, E.; Modak, S.; Heller, G.; Dupont, B.; Cheung, N.-K. V; et al. Unlicensed NK cells target neuroblastoma following anti-GD2 antibody treatment. *J. Clin. Invest.* 2012, 122, 3260–3270, doi:10.1172/JCI62749.

69. Scheid, C.; Pettengell, R.; Ghielmini, M.; Radford, J.A.; Morgenstern, G.R.; Stern, P.L.; Crowther, D. Time-course of the recovery of cellular immune function after high-dose chemotherapy and peripheral blood progenitor cell transplantation for high-grade non-Hodgkin's lymphoma. *Bone Marrow Transplant.* 1995, 15, 901–906.
70. Perez-Garcia, A.; Cabezudo, E.; Lopez-Jimenez, J.; Marugan, I.; Peralta, T.; Arnan, M.; Ramos-Oliva, P.; Benet, I.; Lopez, S.; Mestre, M.; et al. Immune Reconstitution of Regulatory T-Cells Following Autologous Hematopoietic Stem Cell Transplantation. *Biol. Blood Marrow Transplant.* 2009, 15, 140, doi:10.1016/j.bbmt.2008.12.426.
71. Ladenstein, R.; Potschger, U.; Valteau-Couanet, D.; Luksch, R.; Castel, V.; Yaniv, I.; Laureys, G.; Brock, P.; Michon, J.M.; Owens, C.; et al. Interleukin 2 with anti-GD2 antibody ch14.18/CHO (dinutuximab beta) in patients with high-risk neuroblastoma (HR-NBL1/SIOPEN): A multicentre, randomised, phase 3 trial. *Lancet. Oncol.* 2018, 19, 1617–1629, doi:10.1016/S1470-2045(18)30578-3.
72. Ye, C.; Brand, D.; Zheng, S.G. Targeting IL-2: An unexpected effect in treating immunological diseases. *Signal Transduct. Target. Ther.* 2018, 3, 2, doi:10.1038/s41392-017-0002-5.
73. Van Haelst Pisani, C.; Kovach, J.S.; Kita, H.; Leiferman, K.M.; Gleich, G.J.; Silver, J.E.; Dennin, R.; Abrams, J.S. Administration of interleukin-2 (IL-2) results in increased plasma concentrations of IL-5 and eosinophilia in patients with cancer. *Blood* 1991, 78, 1538–1544.
74. Ozkaynak, M.F.; Gilman, A.L.; London, W.B.; Naranjo, A.; Diccianni, M.B.; Tenney, S.C.; Smith, M.; Messer, K.S.; Seeger, R.; Reynolds, C.P.; et al. A Comprehensive Safety Trial of Chimeric Antibody 14.18 With GM-CSF, IL-2, and Isotretinoin in High-Risk Neuroblastoma Patients Following Myeloablative Therapy: Children's Oncology Group Study ANBL0931. *Front. Immunol.* 2018, 9, 1355, doi:10.3389/fimmu.2018.01355.
75. Goldmann, O.; Beineke, A.; Medina, E. Identification of a novel subset of myeloid-derived suppressor cells during chronic staphylococcal infection that resembles immature eosinophils. *J. Infect. Dis.* 2017, 216, 1444–1451, doi:10.1093/infdis/jix494.
76. Kushner, B.H.; Cheung, I.Y.; Modak, S.; Kramer, K.; Ragupathi, G.; Cheung, N.-K. V Phase I trial of a bivalent gangliosides vaccine in combination with  $\beta$ -glucan for high-risk neuroblastoma in second or later remission. *Clin. Cancer Res.* 2014, 20, 1375–1382, doi:10.1158/1078-0432.CCR-13-1012.
77. Qasim, W.; Zhan, H.; Samarasinghe, S.; Adams, S.; Amrolia, P.; Stafford, S.; Butler, K.; Rivat, C.; Wright, G.; Somana, K.; et al. Molecular remission of infant B-ALL after infusion of universal TALEN gene-edited CAR T cells. *Sci. Transl. Med.* 2017, 9, eaaj2013, doi:10.1126/scitranslmed.aaj2013.

78. Park, J.H.; Rivière, I.; Gonen, M.; Wang, X.; Sénéchal, B.; Curran, K.J.; Sauter, C.; Wang, Y.; Santomasso, B.; Mead, E.; et al. Long-term follow-up of CD19 CAR therapy in acute lymphoblastic leukemia. *N. Engl. J. Med.* 2018, 378, 449–459, doi:10.1056/NEJMoa1709919.
79. Kochenderfer, J.N.; Somerville, R.P.T.; Lu, T.; Yang, J.C.; Sherry, R.M.; Feldman, S.A.; McIntyre, L.; Bot, A.; Rossi, J.; Lam, N.; et al. Long-Duration Complete Remissions of Diffuse Large B Cell Lymphoma after Anti-CD19 Chimeric Antigen Receptor T Cell Therapy. *Mol. Ther.* 2017, 25, 2245–2253, doi:10.1016/j.ymthe.2017.07.004.
80. Tawara, I.; Kageyama, S.; Miyahara, Y.; Fujiwara, H.; Nishida, T.; Akatsuka, Y.; Ikeda, H.; Tanimoto, K.; Terakura, S.; Murata, M.; et al. Safety and persistence of WT1-specific T-cell receptor gene2transduced lymphocytes in patients with AML and MDS. *Blood* 2017, 130, 1985–1994, doi:10.1182/blood-2017-06-791202.
81. Tesfaye, M.; Savoldo, B. Adoptive Cell Therapy in Treating Pediatric Solid Tumors. *Curr. Oncol. Rep.* 2018, 20, 73, doi:10.1007/s11912-018-0715-9.
82. Grupp, S.A.; Prak, E.L.; Boyer, J.; McDonald, K.R.; Shusterman, S.; Thompson, E.; Callahan, C.; Jawad, A.F.; Levine, B.L.; June, C.H.; et al. Adoptive transfer of autologous T cells improves T-cell repertoire diversity and long-term B-cell function in pediatric patients with neuroblastoma. *Clin. Cancer Res.* 2012, 18, 6732–6741, doi:10.1158/1078-0432.CCR-12-1432.
83. Kanold, J.; Paillard, C.; Tchirkov, A.; Lang, P.; Kelly, A.; Halle, P.; Isfan, F.; Merlin, E.; Marabelle, A.; Rochette, E.; et al. NK Cell immunotherapy for high-risk neuroblastoma relapse after haploidentical HSCT. *Pediatr. Blood Cancer* 2012, 59, 739–742, doi:10.1002/pbc.24030.
84. Federico, S.M.; McCarville, M.B.; Shulkin, B.L.; Sondel, P.M.; Hank, J.A.; Hutson, P.; Meagher, M.; Shafer, A.; Ng, C.Y.; Leung, W.; et al. A pilot trial of humanized anti-GD2 monoclonal antibody (hu14.18K322A) with chemotherapy and natural killer cells in children with recurrent/refractory neuroblastoma. *Clin. Cancer Res.* 2017, 23, 6441–6449, doi:10.1158/1078-0432.CCR-17-0379.
85. Modak, S.; Le Luque, J.B.; Cheung, I.Y.; Goldman, D.A.; Ostrovnya, I.; Doubrovina, E.; Basu, E.; Kushner, B.H.; Kramer, K.; Roberts, S.S.; et al. Adoptive immunotherapy with haploidentical natural killer cells and Anti-GD2 monoclonal antibody m3F8 for resistant neuroblastoma: Results of a phase I study. *Oncoimmunology* 2018, 7, e1461305, doi:10.1080/2162402X.2018.1461305.
86. Singh, N.; Kulikovskaya, I.; Barrett, D.M.; Binder-Scholl, G.; Jakobsen, B.; Martinez, D.; Pawel, B.; June, C.H.; Kalos, M.D.; Grupp, S.A. T cells targeting NY-ESO-1 demonstrate efficacy against disseminated neuroblastoma. *Oncoimmunology* 2016, 5, e1040216, doi:10.1080/2162402X.2015.1040216.

87. Quintarelli, C.; Orlando, D.; Boffa, I.; Guercio, M.; Polito, V.A.; Petretto, A.; Lavarello, C.; Sinibaldi, M.; Weber, G.; Del Bufalo, F.; et al. Choice of costimulatory domains and of cytokines determines CAR T-cell activity in neuroblastoma. *Oncoimmunology* 2018, 7, e1433518, doi:10.1080/2162402X.2018.1433518.
88. Heczey, A.; Liu, D.; Tian, G.; Courtney, A.N.; Wei, J.; Marinova, E.; Gao, X.; Guo, L.; Yvon, E.; Hicks, J.; et al. Invariant NKT cells with chimeric antigen receptor provide a novel platform for safe and effective cancer immunotherapy. *Blood* 2014, 124, 2824–2833, doi:10.1182/blood-2013-11-541235.
89. Heczey, A.; Louis, C.U.; Savoldo, B.; Dakhova, O.; Durett, A.; Grilley, B.; Liu, H.; Wu, M.F.; Mei, Z.; Gee, A.; et al. CAR T Cells Administered in Combination with Lymphodepletion and PD-1 Inhibition to Patients with Neuroblastoma. *Mol. Ther.* 2017, 25, 2214–2224, doi:10.1016/j.ymthe.2017.05.012.
90. Yang, L.; Ma, X.; Liu, Y.-C.; Zhao, W.; Yu, L.; Qin, M.; Zhu, G.; Wang, K.; Shi, X.; Zhang, Z.; et al. Chimeric Antigen Receptor 4SCAR-GD2-Modified T Cells Targeting High-Risk and Recurrent Neuroblastoma: A Phase II Multi-Center Trial in China. *Blood* 2017, 130, 3335.
91. Künkele, A.; Taraseviciute, A.; Finn, L.S.; Johnson, A.J.; Berger, C.; Finney, O.; Chang, C.A.; Rolczynski, L.S.; Brown, C.; Mgebroff, S.; et al. Preclinical assessment of CD171-directed CAR T-cell adoptive therapy for childhood neuroblastoma: CE7 epitope target safety and product manufacturing feasibility. *Clin. Cancer Res.* 2017, 23, 466–477, doi:10.1158/1078-0432.CCR-16-0354.
92. Walker, A.J.; Majzner, R.G.; Zhang, L.; Wanhainen, K.; Long, A.H.; Nguyen, S.M.; Lopomo, P.; Vigny, M.; Fry, T.J.; Orentas, R.J.; et al. Tumor Antigen and Receptor Densities Regulate Efficacy of a Chimeric Antigen Receptor Targeting Anaplastic Lymphoma Kinase. *Mol. Ther.* 2017, 25, 2189–2201, doi:10.1016/j.ymthe.2017.06.008.
93. Chen, Y.; Sun, C.; Landoni, E.; Metelitsa, L.; Dotti, G.; Savoldo, B. Eradication of neuroblastoma by T cells redirected with an optimized GD2-specific chimeric antigen receptor and interleukin-15. *Clin. Cancer Res.* 2019, 25, 2915–2924, doi:10.1158/1078-0432.CCR-18-1811.
94. Du, H.; Hirabayashi, K.; Ahn, S.; Kren, N.P.; Montgomery, S.A.; Wang, X.; Tiruthani, K.; Mirlekar, B.; Michaud, D.; Greene, K.; et al. Antitumor Responses in the Absence of Toxicity in Solid Tumors by Targeting B7-H3 via Chimeric Antigen Receptor T Cells. *Cancer Cell* 2019, 35, 221–237, doi:10.1016/j.ccell.2019.01.002.
95. Majzner, R.G.; Theruvath, J.L.; Nellan, A.; Heitzeneder, S.; Cui, Y.; Mount, C.W.; Rietberg, S.P.; Linde, M.H.; Xu, P.; Rota, C.; et al. CAR T cells targeting B7-H3, a pan-cancer antigen, demonstrate potent preclinical activity against pediatric solid tumors and brain tumors. *Clin. Cancer Res.* 2019, 25, 2560–2574, doi:10.1158/1078-0432.CCR-18-0432.

96. Yankelevich, M.; Kondadasula, S.V.; Thakur, A.; Buck, S.; Cheung, N.K.V.; Lum, L.G. Anti-CD3×anti-GD2 bispecific antibody redirects T-cell cytolytic activity to neuroblastoma targets. *Pediatr. Blood Cancer* 2012, 59, 1198–1205, doi:10.1002/pbc.24237.
97. Yankelevich, M.; Modak, S.; Chu, R.; Lee, D.W.; Thakur, A.; Cheung, N.-K.V.; Lum, L.G. Phase I study of OKT3 x hu3F8 bispecific antibody (GD2Bi) armed T cells (GD2BATs) in GD2-positive tumors. *J. Clin. Oncol.* 2019, 14, 2533, doi:10.1200/jco.2019.37.15\_suppl.2533.
98. Le, T.P.; Thai, T.H. The state of cellular adoptive immunotherapy for neuroblastoma and other pediatric solid tumors. *Front. Immunol.* 2017, 8, 1640, doi:10.3389/fimmu.2017.01640.
99. Zage, P. Novel Therapies for Relapsed and Refractory Neuroblastoma. *Children* 2018, 5, 148, doi:10.3390/children5110148.
100. Long, A.H.; Haso, W.M.; Shern, J.F.; Wanhainen, K.M.; Murgai, M.; Ingaramo, M.; Smith, J.P.; Walker, A.J.; Kohler, M.E.; Venkateshwara, V.R.; et al. 4-1BB costimulation ameliorates T cell exhaustion induced by tonic signaling of chimeric antigen receptors. *Nat. Med.* 2015, 21, 581–590, doi:10.1038/nm.3838.
101. McLellan, A.D.; Ali Hosseini Rad, S.M. Chimeric antigen receptor T cell persistence and memory cell formation. *Immunol. Cell Biol.* 2019, 97, 664–674, doi:10.1111/imcb.12254.
102. Martinez, M.; Moon, E.K. CAR T cells for solid tumors: New strategies for finding, infiltrating, and surviving in the tumor microenvironment. *Front. Immunol.* 2019, 10, 128, doi:10.3389/fimmu.2019.00128.
103. Gattinoni, L.; Zhong, X.S.; Palmer, D.C.; Ji, Y.; Hinrichs, C.S.; Yu, Z.; Wrzesinski, C.; Boni, A.; Cassard, L.; Garvin, L.M.; et al. Wnt signaling arrests effector T cell differentiation and generates CD8+ memory stem cells. *Nat. Med.* 2009, 15, 808–813, doi:10.1038/nm.1982.
104. Louis, C.U.; Savoldo, B.; Dotti, G.; Pule, M.; Yvon, E.; Myers, G.D.; Rossig, C.; Russell, H.V.; Diouf, O.; Liu, E.; et al. Antitumor activity and long-term fate of chimeric antigen receptor-positive T cells in patients with neuroblastoma. *Blood* 2011, 118, 6050–6056, doi:10.1182/blood-2011-05-354449.
105. Sommermeyer, D.; Hudecek, M.; Kosasih, P.L.; Gogishvili, T.; Maloney, D.G.; Turtle, C.J.; Riddell, S.R. Chimeric antigen receptor-modified T cells derived from defined CD8+ and CD4+ subsets confer superior antitumor reactivity in vivo. *Leukemia* 2016, 30, 492–500, doi:10.1038/leu.2015.247.
106. Turtle, C.J.; Hanafi, L.A.; Berger, C.; Hudecek, M.; Pender, B.; Robinson, E.; Hawkins, R.; Chaney, C.; Cherian, S.; Chen, X.; et al. Immunotherapy of non-Hodgkin's lymphoma with a defined ratio of CD8+ and CD4+ CD19-specific chimeric antigen receptor-modified T cells. *Sci. Transl. Med.* 2016, 30, 492–500, doi:10.1126/scitranslmed.aaf8621.

107. Chong, E.A.; Melenhorst, J.J.; Lacey, S.F.; Ambrose, D.E.; Gonzalez, V.; Levine, B.L.; June, C.H.; Schuster, S.J. PD-1 blockade modulates chimeric antigen receptor (CAR)-modified T cells: Refueling the CAR. *Blood* 2017, 129, 1039–1041, doi:10.1182/blood-2016-09-738245.
108. Long, A.H.; Highfill, S.L.; Cui, Y.; Smith, J.P.; Walker, A.J.; Ramakrishna, S.; El-Etriby, R.; Galli, S.; Tsokos, M.; Orentas, R.J.; et al. Reduction of MDSCs with all-trans retinoic acid improves CAR therapy efficacy for sarcomas. *Cancer Immunol. Res.* 2016, 4, 869–880, doi:10.1158/2326-6066.CIR-15-0230.
109. Kotecki, N.; Awada, A. Checkpoints inhibitors in the (neo)adjuvant setting of solid tumors. *Curr. Opin. Oncol.* 2019, 31, 429–444, doi:10.1097/cco.0000000000000565.
110. Hargadon, K.M.; Johnson, C.E.; Williams, C.J. Immune checkpoint blockade therapy for cancer: An overview of FDA-approved immune checkpoint inhibitors. *Int. Immunopharmacol.* 2018, 62, 29–39, doi:10.1016/j.intimp.2018.06.001.
111. Rigo, V.; Emionite, L.; Daga, A.; Astigiano, S.; Corrias, M.V.; Quintarelli, C.; Locatelli, F.; Ferrini, S.; Croce, M. Combined immunotherapy with anti-PDL-1/PD-1 and anti-CD4 antibodies cures syngeneic disseminated neuroblastoma. *Sci. Rep.* 2017, 25, 14049, doi:10.1038/s41598-017-14417-6.
112. Siebert, N.; Zumpe, M.; Jüttner, M.; Troschke-Meurer, S.; Lode, H.N. PD-1 blockade augments anti-neuroblastoma immune response induced by anti-GD2 antibody ch14.18/CHO. *Oncoimmunology* 2017, 6, e1343775, doi:10.1080/2162402X.2017.1343775.
113. Srinivasan, P.; Wu, X.; Basu, M.; Rossi, C.; Sandler, A.D. PD-L1 checkpoint inhibition and anti-CTLA-4 whole tumor cell vaccination counter adaptive immune resistance: A mouse neuroblastoma model that mimics human disease. *PLoS Med.* 2018, 15, e1002497, doi:10.1371/journal.pmed.1002497.
114. Merchant, M.S.; Wright, M.; Baird, K.; Wexler, L.H.; Rodriguez-Galindo, C.; Bernstein, D.; Delbrook, C.; Lodish, M.; Bishop, R.; Wolchok, J.D.; et al. Phase I clinical trial of ipilimumab in pediatric patients with advanced solid tumors. *Clin. Cancer Res.* 2016, 22, 1364–1370, doi:10.1158/1078-0432.CCR-15-0491.
115. Weber, R.; Fleming, V.; Hu, X.; Nagibin, V.; Groth, C.; Altevogt, P.; Utikal, J.; Umansky, V. Myeloid-derived suppressor cells hinder the anti-cancer activity of immune checkpoint inhibitors. *Front. Immunol.* 2018, 9, 1310, doi:10.3389/fimmu.2018.01310.
116. Eissler, N.; Mao, Y.; Brodin, D.; Reuterswärd, P.; Andersson Svahn, H.; Johnsen, J.I.; Kiessling, R.; Kogner, P. Regulation of myeloid cells by activated T cells determines the efficacy of PD-1 blockade. *Oncoimmunology* 2016, 5, e1232222, doi:10.1080/2162402X.2016.1232222.

117. Eranki, A.; Srinivasan, P.; Ries, M.; Kim, A.; Lazarski, C.A.; Rossi, C.T.; Khokhlova, T.D.; Wilson, E.; Knoblach, S.; Sharma, K. V; et al. High Intensity Focused Ultrasound (HIFU) Triggers Immune Sensitization of Refractory Murine Neuroblastoma to Checkpoint Inhibitor Therapy. *Clin. Cancer Res.* 2019, doi:10.1158/1078-0432.CCR-19-1604.
118. Matthay, K.K. Interleukin 2 plus anti-GD2 immunotherapy: Helpful or harmful? *Lancet. Oncol.* 2018, 19, 1549–1551, doi:10.1016/S1470-2045(18)30627-2.
119. Nierkens, S.; Lankester, A.C.; Egeler, R.M.; Bader, P.; Locatelli, F.; Pulsipher, M.A.; Bollard, C.M.; Boelens, J.J. Challenges in the harmonization of immune monitoring studies and trial design for cell-based therapies in the context of hematopoietic cell transplantation for pediatric cancer patients. *Cytotherapy* 2015, 17, 1667–1674, doi:10.1016/j.jcyt.2015.09.008.
120. Bate-Eya, L.T.; Ebus, M.E.; Koster, J.; den Hartog, I.J.M.; Zwijnenburg, D.A.; Schild, L.; van der Ploeg, I.; Dolman, M.E.M.; Caron, H.N.; Versteeg, R.; et al. Newly-derived neuroblastoma cell lines propagated in serum-free media recapitulate the genotype and phenotype of primary neuroblastoma tumours. *Eur. J. Cancer* 2014, 50, 628–637, doi:10.1016/j.ejca.2013.11.015.
121. Vlachogiannis, G.; Hedayat, S.; Vatsiou, A.; Jamin, Y.; Fernández-Mateos, J.; Khan, K.; Lampis, A.; Eason, K.; Huntingford, I.; Burke, R.; et al. Patient-derived organoids model treatment response of metastatic gastrointestinal cancers. *Science* 2018, 359, 920–926, doi:10.1126/science.aao2774.
122. Wu, T.; Wu, X.; Wang, H.-Y.; Chen, L. Immune contexture defined by single cell technology for prognosis prediction and immunotherapy guidance in cancer. *Cancer Commun.* 2019, 39, 21, doi:10.1186/s40880-019-0365-9.



# Chapter 3

# **Functional immune monitoring in patients with high-risk neuroblastoma during chemo- and immunotherapy reveals T cell unresponsiveness**

---

Celina L. Szanto<sup>1,2</sup>, Sara Tamminga<sup>1</sup>, Eveline M. Delemarre<sup>1</sup>, Coco C.H. de Koning<sup>1</sup>, Denise A.M.H. van den Beemt<sup>1</sup>, Michelle L. Tas<sup>2</sup>, Miranda P. Dierselhuis<sup>2</sup>, Lieve G.A.M. Tytgat<sup>2</sup>, Max M. van Noesel<sup>2</sup>, Kathelijne C.J.M. Kraal<sup>2</sup>, Jaap-Jan Boelens<sup>3</sup>, Alwin D. R. Huitema<sup>4,5</sup>, Stefan Nierkens<sup>1,2</sup>

<sup>1</sup> Center for Translational Immunology, University Medical Center Utrecht, Utrecht University, Utrecht, The Netherlands

<sup>2</sup> Princess Máxima Center for Pediatric Oncology, Utrecht University, Utrecht, The Netherlands

<sup>3</sup> Stem Cell Transplantation and Cellular Therapies Program, Department of Pediatrics, Memorial Sloan Kettering Cancer Center, New York, United States

<sup>4</sup> Department of Clinical Pharmacy, University Medical Center Utrecht, Utrecht University, Utrecht, The Netherlands

<sup>5</sup> Department of Pharmacy & Pharmacology, Netherlands Cancer Institute, Amsterdam, The Netherlands

*Submitted*

## Abstract

Neuroblastoma (NBL) is the most common extracranial solid tumor in childhood. Despite intensive treatment, children with high-risk (HR) disease have a poor prognosis. Immunotherapy has shown a significant improvement in event-free survival in HR NBL patients receiving chimeric anti-GD2 in combination with cytokines and isotretinoin after high-dose chemotherapy followed by stem cell rescue. However, response to immunotherapy varies widely, and often therapy is stopped due to severe toxicity. Thus, there is a clinical need for objective markers to predict efficacy, toxicity and adequate timing of treatment. In addition, immune monitoring during treatment can provide knowledge on the presence and function of the immune system after autologous hematopoietic stem cell transplantation (ASCT).

The aim of this study was to describe the dynamics of immune cell subsets and their function at diagnosis and during therapy in HR NBL patients. We performed in-depth immune monitoring in peripheral blood of 25 HR NBL patients at diagnosis, during induction chemotherapy, before high dose conditioning and during immunotherapy.

The dynamics of immune cells during multi-agent chemotherapy varied largely between patients. IL-2 and GM-CSF induced expansion of suppressive regulatory T-cells (Tregs). In addition, GM-CSF increased eosinophil and monocyte count significantly, and showed an increase of lymphocyte counts. IL-2 administration resulted in a significant increase of total lymphocyte population and CD56+ and CD16+ NK cells. The measurement of 92 proteins in plasma samples showed distinct clustering between samples drawn before and after IL-2 or GM-CSF treatment.

Patient's Tregs were functional albeit with a slightly reduced ability to suppress T-cell proliferation when compared to Tregs from healthy controls. In contrast, we found that patient T-cell proliferation was significantly impaired at diagnosis and after ASCT.

Our findings show that the status of the immune system is highly variable between patients post-ASCT. Nevertheless, the immune status is not taken into account for dose calculation or timing of treatment in the immunotherapy protocols. Moreover, we showed that treating patients with immunotherapy does not restore the corrupted effector T-cell function, but instead induces an expansion of functional Tregs. These new insights justify standardized immune monitoring in NBL patients before and during therapy to gather data on the association of the immune status of a patient and clinical outcome.

## Introduction

Neuroblastoma (NBL) is the most common extracranial solid tumor in children, accounting for approximate 15% of all pediatric oncology deaths worldwide<sup>1</sup>. Patients are stratified as low, intermediate or high-risk (HR), depending on different factors (e.g. age, tumor stage and several genetic components; such as MYCN amplification)<sup>2</sup>. HR NBL patients are treated with multimodal therapy, which can consist of chemotherapy, high-dose chemotherapy followed by autologous hematopoietic cell transplantation (ASCT), resection of the tumor, local radiation and maintenance immunotherapy consisting of anti-GD2 monoclonal antibody, the cytokines IL-2 and GM-CSF and isotretinoin. Despite intense treatment, HR NBL patients have a 5-year event-free survival (EFS) of <50%<sup>3,4</sup>.

Dinutuximab, a monoclonal antibody used in NBL immunotherapy, targets GD2 on the surface of NBL cells and signals antibody-dependent cell-mediated cytotoxicity (ADCC) and complement-dependent cytotoxicity (CDC)<sup>5</sup>. The rationale to add GM-CSF and IL-2 is to increase production and functional activity of natural killer (NK) cells, lymphocytes, monocytes/macrophages and neutrophils<sup>6,7</sup>.

The dose and timing of these compounds are currently highly empirical and do not take the immune status into account. Fast immune reconstitution during chemotherapy and higher absolute lymphocyte and monocyte counts have been associated with improved overall outcome in multiple cancers.<sup>9–11</sup> Nassin et al. showed that most patients with HR NBL do not have full immune reconstitution at the start of immunotherapy and that immune recovery may correlate with disease-related outcomes in patients with HR disease<sup>8</sup>. This result was based on the evaluation of total white blood cell count (WBC), hemoglobin, platelet count, absolute neutrophil, lymphocyte (including CD3+CD4+ and CD3+CD8+ T-cell counts, CD56+CD16+/- NK cell counts, CD19+ B cells) and monocyte counts (CD14+ and CD16+). Therefore, it may be hypothesized that post-transplant immune reconstitution occurs with disparate kinetics in different patients, which may affect treatment efficacy of immune-targeting therapy. A comprehensive understanding of the status of the immune system in these patients may be instrumental for the further development of immunotherapeutic interventions after ASCT. However, no studies have monitored the immune status in NBL patients during chemotherapy and immunotherapy and included functional analysis.

Therefore, we aimed to monitor the immune status comprehensively in NBL patients during chemo- and immunotherapy. In addition, the effect of IL-2 and GM-CSF on leukocyte and lymphocyte subpopulations and the (effector) cell functions during immunotherapy were studied.

## Materials and methods

### Patients ant treatment

HR NBL patients diagnosed between January 2015 and January 2018 and treated in the Princess Máxima Center for Pediatric Oncology (Utrecht, the Netherlands) or Uniklinik Köln (Cologne, Germany) were included in this study. Patients were treated following the same treatment protocol (Dutch NBL2009 trial and NB2013-HR pilot GPOH/DCOG trial). Staging was performed according to the International NBL Staging System (INSS)<sup>12</sup>. MYCN and ALK amplification status was determined with FISH, SNP-array was used for the determination of CNVs in 1p and 17q. The study was approved by the Medical Ethical Committees (Academic Medical Center, Amsterdam, the Netherlands; NL50762.018.14 and the university of Cologne, German trial 2013-004481-34). Written informed consent was obtained from the parents or guardians before enrollment in accordance with the Declaration of Helsinki.

### Sample collection

For patients included in the Princess Máxima Center, peripheral blood samples (EDTA) were transported to the laboratory at room temperature (RT) immediately after blood withdrawal and a cell subset enumeration tube was analyzed using flow cytometry within 24h after blood withdrawal. Plasma was isolated after centrifugation and stored at -80°C until analysis. All other experiments were performed on thawed peripheral blood mononuclear cells PBMCs (frozen in fetal calf serum (Bodinco) containing 10% dimethyl sulphoxide (Sigma-Aldrich)), stored in liquid nitrogen in the biobank of the University Medical Center Utrecht (UMCU). Control donor PBMCs, taken from healthy adult volunteers, served as control group.

In the Princess Máxima Center, peripheral blood samples were taken at diagnosis (1 sample from 7 patients), after each N5/N6 cycle (1-3 samples from 18 patients), before the high dose conditioning regimen (1 sample from 7 patients), at start of immunotherapy (1 sample from 7 patients) and after 3 and 6 cycles of immunotherapy (1-2 samples from 8 patients) as depicted in Supplementary Figure 1. In the Uniklinik Köln, peripheral blood samples were taken at start of immunotherapy and every 2 weeks during immunotherapy cycle 1-5. Samples were shipped at RT to the laboratory in Utrecht and processed within 24h as described above.

### Immune monitoring whole blood

Fresh 50 ml whole blood was stained in the dark with the following antibodies: CD45-PerCP-Cy5.5, CD14-PE, CD3-Alexa-Fluor700, CD4-APC-eFluor780, CD8-PE-Cy7, CD19-FITC, CD16-BV510, CD56-APC (Biolegend). After 15 min incubation at RT, erythrocytes were lysed for

minimal 15 min using BD FACS™ Lysing Solution (BD Biosciences). Stained cells were acquired using TruCount™ Tubes (BD Biosciences, Erembodegem, Belgium) to obtain absolute numbers on a BD LSRFortessa™ (BD Biosciences).

### Treg phenotyping

PBMCs were isolated using ficoll density gradient centrifugation and stained for Tregs using the following extracellular antibodies: CD3-AF700, CD4-eFluor780, CD8-PE-Cy7, CD25-PE, CD127-BV421, CD45RO-BV711 (Biolegend). For the intracellular staining, cells were permeabilized after extracellular staining, using the eBioscience kit (eBioscience, Thermo Fisher Scientific Inc) and stained intracellularly for FoxP3 expression. All samples were measured within 24h after staining on a BD LSR Fortessa. All flow cytometry data was analyzed with FlowJo software version 10.6.0 (Tree Star). Output CSV data files were further analyzed using Rstudio (version 1.2.1335).

### Proliferation assay

To assess proliferation of T-cells, PBMCs were labelled with CTV and cultured in a round-bottom 96-well plate for 3 days at 37°C and 5% CO<sub>2</sub>. 25.000 PBMCs were cultured in duplicates in the presence of anti-CD3 (0.5mg/ml, 16-0037-81; ThermoFisher), the mitogen phytohaemagglutinin P (PHA, 1,25mg/ml) or without stimuli. On day 3 supernatants were collected (pooled from duplo's) and stored (as described below). Proliferation of PBMCs was analyzed using flow cytometry.

### Suppression assay

Patient and healthy donor (HD) CD4+CD25highCD127low Tregs were sorted using BD FACSAria™. Tregs were added to CTV labelled effector cells in a cross-over manner: 1) Tregs patient + effector cells patient; 2) Tregs patient + effector cells HD; 3) Tregs HD + effector cells patient; 4) Tregs HD + effector cells HD. Soluble anti-CD3 (16-0037-81; ThermoFisher) was used as a stimulus. At day 3, the proliferation of effector cells was analyzed with flow cytometry.

### Protein profiling

Supernatant from the proliferation and suppression assays was collected after 3 days of culture, and stored at -80°C until cytokine measurement. Interferon- $\gamma$  (IFN- $\gamma$ ), tumor necrosis factor  $\alpha$  (TNF $\alpha$ ), soluble IL-2R, IL-2, IL-10, IL-13 and IL-17 were measured using multiplex immunoassays (Luminex Technology). The multiplex immunoassay was performed as described previously by the MultiPlex Core Facility of the UMCU<sup>13</sup>. Plasma samples were analyzed using the Proseek Multiplex Immuno-oncology immunoassay panel. Proseek is a high-throughput multiplex immunoassay based on proximity extension assay (PEA) technology that enables the analyses of

92 immuno-oncology related biomarkers simultaneously (Proseek Multiplex, Olink Bioscience, Uppsala, Sweden). In short, PEA technology makes use of antibody pairs linked with matching DNA-oligonucleotides per protein of interest. These oligonucleotides hybridize when brought into proximity after binding the protein and are extended by DNA polymerase, thereby forming PCR targets. These targets are quantified by real-time PCR. Obtained results are expressed in normalized protein expression (NPX) values, which are in a log scale.

## Statistics

Statistical analysis was performed using the Mann-Whitney U test, comparing differences between groups before and after administration of IL-2 and GM-CSF. Heatmaps for protein profiling data were generated using the heatmap.2 function from the gplots package using R software.

## Results

### Patient characteristics

Twenty-five patients were included in this study (Table 1) with a median age at diagnosis of 3.9 years (range 0.3-10.8). A slight majority (56%, n=14) had complete response or partial response after induction chemotherapy. These patients continued therapy following the HR treatment protocol. Non-responders (44%, n=11), received additional chemotherapy (2-4 N8 cycles [etoposide, topotecan, cyclophosphamide]) and 14% (n=4) received <sup>131</sup>I-metaiodobenzylguanidine (<sup>131</sup>I-MIBG) therapy. Transplantation conditioning regimens varied between patients, with 52% (n=13) of patients receiving busulfan and melphalan (Bu-Mel). Following ASCT, 16 out of 20 patients (80%) received dinutuximab immunotherapy in combination with cytokines. The four patients that did not receive immunotherapy had progressive disease or died before start. The mean time to from ASCT to start immunotherapy was 137 days after ASCT (range 32-193 days). The median time of last follow up for surviving patients was 2.14 years (range 0.65-3.67). The median event-free survival (EFS) was 1.65 years (range 0.11-3.67).

**Table 1.** Patient Characteristics and time of sampling

	<b>Total (n=25)</b>
<b>Gender</b> male/female	14 (56%) / 11 (44%)
<b>Median age at diagnosis, yr, (range)</b>	3.9 (0.3-10.8)
<b>Stage 3 disease</b>	1 (4%)
<b>Stage 4 disease</b>	24 (96%)
<b>Genetics</b>	
<b>MYCN</b> Neg/Gain/Amp	18 (72%) / 2 (8%) / 5 (20%)
<b>1p</b> normal/partial loss/loss/gain	14 (56%) / 9 (36%) / 1 (4%) / 1 (4%)
<b>17q</b> normal/partial gain/gain/ unknown	1 (4%) / 10 (40%) / 11 (44%) / 3 (12%)
<b>ALK</b> mutation yes/no/gain/ unknown	5 (20%) / 16 (64%) / 1 (4%) / 3 (12%)
<b>CR or PR after induction chemotherapy (3x N5N6)</b>	14 (56%)
<b>HD + ASCT</b>	20 (80%)
<b>Conditioning Regimen</b>	
Busulfan/melphalan	14/20 (70%)
Carboplatin/etoposide/melphalan	6/20 (30%)
<b>CD34+ cell dose x 10<sup>6</sup>/kg, (range)</b>	2.47 (0.59-21.73)
<b>Immunotherapy</b>	16 (64%)
<b>Time to immunotherapy, d, (range)</b>	137 (108-193)
<b>Event: progression or relapse</b>	7 (31%)
<b>Event: Refractory Disease</b>	3 (14%)
<b>Event: Toxicity</b>	1 (5%)
<b>Alive at last FU</b>	14 (56%)
<b>Median EFS, yr (range)</b>	1.65 (0.11-3.67)
<b>Median follow up OS, yr, (range)</b>	2.14 (0.65-3.67)

### Immune profiles at diagnosis, during induction chemotherapy and before high dose conditioning show broad variation between patients

To explore the immune status in the period before ASCT, immune profiles were generated from absolute leukocyte, lymphocyte, monocyte, neutrophil, eosinophil and lymphocyte subsets B-cells, NK-cells and T-cells (Figure 1) after each N5/N6 chemotherapy cycle (N5= cisplatin, etoposide, vindesine, N6= vincristine, dacarbazine, ifosfamide, doxorubicin) and before high-dose conditioning. Large variability between cell counts between patients and between treatment cycles within individual patients was observed. Absolute leukocyte counts increased, mainly due to increase of absolute neutrophils. During therapy absolute neutrophil counts varied the most between patients (range 0.002-18.38 x10<sup>3</sup>/mL compared to 1.08-2.98 x10<sup>3</sup>/mL at diagnosis). No correlation was found between absolute cell counts and occurrence of an event or MYCN status (data not shown). Absolute lymphocyte counts remained similar between patients, while

NK-cells and T-cells showed large variability between patients. Monocytes increased after diagnosis and varied between patients and between treatment cycles. Eosinophils remained similar between cycles and patients. CD19+ B cells decreased after the first round of induction chemotherapy (1<sup>st</sup> N5N6) and remained low during chemotherapy.

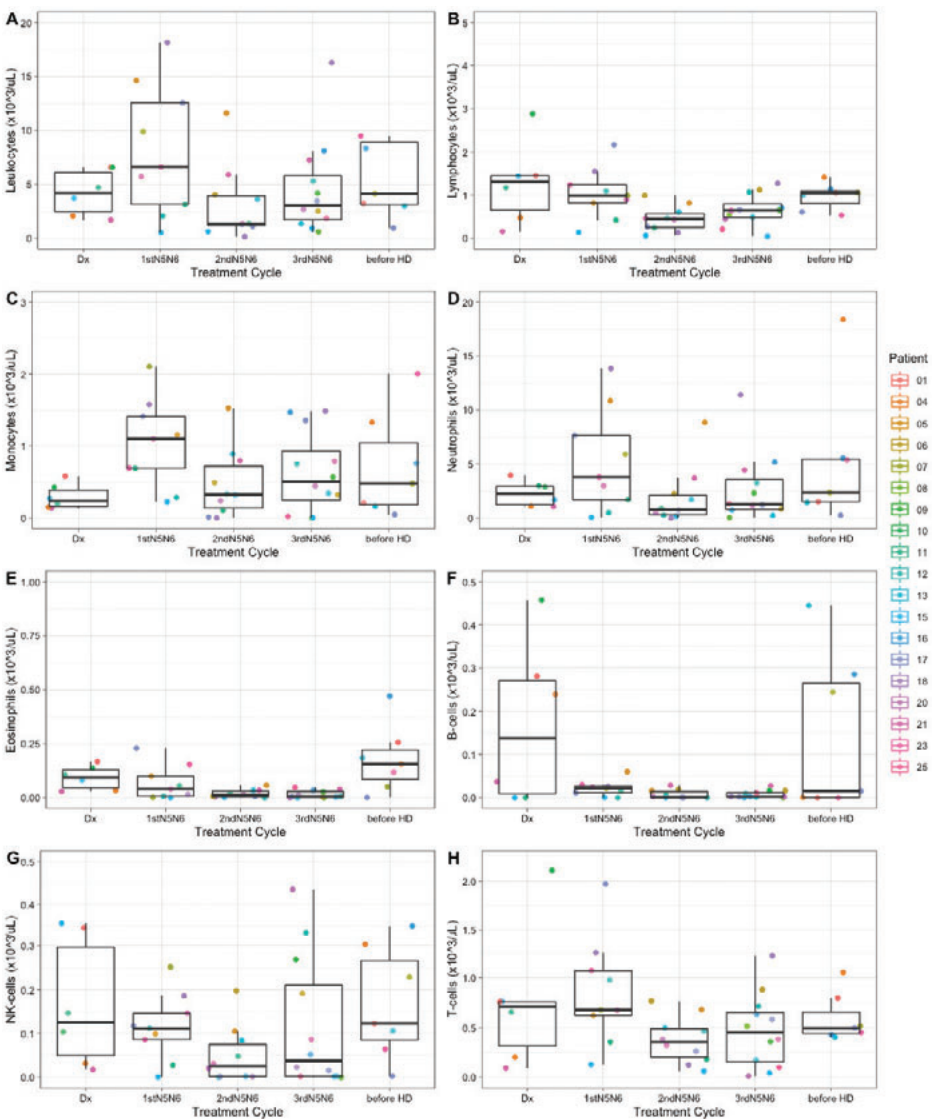


**Figure 1. Immune profiles at diagnosis, during induction chemotherapy and before high-dose conditioning**  
Each colored dot indicates absolute counts or cell percentages from one patient. Absolute counts are depicted at diagnosis, after 1<sup>st</sup> round of N5/N6 induction chemotherapy, after the 2<sup>nd</sup> round of N5/N6 induction chemotherapy, after the 3<sup>rd</sup> round of N5/N6 induction chemotherapy and before high dose conditioning from 6, 9, 11, 12 and 7 patients respectively.

### **Immune profiles during immunotherapy show effect of IL-2 and GM-CSF on leukocyte and lymphocyte subsets**

Total lymphocytes increased significantly after IL-2 ( $p=0.01$ ), due to a significant increase of NK cells ( $p=0.007$ ) (Figure 2, and supplementary figure 2 and 3). IL-2 had no effect on total CD3+ T-cell ( $p=0.67$ ), CD19+ B cell ( $p=0.70$ ) populations and monocytes ( $p=0.57$ ). Neutrophils decreased significantly after IL-2 administration ( $p=0.01$ ), while eosinophils showed an increase in peripheral blood after IL-2 ( $p=0.19$ ). Administration of GM-CSF resulted in a significant increase of eosinophils ( $p=0.0002$ ) (Figure 3). These eosinophils remained present after Ficoll density centrifugation suggesting that these cells are low density eosinophils (Supplementary Figure 4). GM-CSF increased neutrophils ( $p=0.07$ ), total lymphocytes ( $p=0.05$ ) and monocytes ( $p=0.03$ ). GM-CSF had no effect of total CD3+ T-cell ( $p=0.28$ ), NK cells ( $p=0.12$ ) and CD19+ B cells ( $p=0.19$ ). Administration of IL-2 in this study increased the frequency of circulating CD4+CD25<sup>high</sup>CD127<sup>dim</sup> FoxP3+ Tregs (Figure 4A). In addition, GM-CSF also increased the frequency of Tregs, although to a lower extent than IL-2 (Figure 4B).

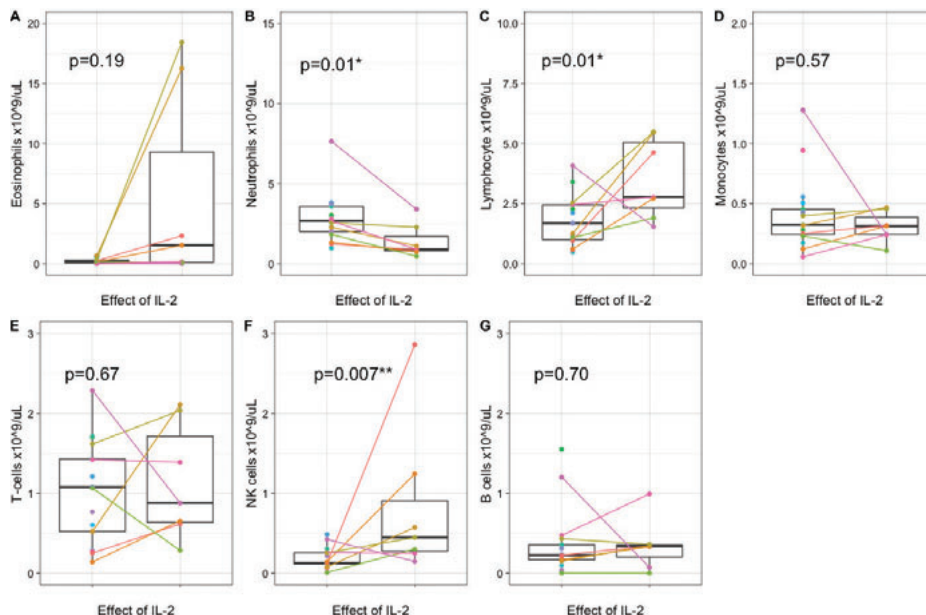


**Figure 2. Immune profiles before and after IL-2**

Each colored dot indicates absolute counts from one patient. From 5 patients, samples were paired before IL-2 (day 1 immunotherapy cycle 2 or 4) and after IL-2 (day 15 immunotherapy cycle 2 or 4). In total 7 paired samples are depicted (colored lines), because two patients were monitored in both IL-2 cycles. Nine single measurements from 9 other patients were included, having a total of 14 patients (11 in study, 3 left over material during IT). (A) A minimal 5-fold increase was noticed for absolute eosinophils (before IL-2 mean 0.22, range 0.00-0.63; after IL-2 mean 5.54, range 0.00-18.43). (B) Absolute neutrophils decrease after IL-2 (before IL-2 mean 2.84, range 0.96-7.64; after IL-2 mean 1.38, range 0.45-3.39). (C) Absolute lymphocytes increase after IL-2 (before IL-2 mean 1.75, range 0.47-4.08; after IL-2 mean 3.50, range 1.53-5.48). (D) Absolute monocytes (before IL-2 mean 0.41, range 0.05-1.27; after IL-2 mean 0.31, range 0.11-0.47). (E) Absolute CD3+ T-cells before and after IL-2 (before IL-2 mean 1.02, range 0.14-2.86; after IL-2 mean 1.14, range 0.29-2.11). (F) Absolute total NK cells increase after IL-2 (before IL-2 mean 0.19, range 0.01-0.48; after IL-2 mean 0.83, range 0.15-2.86). (G) Absolute CD19+ B cells before and after IL-2 (before IL-2 mean 0.36, range 0.002-1.55; after IL-2 mean 0.35, range 0.001-0.99).

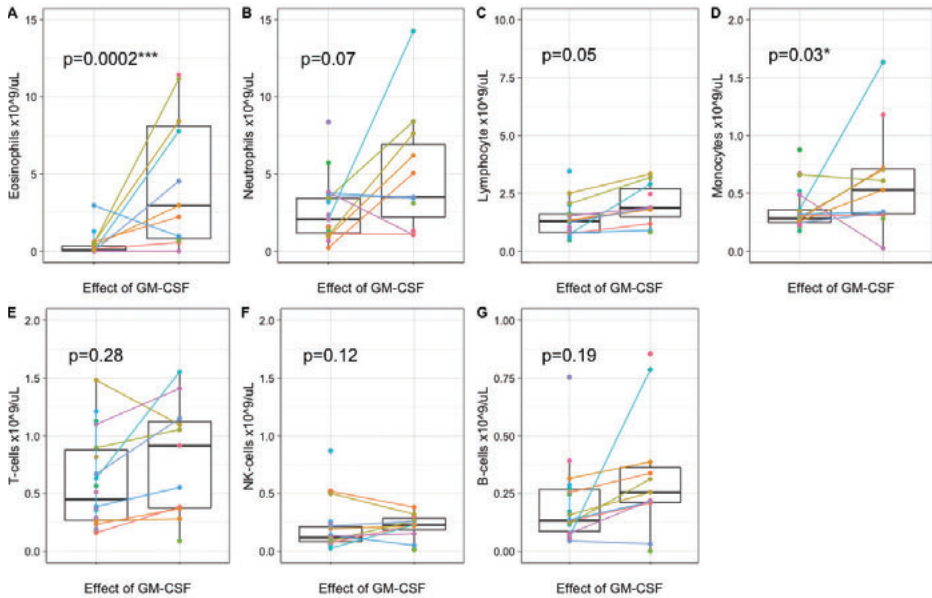
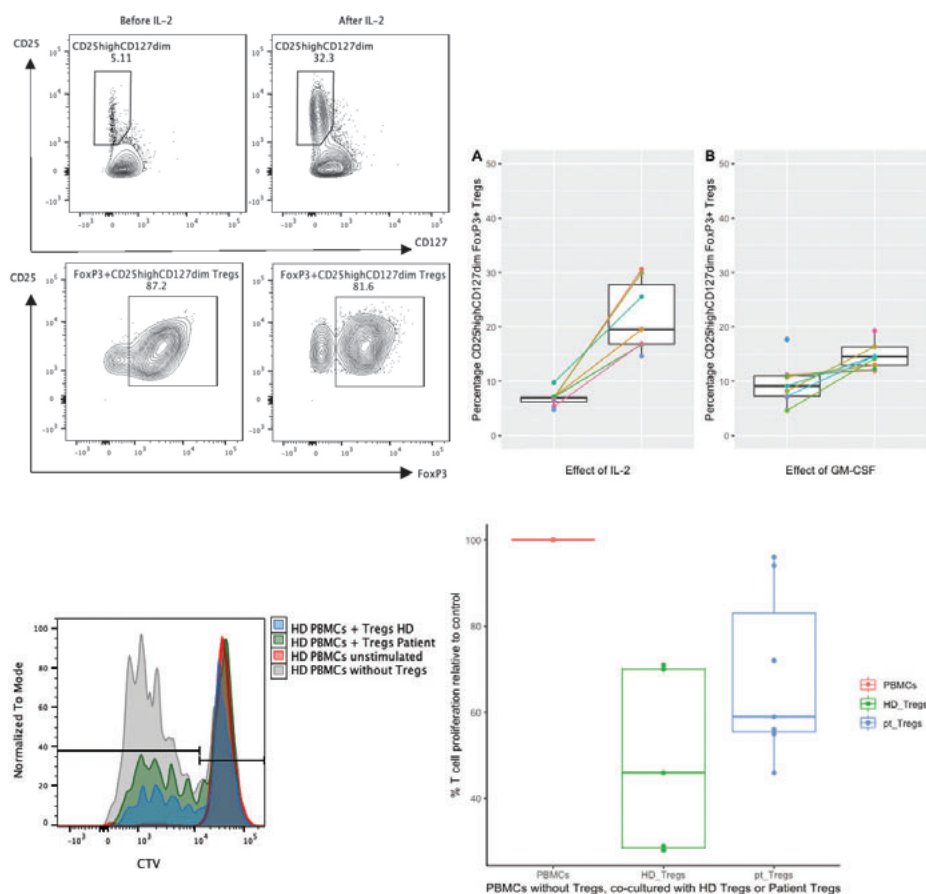


**Figure 3. Immune profiles before and after GM-CSF**

Each colored dot indicates absolute counts from one patient. From 5 patients, samples were paired before GM-CSF (day 1 immunotherapy cycle 1,3 or 5) and after GM-CSF (day 15 immunotherapy cycle 1,3 or 5). In total 9 paired samples are depicted (colored lines), because two patients were monitored during all 3 GM-CSF cycles. 12 single measurements from 12 other patients were included, having a total of 17 patients (11 in study, 6 left over material during IT). (A) A minimal 5-fold increase was noticed for absolute eosinophils (before GM-CSF mean 0.32, range 0.01-2.95; after GM-CSF mean 4.61, range 0.002-11.43). (B) Absolute neutrophils increase after GM-CSF (before GM-CSF mean 2.55, range 0.22-8.37; after GM-CSF mean 5.00, range 1.06-14.26). (C) Absolute lymphocytes increase after GM-CSF (before GM-CSF mean 1.38, range 0.47-3.47; after GM-CSF mean 2.02, range 0.82-3.33). (D) Absolute monocytes increase after GM-CSF (before GM-CSF mean 0.36, range 0.17-0.86; after GM-CSF mean 0.60 range 0.03-1.63). (E) Absolute CD3+ T-cells before and after GM-CSF (before GM-CSF mean 0.64, range 0.16-2.27 after GM-CSF mean 0.80 range 0.09-1.16). (F) Absolute total NK cells before and after GM-CSF (before GM-CSF mean 0.19, range 0.03-0.87; after GM-CSF mean 0.22 range 0.02-0.38). (G) Absolute CD19+ B cells before and after GM-CSF (before GM-CSF mean 0.24, range 0.05-1.34; after GM-CSF mean 0.33, range 0.001-0.85).



**Figures 4. Regulatory T-cell profiles during immunotherapy and their suppressive capacity**

(A) Example of gating of CD25highCD127dim cells within the CD3+CD4+ T-cell population and gating of FoxP3 within the CD25highCD127dim cell population before and after IL-2 administration. (B) Percentages of Tregs (within CD3+CD4+ T-cell population) increase 4-5-fold after IL-2 administration and increase 1-2-fold after GM-CSF administration. (C) CTV staining of PBMCs of a HD co-cultured without Tregs (grey), with Tregs of patient (green), or Tregs of HD (blue), or unstimulated (red). (D) Relative percentages of proliferation of HD CD3+ T-cells co-cultured with patient Tregs (blue) or HD Tregs (green) compared to proliferation without Tregs (red). CD3+ T-cell proliferation was measured in patient 1 (during cycle 2 and 4), patient 2 (during cycle 1,2 and 5) and patient 3 (during cycle 1 and 2).

## Treg suppression and impaired T-cells proliferation during therapy

Co-cultures of healthy donor PBMCs with patient's Tregs at different time points during immunotherapy showed suppression of T-cell proliferation (Figure 4C and Figure 4D). In 2 of the 7 measurements (patient 1 cycle 2 and patient 3 cycle 1), no T-cell suppression was noticed. Further, we noticed that T-cells, isolated from patients during immunotherapy did not proliferate *in vitro* after anti-CD3 stimulation (Figure 5A). This was strongly supported by

the cytokine concentrations measured in the supernatants (Figure 5B). Therefore, we purified lymphocytes without Tregs and low-density eosinophils to remove any possible interfering cell populations and stimulated them similarly. Purified lymphocytes showed again no proliferation (data not shown). In addition, PBMCs were stimulated with PHA. PHA was able to induce T-cell proliferation *in vitro*.

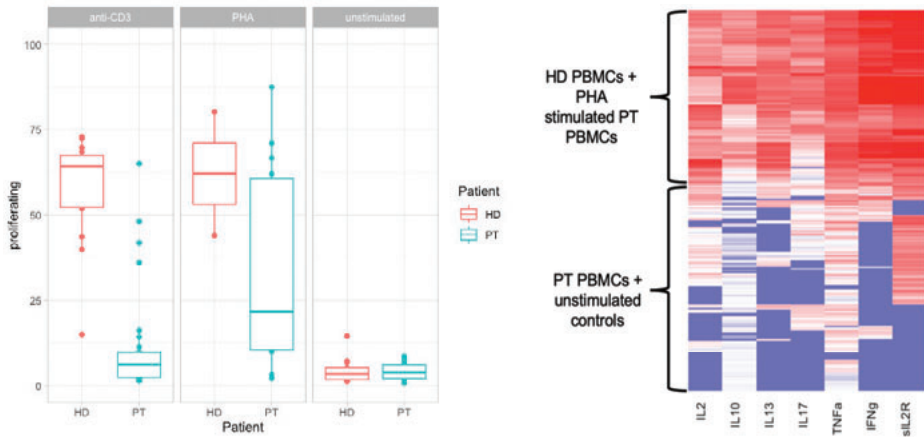


**Figure 5 Impaired proliferation of T-cells**

(A) PBMCs of HDs (red) and patients (blue) were stimulated with anti-CD3 (0.5 mg/ml) or PHA (1,25mg/ml). T-cell proliferation of each individual sample are shown (duplo's were pooled); PBMCs HD (n=8), PBMCs patients (n=12). (B) Supernatants (HD n=15, patients n=17) was analyzed using Luminex-based multiplex immunoassays. The heatmap shows the log concentration of all cytokines (IL-2, IL-10, IL-13, IL-17, TNFα, IFNγ and soluble IL-2R) with low levels indicated in blue and high levels indicated in red.

## Olink protein profiling

As a proof of concept, Olink protein analyses was performed in plasma samples of 6 patients. Protein profiling showed distinct patterns between pre- and post- IL-2 and pre- and post- GM-CSF samples. Samples from corresponding timepoints clustered partly together and protein profiles were similar between treatment cycles (Figure 6).

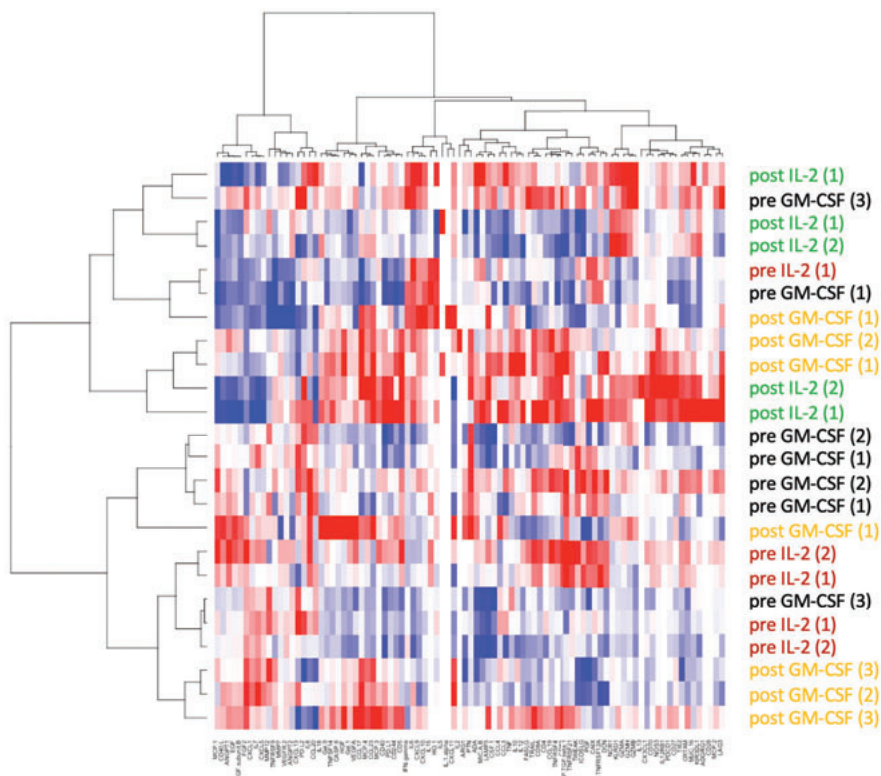


**Figure 6 Olink protein profiling**

Heatmap of 24 plasma protein profiles showing distinct patterns between treatment cycles. Pre- and post- IL-2 and GM-CSF samples are indicated with (1), (2), (3), corresponding for the first, second or third IL-2 or GM-CSF cycle respectively.

## Discussion

In this study we showed large variability between patient's immune status during chemotherapy. Overall increased neutrophil, lymphocyte and monocyte levels after GM-CSF, and increased NK cell populations after IL-2 were found. Both IL-2 and GM-CSF induced a remarkable expansion of suppressive Tregs and increased circulating eosinophils. In addition, we observed that T-cell proliferation was severely impaired in NBL patients.

Total number of leukocytes, thrombocytes and erythrocytes are routinely monitored in the clinic following therapy to prepare for possible short-term complications. Absolute lymphocyte counts, their subsets and diversity (phenotype) are rarely monitored and not used as prognostic criteria or treatment guidance. We show that patients with NBL have normal immune profiles at diagnosis, including lymphocyte (CD3+, CD16/CD56+ and CD19+) subsets ranging within normal

limits based on age<sup>14</sup>. Although chemotherapeutic agents can be immunosuppressant, the only subset that was completely depressed were peripheral blood B-lymphocytes. We noticed large inter-patient variability between treatment cycles during chemotherapy. Large variability in NK cell and monocyte levels may suggest a difference in ADCC capability between patients when subjected to mAb-treatment, while the variability in CD3+ T-cells and CD19+ B-cells and their products may be important measures for generating memory responses to prevent relapses. Follow-up studies are needed to clarify this. To our knowledge, this is the first time immune subsets are monitored longitudinally during chemotherapy of NBL patients. An emerging crucial question is how to incorporate chemoimmunotherapy into the multi-modulatory treatment protocol<sup>15</sup>. Pre-clinical studies in NBL models and two phase II trials demonstrated that chemotherapy with monoclonal antibodies provides synergistic benefits<sup>16,17</sup>. As CD56+ and CD16+ NK subsets are present during chemotherapy in normal ranges, we hypothesize that administering immunotherapy upfront may indeed provide synergistic benefits when guided through immune monitoring protocols.

The efficacy of anti-GD2 targeted therapy relies on ADCC mediated by GM-CSF and IL-2 activated NK cells. We found that both NK cell populations (cytokine releasing CD56bright CD16+/- NK cells and cytotoxic CD56dimCD16+ NK cells) increased after IL-2 administration. However, the ratio cytotoxic/cytokine releasing NK cells remained lower (at start IT large variation in percentages cytotoxic NK cells (30-80% instead of 90% normally) before and after IL-2. Whether this impacts the success of anti-GD2 therapy early after ASCT<sup>8</sup> needs to be established.

We noticed a strong increase of CD127dimCD25highFoxP3 + Tregs after IL-2 and GM-CSF administration. This increase has been described before, however, in many cases without confirming FoxP3 positivity. Using functional suppression assays in a cross-over format we showed that these Tregs have suppressive capacity at multiple timepoints during immunotherapy. These data are in line with preclinical data that have shown that the Tregs inhibit anti-NBL immune responses before and after ASCT<sup>18-20</sup>. Combining chemotherapy with anti-GD2 and GM-CSF might limit Tregs as cyclophosphamide has shown to selectively target Tregs, mitigating immunosuppression and promoting anti-tumor T-cell immunity<sup>21</sup>.

Interestingly, we noticed impaired T-cell proliferation after ASCT and a lack of IFN- $\gamma$ , TNF- $\alpha$ , IL-2, IL-10, IL-13, IL-17 and sIL2-R production after anti-CD3 stimulation. Impaired T-cell proliferation was shown previously 3-12 months post-ASCT in patients with breast cancer, amyloidosis, multiple myeloma and non-Hodgkin's lymphoma undergoing ASCT<sup>22-24</sup>. In this cohort, 3 out of 5 patients showed impaired T-cell proliferation at diagnosis. It has been reported that primary

human NBL cells inhibit T-cell proliferation through high arginase activity<sup>25</sup>. The resulting arginine depletion leads to T-cell cycle arrest, impaired proliferation and reduced activation<sup>26,27</sup>. Although we noticed impaired proliferation at diagnosis and after ASCT, it is debatable if the impaired proliferation after ASCT is caused by the tumor and/or by the intensive treatment regimen. To determine which specific pathways of T-cell proliferation are impaired, and whether they can be modulated, requires additional analyses.

The eosinophilia we observed in patients could be caused by IL-2 administration as it is reported that IL-2 (via IL-5) induces peripheral eosinophilia in immunotherapy treated cancer patients<sup>28</sup>. This is consistent with our data showing eosinophil percentages spiking at IL-2 doses. The effect of eosinophilia on treatment efficacy remains unclear. It has been reported that IL-2 is correlated with degranulation of eosinophils within the tumor micro environment<sup>29,30</sup>. On the other hand, eosinophils are known for extravascular degranulation in cancer patients, leading to release of toxic eosinophil products at extravascular sites and in the circulation. This contributes to the pathogenesis of capillary leak syndrome, a severe complication in IL-2 therapy<sup>28</sup>. However, tumor-associated tissue eosinophilia is associated with both good and poor prognosis, reflecting conflicting results as determination criteria vary between researchers<sup>31</sup>. It should be considered that we only report blood eosinophilia, which has been associated with TGF- $\beta$  production<sup>32</sup>. This is known both as a suppressor and promotor of tumor growth, and also for its function in generating Tregs by inducing FoxP3 expression. The effect of eosinophilia on outcome must be studied in larger patient groups.

This study has some limitations. First of all, successful patient sampling was low due to a drop out of patients from the study due to relapse/progression disease and transfer to other trials (e.g. BEACON), failure of blood sampling and logistic issues. Secondly, we could only monitor immune status in peripheral blood. Phenotyping tumor-infiltrating lymphocytes (TILs), or monitoring lymphocytes in tissues would help to elucidate the mechanisms of therapy. Larger sample size would be required to confirm these finding and relate them to clinical parameters and outcome.

In conclusion, immune monitoring in HR NBL patients demonstrated large patient variability. Standardized immune monitoring in larger patient groups via international collaboration is required to be able to relate the variability in numbers and function of immune cells to treatment efficacy.

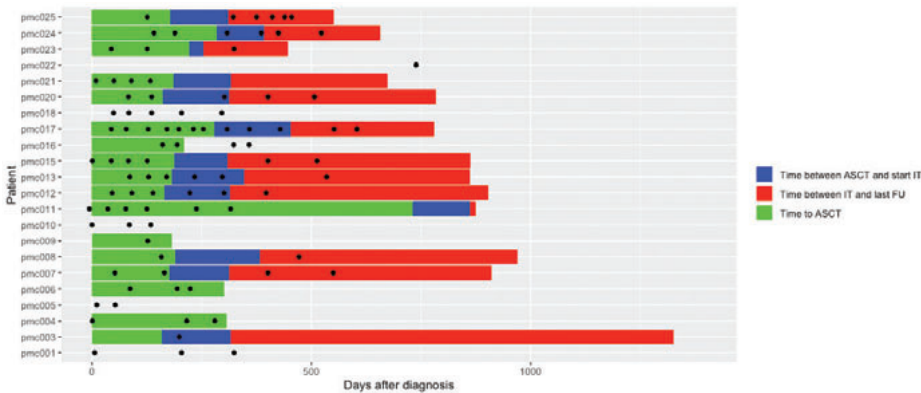
## References

1. Howlander N, Noone A, Krapcho M, et al. SEER Cancer Statistics Review, 1975-2016. *Nat/ Cancer Inst.* 2016.
2. Cohn SL, Pearson ADJ, London WB, et al. The International Neuroblastoma Risk Group (INRG) classification system: An INRG task force report. *J Clin Oncol.* 2009;27(2):289-97. doi:10.1200/JCO.2008.16.6785.
3. Park JR, Bagatell R, London WB, et al. Children's Oncology Group's 2013 blueprint for research: Neuroblastoma. *Pediatr Blood Cancer.* 2013;60(6):985-93. doi:10.1002/pbc.24433.
4. Pinto NR, Applebaum M a., Volchenboum SL, et al. Advances in risk classification and treatment strategies for neuroblastoma. *J Clin Oncol.* 2015;33(27):3008-3017. doi:10.1200/JCO.2014.59.4648.
5. Yu AL, Gilman AL, Ozkaynak MF, et al. Anti-GD2 Antibody with GM-CSF, Interleukin-2, and Isotretinoin for Neuroblastoma. *N Engl J Med.* 2010;363(14):1324-1334. doi:10.1056/NEJMoa0911123.
6. Masucci G, Ragnhammar P, Wersäll P, Mellstedt H. Granulocyte-monocyte colony-stimulating-factor augments the interleukin-2-induced cytotoxic activity of human lymphocytes in the absence and presence of mouse or chimeric monoclonal antibodies (mAb 17-1A). *Cancer Immunol Immunother.* 1990;31(4):231-235. doi:10.1007/BF01789174.
7. Hank J a, Robinson RR, Surfus J, et al. Augmentation of antibody dependent cell mediated cytotoxicity following in vivo therapy with recombinant interleukin 2. *Cancer Res.* 1990;50(17):5234-5239. doi:10.1158/0008-5472.can-10-2211.
8. Nassin ML, Nicolaou E, Gurbuxani S, Cohn SL, Cunningham JM, LaBelle JL. Immune Reconstitution Following Autologous Stem Cell Transplantation in Patients with High-Risk Neuroblastoma at the Time of Immunotherapy. *Biol Blood Marrow Transplant.* 2018;24(3):452-459.. doi:https://doi.org/10.1016/j.bbmt.2017.11.012.
9. Galvez-Silva J, Maher OM, Park M, et al. Prognostic Analysis of Absolute Lymphocyte and Monocyte Counts after Autologous Stem Cell Transplantation in Children, Adolescents, and Young Adults with Refractory or Relapsed Hodgkin Lymphoma. *Biol Blood Marrow Transplant.* 2017;23(8):1276-1281. doi:10.1016/j.bbmt.2017.04.013.
10. Kim HT, Armand P, Frederick D, et al. Absolute lymphocyte count recovery after allogeneic hematopoietic stem cell transplantation predicts clinical outcome. *Biol Blood Marrow Transplant.* 2015;21(5):873-80. doi:10.1016/j.bbmt.2015.01.019.

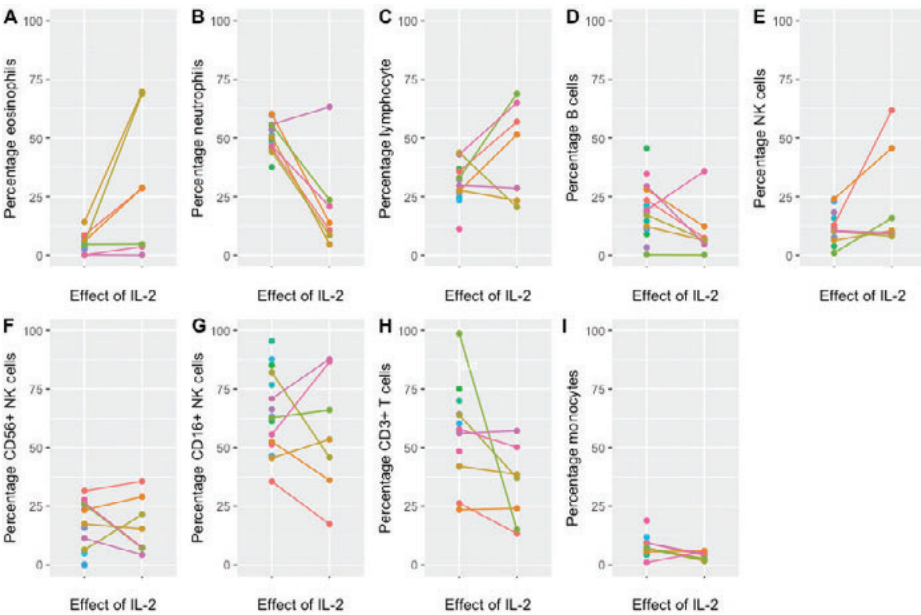
11. Thoma MD, Huneke TJ, DeCook LJ, et al. Peripheral blood lymphocyte and monocyte recovery and survival in acute leukemia postmyeloablative allogeneic hematopoietic stem cell transplant. *Biol Blood Marrow Transplant.* 2012;18(4):600-7. doi:10.1016/j.bbmt.2011.08.007.
12. Brodeur GM, Pritchard J, Berthold F, et al. Revisions of the international criteria for neuroblastoma diagnosis, staging, and response to treatment. *J Clin Oncol.* 1993;11(8):1466-77. doi:10.1200/JCO.1993.11.8.1466.
13. De Jager W, Prakken BJ, Bijlsma JWW, Kuis W, Rijkers GT. Improved multiplex immunoassay performance in human plasma and synovial fluid following removal of interfering heterophilic antibodies. *J Immunol Methods.* 2005;300(2):124-35. doi:10.1016/j.jim.2005.03.009.
14. Tosato F, Bucciol G, Pantano G, et al. Lymphocytes subsets reference values in childhood. *Cytom Part A.* 2015;87(1):81-5. doi:10.1002/cyto.a.22520.
15. Kushner BH. Chemoimmunotherapy for high-risk neuroblastoma. *Lancet Oncol.* 2017;18(7):845-846. doi:10.1016/S1470-2045(17)30337-6.
16. Mody R, Naranjo A, Van Ryn C, et al. Irinotecan–temozolomide with temsirolimus or dinutuximab in children with refractory or relapsed neuroblastoma (COG ANBL1221): an open-label, randomised, phase 2 trial. *Lancet Oncol.* 2017;18(7):946-957. doi:10.1016/S1470-2045(17)30355-8.
17. Furman WL, Federico SM, McCarville MB, et al. A Phase II trial of Hu14.18K322A in combination with induction chemotherapy in children with newly diagnosed high-risk neuroblastoma. *Clin Cancer Res.* 2019;10(3):320-897. doi:10.1158/1078-0432.CCR-19-1452.
18. Jing W, Gershan JA, Johnson BD. Depletion of CD4 T cells enhances immunotherapy for neuroblastoma after syngeneic HSCT but compromises development of antitumor immune memory. *Blood.* 2009;30 113(18):4449-57. doi:10.1182/blood-2008-11-190827.
19. Jing W, Yan X, Hallett WHD, Gershan JA, Johnson BD. Depletion of CD25+ T cells from hematopoietic stem cell grafts increases posttransplantation vaccine-induced immunity to neuroblastoma. *Blood.* 2011;117(25):6952-62. doi:10.1182/blood-2010-12-326108.
20. Johnson BD, Jing W, Orentas RJ. CD25+ regulatory T cell inhibition enhances vaccine-induced immunity to neuroblastoma. *J Immunother.* 2007;30(2):203-14. doi:10.1097/01.cji.0000211336.91513.dd.
21. Ghiringhelli F, Menard C, Puig PE, et al. Metronomic cyclophosphamide regimen selectively depletes CD4 +CD25+ regulatory T cells and restores T and NK effector functions in end stage cancer patients. *Cancer Immunol Immunother.* 2007;56(5):641-8. doi:10.1007/s00262-006-0225-8.

22. Avigan D, Wu Z, Joyce R, et al. Immune reconstitution following high-dose chemotherapy with stem cell rescue in patients with advanced breast cancer. *Bone Marrow Transplant.* 2000;26(2):169-76. doi:10.1038/sj.bmt.1702474.
23. Akpek G, Lenz G, Lee SM, et al. Immunologic recovery after autologous blood stem cell transplantation in patients with AL-amyloidosis. *Bone Marrow Transplant.* 2001;28(12):1105-9. doi:10.1038/sj.bmt.1703298.
24. van der Velden AMT, Claessen AME, van Velzen-Blad H, Biesma DH, Rijkers GT. Development of T cell-mediated immunity after autologous stem cell transplantation: Prolonged impairment of antigen-stimulated production of  $\gamma$ -interferon. *Bone Marrow Transplant.* 2007;40(3):261-6. doi:10.1038/sj.bmt.1705706.
25. Mussai F, Egan S, Hunter S, et al. Neuroblastoma arginase activity creates an immunosuppressive microenvironment that impairs autologous and engineered immunity. *Cancer Res.* 2015;75(15):3043-53. doi:10.1158/0008-5472.CAN-14-3443.
26. Rodriguez PC, Quiceno DG, Ochoa AC. L-arginine availability regulates T-lymphocyte cell-cycle progression. *Blood.* 2007;109(4):1568-1573. doi:10.1182/blood-2006-06-031856.
27. Zea AH, Rodriguez PC, Culotta KS, et al. L-Arginine modulates CD3 $\zeta$  expression and T cell function in activated human T lymphocytes. *Cell Immunol.* 2004;232(2):21-31. doi:10.1016/j.cellimm.2005.01.004.
28. Van Haelst Pisani C, Kovach JS, Kita H, et al. Administration of interleukin-2 (IL-2) results in increased plasma concentrations of IL-5 and eosinophilia in patients with cancer. *Blood.* 1991;78(6):1538-44 DOI: 10.1007/bf01629431.
29. Huland E, Huland H. Tumor-associated eosinophilia in interleukin-2-treated patients: evidence of toxic eosinophil degranulation on bladder cancer cells. *J Cancer Res Clin Oncol.* 1992;118(6):463-7. doi:10.1007/BF01629431.
30. Simon HU, Plötz S, Simon D, et al. Interleukin-2 primes eosinophil degranulation in hypereosinophilia and Wells' syndrome. *Eur J Immunol.* 2003;33(4):834-9. doi:10.1002/eji.200323727.
31. Gatault S, Legrand F, Delbeke M, Loiseau S, Capron M. Involvement of eosinophils in the anti-tumor response. In: *Cancer Immunology, Immunotherapy.*; 2012;61(9):1527-34. doi:10.1007/s00262-012-1288-3.
32. Wong DTW, Elovic A, Matossian K, et al. Eosinophils from patients with blood eosinophilia express transforming growth factor  $\beta$  1. *Blood.* 1991;78(10):2702-7. doi:10.1182/blood.v78.10.2702.bloodjournal78102702.

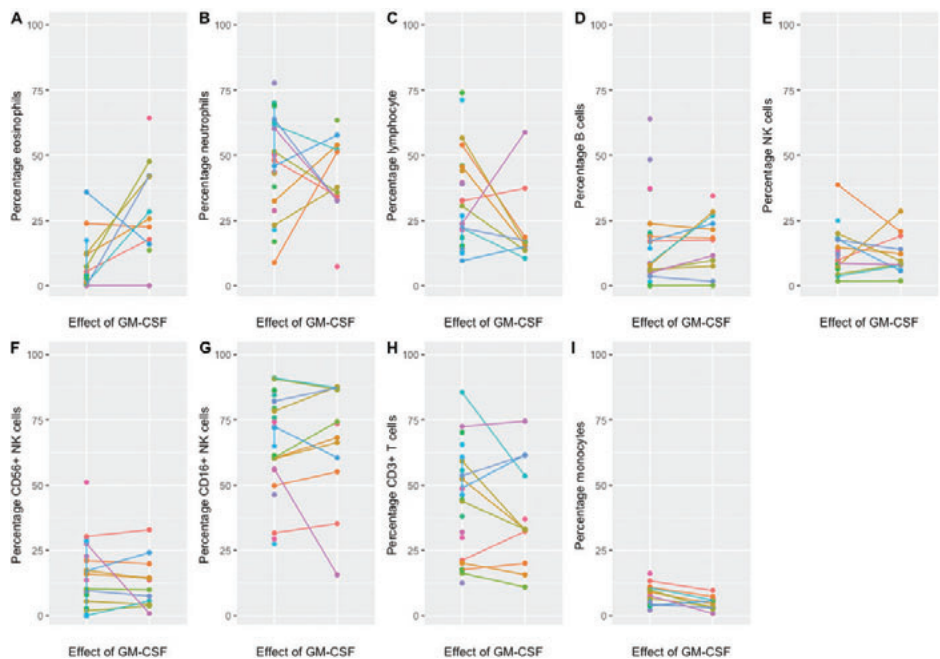
Supplementary figures:



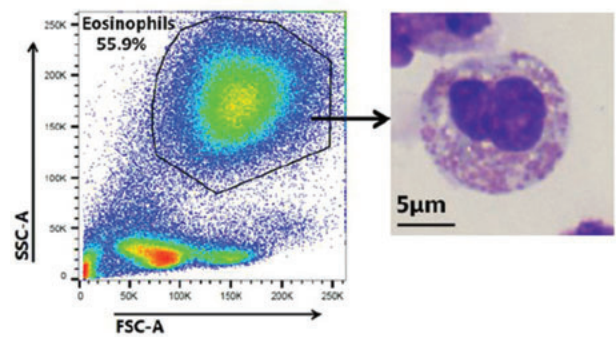
Suppl. Figure 1: Timing of sampling



Suppl. Figure 2: Percentages subsets before and after IL-2



Suppl. Figure 3: Percentages subsets before and after GM-CSF



Suppl. Figure 4: Cytospin low density eosinophils



# Chapter 4

# **Quantification of total dinutuximab concentrations in neuroblastoma patients with liquid chromatography tandem mass-spectrometry**

---

Mohsin El Amrani<sup>1</sup>, Celina L. Szanto<sup>2</sup>, C. Erik Hack<sup>2</sup>, Alwin D.R. Huitema<sup>1,3</sup>, Stefan Nierkens<sup>2,4</sup>, Erik M. van Maarseveen<sup>1</sup>

<sup>1</sup> Department of Clinical Pharmacy, University Medical Center Utrecht, Utrecht University, Utrecht, The Netherlands

<sup>2</sup> Center for Translational Immunology, University Medical Center Utrecht, Utrecht University, Utrecht, The Netherlands

<sup>3</sup> Department of Pharmacy & Pharmacology, Netherlands Cancer Institute, Amsterdam, The Netherlands

<sup>4</sup> Princess Máxima Center for Pediatric Oncology, Utrecht University, Utrecht, The Netherlands

*Analytical and Bioanalytical Chemistry*. 2018 Sep; 410(23), 5849-5858.

## Abstract

Neuroblastoma is one of the most commonly found solid tumors in children. The monoclonal antibody dinutuximab (DNX) targets the sialic acid-containing glycosphingolipid GD2 expressed on almost all neuroblastoma tumor cells and induces cell lysis. However, the expression of GD2 is not limited to tumor cells only, but is also present on central nerve tissue and peripheral nerve cells explaining dinutuximab toxicity. The most common adverse reactions are pain and discomfort, which may lead to discontinuation of the treatment. Furthermore, there is little to no data available on exposure and effect relationships of dinutuximab. We, therefore, developed an easy method in order to quantify dinutuximab levels in human plasma.

Ammonium sulfate (AS) was used to precipitate all immunoglobulins (IgG's) in human plasma. After centrifugation, supernatant containing albumin was decanted and the precipitated IgG fraction was re-dissolved in a buffer containing 0.5% sodium dodecyl sulfate (SDS). Samples were then reduced, alkylated and digested with trypsin. Finally, a signature peptide in complementarity-determining region 1 of DNX heavy chain was quantified on LC-MS/MS using a stable isotopically labeled peptide as internal standard. AS purification efficiently removed 97.5% of the albumin fraction in the supernatant layer. The validation performed on DNX showed that within-run and between-run coefficients of variation (CV's) for lower limit of quantification (LLOQ) were 5.5% and 1.4%, respectively. The overall CV's for quality control (QC) Low, QC Med and QC High levels were <5%. Linearity in the range 1 – 32 mg/L was excellent ( $r^2 > 0.999$ ). Selectivity, stability and matrix effect were in concordance with EMA guidelines. In conclusion, a method to quantify DNX in human plasma was successfully developed. In addition, the high and robust process efficiency enabled the utilization of a stable isotopically labelled (SIL) peptide instead of SIL DNX, which was commercially unavailable.

## Introduction

Neuroblastoma (NB) is the third most common childhood cancer with a prevalence of 10.2 cases per million children under the age of 15 years [1]. NB is an embryonic cancer of the post-ganglionic sympathetic nervous system which is usually formed in nerve tissues of the adrenal gland, neck, chest or spinal cord [2]. Early diagnosis of high risk NB is very difficult, however depending on the stage of the disease, tumors can clearly be seen as a lump under the skin. Treatment strategies of NB is dependent on the risk group it has been categorized to, since some cases of NB can show spontaneous and complete regression [1, 3-5]. However, the long-term survival of high risk NB is between 35 to 45% despite multimodal treatment [6-8]. Therefore, a new treatment strategy based on the chimeric, mouse-human, monoclonal antibody dinutuximab (CH14.18/SP2/0; Unituxin™; DNX) has been developed to target and eradicate remaining NB cells in order to prevent relapse [9, 10]. DNX was approved by European Medicines Agency (EMA) and Food and Drug Administration (FDA) in 2015 and is used in combination with granulocyte-macrophage colony-stimulating factor, interleukin-2, and isotretinoin [10, 11]. This therapeutic antibody targets the sialic acid-containing glycosphingolipid GD2 which is overexpressed on almost all NB tumor cells and induces cell lysis through complement-dependent cytotoxicity and cell necrosis and apoptosis through antibody-dependent cell-mediated cytotoxicity [8, 10, 12, 13]. However, treatment with DNX causes neuropathic pain due to GD2 presence on nerve cells, this necessitates the use of opioids prior to, during and for 2 h after administration of DNX in order to manage pain [10]. A method to quantify DNX levels in plasma can potentially lead to new insights for personalized dosing to increase efficacy and reduce toxicity. Furthermore, it has been estimated that up to 37% of patients develop anti-drug antibodies (ADA) which could have a profound impact on drug clearance [14-16], and thus therapeutic drug monitoring of these patients is of great value.

To date, three ligand binding assays are described, two based on anti-idiotypic antibodies to DNX and the other is a cell-based enzyme-linked immunosorbent assay (ELISA) using GD2 expressing melanoma cell line [17-19]. However, the generation of these cell lines and antibodies requires specific skills and facilities. Recently, the introduction of highly-sensitive liquid chromatography tandem mass spectrometry (LC-MS/MS) technology has enabled monoclonal antibody quantification. LC-MS/MS possesses notable advantages over ELISA methods such as faster assay setup times, wider linear dynamic range and most importantly higher selectivity [20, 21]. Therefore, we have developed an easy method to quantify total DNX in plasma using a novel sample preparation in combination with tandem mass-spectrometry analysis.

## Materials and Methods

### Chemicals and reagents

Dinutuximab (CH14.18/SP2/0; Unituxin®; DNX) was obtained from United Therapeutics Europe, Ltd (Chertsey, United Kingdom) as a solution of 3.5 mg/ml. Dinutuximab beta (CH14.18/CHO; Isquette®; DNX-β) was obtained from Retschler Biotechnologie GmbH (Laupheim, Germany) as a solution of 4.5 mg/ml. As internal standard (IS) stable isotopically labeled (SIL) peptide "ASGSSFTGYNMNWV(R 13C<sub>6</sub>,15N<sub>4</sub>)" was obtained from Pepscan Presto BV (Lelystad, The Netherlands). TPCK-Trypsin was supplied by Thermo Scientific as a lyophilized powder and was dissolved in acetic acid (50mM) to a concentration of 10 µg/µL, aliquoted in Eppendorf LoBind Microcentrifuge tubes and stored at -80 °C. All other chemicals, reagents and LC-MS grade mobile phase solvents were obtained from Sigma-Aldrich (Saint Louis, MO).

### Preparation of standards, internal standard and quality control samples

The working DNX standard solution (32 µg/mL) was prepared by pipetting 30 µL stock solution Unituxin (3.5 µg/µL) and 180 µL pooled plasma in a LoBind Eppendorf tube to obtain a concentration of 500 µg/mL. This solution was further diluted to 32 µg/mL in pooled plasma and aliquots were stored at -80 °C. Standard concentrations of 1, 2, 4, 8, 16 and 32 µg/mL were freshly prepared from the working standard solution by serial dilution in pooled plasma. The working internal standard SIL peptide solution "ASGSSFTGYNMNWV(R 13C<sub>6</sub>,15N<sub>4</sub>)" at a concentration of 0.5 mg/L was prepared in tris(hydroxymethyl)aminomethane (Tris) buffer pH 8.5, 100mM containing 0.5% octyl glucoside (OG). Quality Control samples (QCs) at lower limit of quantification (LLOQ) (1 µg/mL), QC low (3 µg/mL), QC med (15 µg/mL) and QC high (25 µg/mL) were prepared in pooled plasma from a separate batch. Aliquots were stored at -80 °C.

### Instrumentation and chromatographic conditions

Sample reduction, alkylation and digestion was performed on Eppendorf™ ThermoMixer C. All measurements were performed on an Ultimate 3000 UHPLC Dionex (Sunnyvale, CA) coupled to a TSQ Quantiva, Thermo Fisher (Waltham, MA). The analytical column was Acclaim™, RSLC 120, C18, 2.1 x 100 mm, 2.2 µm particle size, Thermo Fisher (Waltham, MA), The Guard column was the SecurityGuard column ULTRA C18, 2.1 mm (Phenomenex) and were maintained at 50 °C. The mobile phases were: (A) 0.1% formic acid in water; (B) 0.1% formic acid in acetonitrile. The LC gradients in minutes per percentage of mobile phase B were 0.0 (min)/2 (% B), 7.5/24, 7.6/85, 8.5/85, 8.6/2 and 10.5/2. The flow rate was 0.6 ml/min and the run time was 10.5 min. The mass spectrometer was operated in positive mode with spray voltage of 3.5 kV, ion transfer tube temperature 350 °C, vaporizer temperature 300 °C, aux gas pressure 15 Arb, sheath gas

pressure 50 Arb, collision energy 30 V, collision gas pressure 2.5 mTorr and radio frequency (RF) lens 110 V. The precursor ions and product ions settings are listed in table 1 for DNX and for the SIL internal standard.

**Table 1.** Mass Spectrometer conditions for selected reaction monitoring (SRM) transitions for the signature peptide (liberated from DNX after digestion with trypsin) and the SIL internal standard

Peptide Sequence	Used as	Precursor (m/z)	Product (m/z)	Product Ion type
ASGSSFTGYNMNWVR	Qualifier	838.88	819.39	Y6
ASGSSFTGYNMNWVR	Quantifier	838.88	1039.47	Y8
ASGSSFTGYNM(O)NWVR	Oxidation check	846.88	1055.47	Y8
ASGSSFTGYNMNWVR	Qualifier	838.88	1140.52	Y9
ASGSSFTGYNMNWVR [13C6,15N4]	Qualifier	843.90	829.39	Y6
ASGSSFTGYNMNWVR [13C6,15N4]	Quantifier	843.90	1049.47	Y8
ASGSSFTGYNM(O)NWVR [13C6,15N4]	Oxidation check	851.90	1065.47	Y8
ASGSSFTGYNMNWVR [13C6,15N4]	Qualifier	843.90	1150.52	Y9

## Sample preparation for LC-MS/MS analysis

Ammonium sulfate (AS) protein precipitation method was chosen because of its inherent simplicity, high sample throughput and fast work flow (Fig. 1). In brief, 10  $\mu$ L (sample, standard or QC) was diluted with 90  $\mu$ L Tris (50 mM, pH 8, 0.5% OG) in 1 mL LoBind 96 well plate. Then, 70  $\mu$ L AS (saturated) was added to each sample followed by 1 minute mixing at room temperature. The 96 well plate was centrifuged at 4000 G for 5 minutes to collect the IgG pellet at the bottom. The supernatant containing albumin was decanted and the pellet was re-dissolved in 50  $\mu$ L Tris (100 mM, pH 9, 0.5% sodium dodecyl sulfate (SDS), 20 mM 1,4-dithiothreitol (DTT)). Then, the well plate was placed in a ThermoMixer at 60 °C, 1000 RPM for 30 minutes to reduce the disulfide bonds. Samples were alkylated by adding 20  $\mu$ L iodoacetamide (IAA) (100mM dissolved in ultrapure water) and placed on a ThermoMixer at 37 °C for 30 min in the dark. Then, 150  $\mu$ L ultrapure water was added and mixed for 1 minute to dilute the SDS and IAA. After mixing, methanol was added to precipitate the IgG fragments and the well plate was centrifuged at 4000 G for 5 minutes. The supernatant containing SDS and IAA was decanted. Then, 90  $\mu$ L IS working solution was added, followed by 10  $\mu$ L Trypsin (2  $\mu$ g/ $\mu$ L) and the samples were placed on the ThermoMixer for overnight digestion at 37 °C, 800 RPM. Trypsin activity was stopped by adding 30  $\mu$ L 10% formic acid, 5% trifluoroacetic acid (TFA) in acetonitrile. Finally, 25  $\mu$ L was injected on an LC-MS/MS.

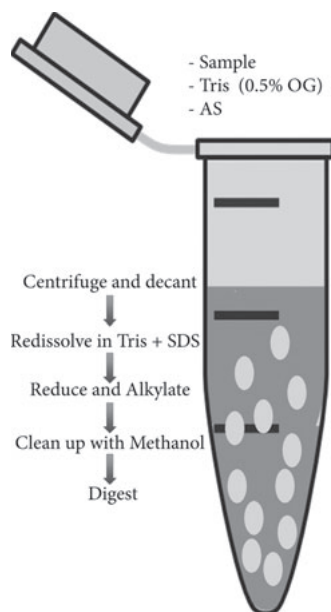


**Figure 1:** Sample purification workflow using AS

## Signature peptide selection

Tryptic digestion is regularly used to obtain peptides to enable low quantification levels of therapeutic monoclonal antibodies (mAb) in plasma with a triple quadrupole mass spectrometer. DNX sequence was obtained from the international immunogenetics information system® (<http://imgt.org>). After in silico digesting the variable chains with the online tool from institute of systems biology (<http://db.systemsbiology.net>), potential signature peptide candidates having amino acids in the range of  $6 < n < 20$  were identified. These amino acids were then screened using pBlast (<https://blast.ncbi.nlm.nih.gov/Blast.cgi?PAGE=Proteins>). Finally, the retention time (RT) of the surrogate peptide candidates were identified on the Q Exactive (Thermo Scientific) and the signal intensity of all peptides were compared.

## Albumin determination

After sample purification with AS, the remaining concentration albumin in the pellet was measure by means of immunonephelometry on the BN ProSpec® System (SIEMENS). In brief, 200  $\mu$ L plasma from a healthy donor was diluted with 1800  $\mu$ L Tris (50 mM, pH 8, 0.5% OG) in a test tube in triplicates. Then, 1400  $\mu$ L AS (saturated) was added to each tube followed by 1 minute mixing at room temperature. Then the test tubes were centrifuged at 4000 G for 5 minutes to collect the IgG pellet at the bottom. The supernatant was decanted to the waste and the pellet was re-dissolved in 200  $\mu$ L phosphate-buffered saline (PBS). The remaining albumin in the pellet and in the original plasma sample were measured on the BN ProSpec.

### AS concentration and DNX recovery

10  $\mu$ L standard 6 (32 mg/L) was pipetted 12 times in lobind 96 deep well plate followed by 90  $\mu$ L Tris (pH 8, 0.5% OG). Then, 50, 60, 70 and 80  $\mu$ L saturated AS was added in triplicates followed by mixing and centrifugation. Samples were then prepared and analyzed according to chapter 2.4.

### Methanol concentration and DNX recovery

10  $\mu$ L standard 6 (32 mg/L) was pipetted 18 times in lobind 96 deep well plate followed by 90  $\mu$ L Tris (pH 8, 0.5% OG). Samples were then prepared according to chapter 2.4 with the following modifications; following alkylation 0, 50, 100, 150, 200, 250  $\mu$ L water was added in triplicates followed by 550, 500, 450, 400, 350, 300  $\mu$ L methanol also in triplicates.

### Comparison between DNX and DNX- $\beta$

A test was performed to determine whether concentrations of DNX and DNX- $\beta$  were similar. A DNX- $\beta$  control sample was prepared at a concentration of 15 mg/L and was run in duplicate against DNX calibration curve. DNX standards and the DNX- $\beta$  control sample were prepared as described in chapter 2.2.

### Patient infusion samples

After obtaining parental informed consent, eight peripheral blood samples of 2 mL (in EDTA-treated tubed) were drawn from one pediatric patient each time before and after DNX infusion. The patient was given a daily infusion of 14.01 mg DNX for 10 - 20 hours during a 4 day treatment period. Peripheral blood samples were centrifuged at 600 G for 15 minutes. Following centrifugation, the supernatant (plasma) was carefully removed from the cell pellet. Plasma was aliquoted into 1-2 volumes of 0.5mL and immediately stored at -80°C. After storage, samples were analyzed in duplicates according to the procedure described in chapter 2.4.

### Validation

The method was validated according to EMA guidelines which dictate the investigation of parameters such as, LLOQ, linearity, selectivity, matrix effect, carry-over, auto sampler stability, freeze/thaw stability, within-run and between-run precision and accuracy [22]. LLOQ was chosen based on the reference ELISA used to generate pharmacokinetic data for FDA approval [23] and was determined by comparing the signal obtained from standard 1 (1 mg/L) against a pooled normal human plasma after sample preparation according to the above described method. The acceptance criterion is that the signal of standard 1 (LLOQ) should be at least 5 times higher than the signal obtained for the pooled normal human plasma at the RT of the signature peptide. The linear dynamic range of the standard curve was established based on theoretical

peak levels that would be obtained in patients and was investigated by measuring 6 standards at concentrations 1.00, 2.00, 4.00, 8.00, 16.00, 32.00 µg/mL for 3 days. The acceptance criterion for the back calculated concentration for LLOQ was 20% of the nominal value and for the remaining standard 15% of the nominal value. Selectivity was tested by evaluating 10 human plasma samples from healthy donors and comparing the MS signal intensity at the RT of the signature peptide against LLOQ signal. The noise signal intensity obtained for the blank plasma samples at the RT of DNX signature peptide should be less than 20% of the LLOQ signal. Matrix effect was tested by spiking human plasma samples from healthy donors at QC low (3 mg/L) and QC high (25 mg/L) and determining the concentration with the calibration curve. The back calculated concentration should be within 15% of the nominal value. Carry-over was tested by injecting digested pooled normal human plasma sample after a high standard. The acceptance criterion, in this case, was a signal obtained at the RT of DNX signature peptide of less than 20% of the LLOQ and a signal obtained for the IS under 5%. Auto sampler stability was tested by re-injecting the validation samples the next day and comparing the results to those of the day before. Freeze and thaw stability was validated by analyzing a QC Low and QC high sample in 5-fold during 3 days at which samples were thawed and tested, and the remaining samples were stored again at -80 °C, and subjected to the same procedure next day. Within-run and between-run precision and accuracy was evaluated during 3 days by analyzing LLOQ (1 µg/mL), QC Low (3 µg/mL), QC Med (15 µg/mL) and QC High (25 µg/mL) in 5 folds each day. The data obtained for each concentration was evaluated with single factor ANOVA. Accuracy was expressed as percentage bias. Within-run and between-run precision was expressed as percent coefficient of variation (% CV) and was calculated by taking the squared root of the mean squares (MS) and dividing this by the overall mean concentration times 100%.

## Results

### Method development

A novel sample preparation method was developed based on an optimized combination of established methods from literature [20, 24-27]. AS purification was found to be a fast, easy and efficient way to remove plasma albumin which comprises of approximately 60% of total plasma proteins. Furthermore, the protein pellet could easily be re-dissolved in working buffers, suggesting that AS did not denature the IgG's and kept the tertiary structure intact. The use of a MS compatible non-ionic surfactant, octyl glucoside (OG), with AS aided in the removal of phospholipids which are notorious MS-ionization suppressants. SDS is a widely used inexpensive ionic detergent, and is very efficient in protein unfolding and solubilization when used under reducing conditions in presence of DTT. However, SDS is not compatible with trypsin nor with MS thus removal prior to these steps is essential. Using our method, SDS was efficiently removed by protein precipitation with methanol, as SDS remains in solution in the aqueous layer. This was verified by evaporating the supernatant layer under nitrogen. Upon the addition of water, foam was clearly visible after agitating the test tube. Methanol precipitation also allowed for efficient removal of the remaining salts. The internal standard was a SIL peptide ASGSSFTGYNMNWV(R 13C<sub>6</sub>, 15N<sub>4</sub>) and was introduced to the samples prior to digestion. The internal standard allowed for correction of ionization suppression and injection volume differences during MS analysis. Importantly, digestion with trypsin needed to be reproducible between different patients because the SIL peptide cannot correct for digestion efficiency. Here, we found that the protein pellet was completely dissolved in all patients containing different levels of IgG's during matrix effect studies

### Signature peptide selection

In silico digestion of the variable light (VL) and heavy chain (VH) provided 10 potential candidates that were between 6 to 20 amino acids long and that could possibly be used as signature peptide (table 2). After performing a protein blast search three peptide candidates (VL1, VL19 and VL67) were found to be endogenous to humans and were dismissed. VL 33 was also dismissed because it contained asparagine followed by glycine. Glycine, a small amino acid group is not capable of shielding asparagine from deamination reaction. The remaining candidates were screened using high resolution mass spectrometry after tryptic digestion (data not shown). Signals for peptide VH68 and VL60 were found to be low, probably due to charge interference caused by the aspartic acid group (D) near the trypsin digestion sites (K and R). Peptide VH24 (ASGSSFTGYNMNWVR) and VH44 (SLEWIGAI DPYYGGTSYNQK) from the complementarity-determining region (CDR) 1 and CDR 2, respectively were found to have the highest signal intensity and both were optimized for collision energy and RF lens settings

on the triple quadrupole. After optimizing the digestion condition, the signal intensity of VH44 was found to be too low to allow for quantification at the required LLOQ of 1 µg/mL. Therefore, VH44 peptide was omitted and the validation was performed on the VH24 peptide. Although VH24 peptide contains a methionine group, no oxidation peaks were found after overnight digestion (data not shown).

**Table 2.** Peptides with amino acids (6<n<20) obtained after in-silico digestion of the variable chains. Results for query cover and identification percentages were obtained from pBlast using human library from Swiss-Prot database

LOCATION	SEQUENCE	MASS	QUERY COVER	IDENTIFICATION
VH24	ASGSSFTGYNMNVVR	1676.7485	100%	73%
VH44	SLEWIGAIDPYGGTSYNQK	2262.0713	80%	63%
VH68	ATLTVDK	747.4247	100%	86%
VH75	SSSTAYMHLK	1124.5405	100%	88%
VL1	EIVMTQSPATLSVSPGER	1901.9637	100%	100%
VL19	ATLSCR	650.3290	100%	100%
VL25	SSQSLVHR	913.4850	75%	100%
VL33	NGNTYLHWYLQKPGQSPK	2131.0719	94%	82%
VL60	FSGVPDR	777.3889	85%	100%
VL67	FSGSGSGTDFTLK	1303.6164	100%	100%

### Level of albumin remaining after AS purification

The albumin concentration of the untreated plasma sample and the AS pellet re-dissolved in PBS buffer were measured in triplicate by means of immunonephelometry. The untreated plasma sample had a mean concentration albumin of 39,5 g/L with a standard deviation (SD) of 0.72 g/L and the AS pretreated plasma sample had a mean remaining albumin concentration of 0.98 g/L with an SD of 0.1g/L. This translates to a highly efficient depletion of 97.5% albumin with AS pretreatment (Fig. 2).

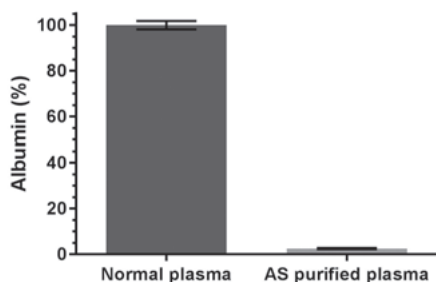


**Figure 2:** Level of albumin remaining without pretreatment (normal plasma) and with AS pretreatment (AS purified plasma), error bars represent SD with n=3

### AS concentration and DNX recovery

This test was performed to determine the concentration AS needed that provides the highest recovery. Increasing concentrations AS were tested starting from 33.3% going up to 44.4%. From the results obtained we see that at 37.5% AS the line started to bend reaching a plateau at an AS concentration of 41.2% (Fig. 3). This translates to 70  $\mu$ L saturated AS per 100  $\mu$ L solution consisting of 10  $\mu$ L sample and 90  $\mu$ L Tris (50mM, pH 8, 0.5% OG).

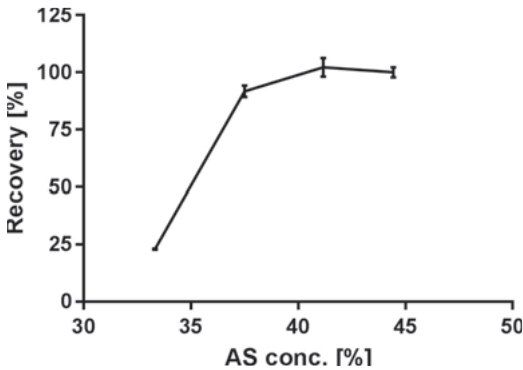


**Figure 3:** Concentration AS plotted against DNX recovery, error bars represent SD with n=3

### Methanol concentration and DNX recovery

The second step in the procedure that could lead to loss of DNX is the water – methanol washing step. Water was used to dilute the SDS and methanol was used to precipitate the proteins in order to obtain a pellet after centrifugation. From the obtained results we see that the highest concentration methanol tested resulted in the lowest recovery (Fig. 4). This is counterintuitive since we expect the opposite. In fact, the reason for the signal drop is not due to loss of DNX in the washing step, but rather due to ionization suppression or trypsin denaturation caused by inefficient removal of SDS. Here, we notice that we need to introduce at least 50  $\mu$ L of water per sample to dilute and remove SDS in the supernatant layer. Using 48% methanol, we noticed a decrease in DNX recovery and therefore, we chose 65% methanol as the optimum concentration which lies in the middle of the plateau. This corresponds to 400 $\mu$ L methanol per 70 $\mu$ L sample diluted with 150 $\mu$ L water.

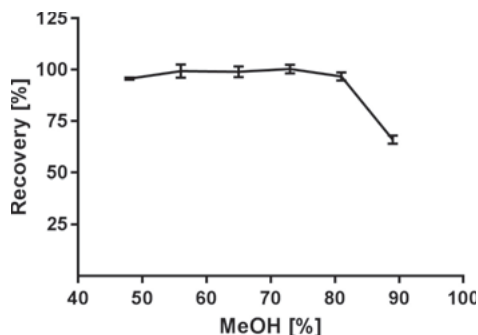


**Figure 4:** Methanol concentration plotted against DNX recovery, error bars represent SD with  $n=3$ .

### Comparison between DNX and DNX- $\beta$

DNX- $\beta$  (CH14.18/CHO; Dinutuximab beta; Isquette) received marketing approval in 2017 and is currently used to treat new patients suffering from NB. DNX (CH14.18/SP2/0; Unituxin) was withdrawn from the market in March 2017. However, patients on Unituxin will continue to receive this formulation. DNX- $\beta$  can be given without co-administration of interleukin-2, which induces inflammatory side effects [28]. These two drugs contain the same peptide sequences, only glycosylation differences can occur due to the different cell lines used. Since measurements are based on signal obtained from the signature peptide these two drugs were found to be well correlated with a bias of 8.8% and RSD of 1.13%. The latter illustrates one of the advantages of antibody quantification using LCMSMS.

### Patient infusion data

One patient was monitored for DNX concentration with the above described method during the 4 day treatment period. Samples were drawn before infusion and at the end of a 10 to 20h DNX infusion. The third dose showed the highest DNX concentration (Fig. 5). This was probably due to relative short resting period (8h) in between dose 2 and 3. The resting period in between dose 1 and 2 and between dose 3 and 4 were 30 hours and 18 hours respectively.

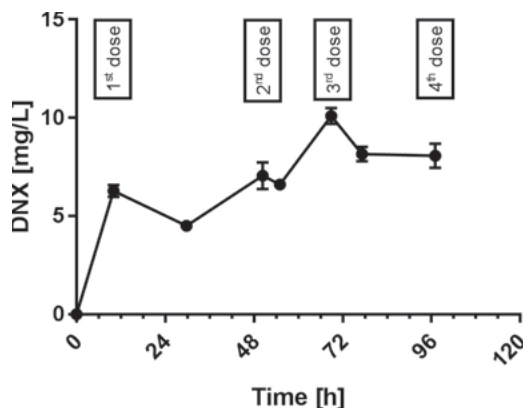


**Figure 5:** DNX concentration data obtained from one patient dosed during 4 days, each time with a 10 - 20 hour infusion of 14.01 mg DNX, error bars represent SD with n=2.

## Validation

The LLOQ was first determined by analyzing DNX spiked in pooled normal human plasma sample at a concentration of 1 µg/mL (Fig. 6). The signal to noise ratio (S/N) was found to be approximately 187, which is well above the EMA guidelines (threshold of S/N >5). Linearity was evaluated during 3 days using the following standards; 1.00, 2.00, 4.00, 8.00, 16.00, 32.00 µg/mL. The back calculated concentrations were found to be in agreement with guidelines with a determination coefficient  $R^2 > 0.999$  (Fig. 7). Selectivity and carry-over were evaluated by analyzing 10 normal human plasma samples and measuring the signal intensity at the RT of the signature peptide in relation to LLOQ signal intensity. Table 3 lists the percentage signal in relation to LLOQ signal for DNX signature peptide and for the SIL IS. Matrix effect was tested by spiking DNX at QC Low and QC High levels in 7 different human plasma samples. The average bias was in concordance with EMA guidelines of 15% (table 4). Auto sampler stability was tested by re-injecting the validation samples after 24 hours. Signal intensities and concentration values were found to be in agreement with previous run (data not show). Freeze and thaw stability was tested during 3 days with overall CV of around 4% for both QC Low and QC High and a bias of 1.4% and 5%, respectively. And finally, within-run and between-run precision and accuracy for LLOQ, QC Low, QC Med and QC High were evaluated during three days in five folds and were found to be well within the acceptance criteria with CV in the range of 5% which is 3 times lower than the set limit see table 5.

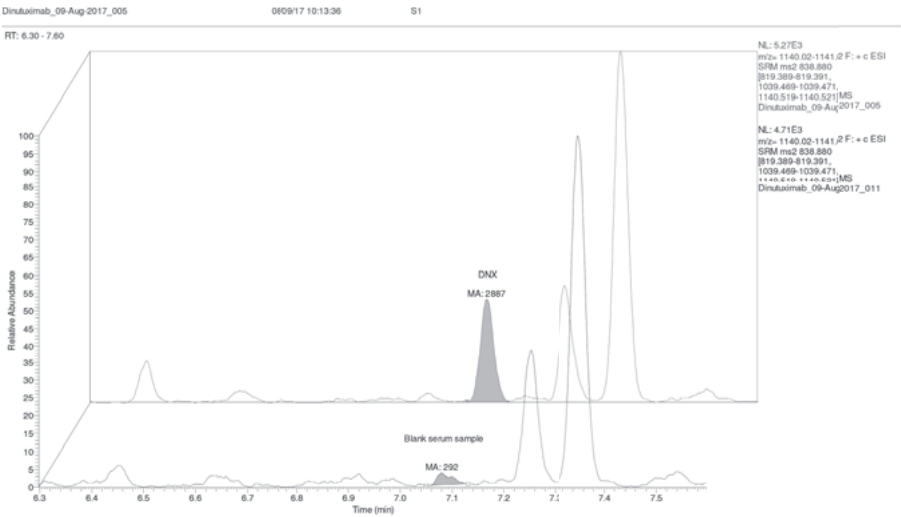


**Figure 6:** LLOQ at 1 µg/mL tested against a blank pooled normal human plasma sample

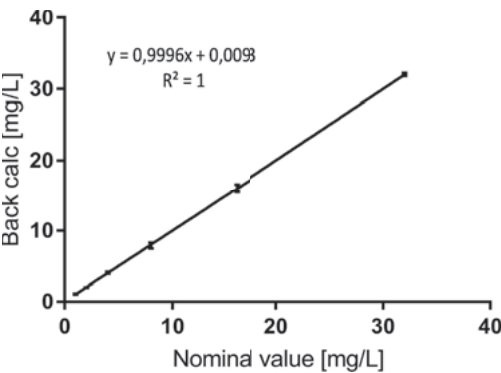


**Figure 7:** Linearity test, standard curve with SD error bars at each standard level tested during three days

**Table 3.** Selectivity and carry over test with randomly chosen blank human plasma samples

Blank human plasma sample	% Signal in relation to LLOQ signal	% Signal in relation to IS signal
Plasma pool – IS (Carry over)	12	0,16
Plasma pool + IS	3	112,05
Sample 1	2	0,08
Sample 2	5	0,06
Sample 3	11	0,02
Sample 4	8	0,04
Sample 5	5	0,06
Sample 6	7	0,03
Sample 7	1	0,07
Sample 8	1	0,05
Sample 9	5	0,00
Sample 10	8	0,03

**Table 4.** Matrix effect test, 7 human plasma samples spiked at QC Low (3mg/L) and QC High level (25mg/L)

Sample nr	Measured [mg/L]	Bias	Measured [mg/L]	Bias [%]
1	2.80	-6,7	24,42	-2,3
2	2.60	-13,3	25,98	3,9
3	3.16	5,2	27,61	10,4
4	3.29	9,5	26,28	5,1
5	3.26	8,6	29,00	16,0
6	3.24	8,2	26,82	7,3
7	3.14	4,7	26,87	7,5

**Table 5 .** Accuracy and precision validation data for QC's at LLOQ, Low, Medium and High levels. Within-run data were based on 5 replicates and between-run data on 3 different days.

QC	Within- run	Precision (% CV)		Accuracy (% bias)
		Between-run	Overall	Overall
LLOQ	5.5	1.4	5.7	6.4
Low	4.4	1.2	4.6	0.2
Med	2.9	2.0	3.5	2.9
High	2.9	3.4	4.5	4.6

## Discussion and Conclusion

A novel sample work-up method utilizing AS in combination with SDS was developed for the quantification of total DNX in human plasma. The AS precipitation method facilitated efficient removal of albumin while retaining a high recovery for DNX. The development of a DNX LC-MS/MS method was performed because of the clinical need for reliable method to quantify DNX in plasma for ongoing pharmacokinetic studies and future drug monitoring. This method measures total (free and bound) DNX concentration in plasma while ELISA methods measure free DNX concentrations. Previous studies in animals and in humans showed that total mAb fraction measured by LC-MS/MS provide similar PK profiles as those obtained by ELISA's free mAb fraction [29-33]. Furthermore, Willrich and colleagues have shown that total infliximab was strongly correlated to free infliximab even in a subset of samples containing anti-drug antibodies [26]. These data show that similar results can be obtained with assays that are fundamentally different. In addition, LC-MS/MS methods are in many ways analytically superior to ligand binding assays due to their high specificity, wider linear dynamic range and higher accuracy and precision.

The method was validated in concordance with the latest EMA/FDA guidelines. Furthermore, excellent validation data were obtained. This was mainly due to the ease of use of the method and to the efficient and robust digestion process which was achieved by incorporating SDS in the sample work-up. Finally, the here described method can be used as a template for the quantification other therapeutic monoclonal antibodies in plasma.

## Acknowledgements

The authors would like to thank Dr. Maarten ten Berg for his assistance with sample procurement.

## References

- [1] J.M. Maris, Recent advances in neuroblastoma, *N Engl J Med*, 362 (2010) 2202-2211.
- [2] J. Hara, Development of treatment strategies for advanced neuroblastoma, *Int J Clin Oncol*, 17 (2012) 196-203.
- [3] S. Tsubota, K. Kadomatsu, Origin and mechanism of neuroblastoma, *Oncoscience*, 4 (2017) 70-72.
- [4] N.L. Carlsen, How frequent is spontaneous remission of neuroblastomas? Implications for screening, *Br J Cancer*, 61 (1990) 441-446.
- [5] K. Yamamoto, R. Hanada, A. Kikuchi, M. Ichikawa, T. Aihara, E. Oguma, T. Moritani, Y. Shimanuki, M. Tanimura, Y. Hayashi, Spontaneous regression of localized neuroblastoma detected by mass screening, *J Clin Oncol*, 16 (1998) 1265-1269.
- [6] K.K. Matthay, C.P. Reynolds, R.C. Seeger, H. Shimada, E.S. Adkins, D. Haas-Kogan, R.B. Gerbing, W.B. London, J.G. Villablanca, Long-term results for children with high-risk neuroblastoma treated on a randomized trial of myeloablative therapy followed by 13-cis-retinoic acid: a children's oncology group study, *J Clin Oncol*, 27 (2009) 1007-1013.
- [7] N.R. Pinto, M.A. Applebaum, S.L. Volchenboum, K.K. Matthay, W.B. London, P.F. Ambros, A. Nakagawara, F. Berthold, G. Schleiermacher, J.R. Park, D. Valteau-Couanet, A.D. Pearson, S.L. Cohn, Advances in Risk Classification and Treatment Strategies for Neuroblastoma, *J Clin Oncol*, 33 (2015) 3008-3017.
- [8] L. Amoroso, R. Haupt, A. Garaventa, M. Ponzoni, Investigational drugs in phase II clinical trials for the treatment of neuroblastoma, *Expert Opin Investig Drugs*, (2017) 1-13.
- [9] V. Castel, V. Segura, A. Canete, Treatment of high-risk neuroblastoma with anti-GD2 antibodies, *Clin Transl Oncol*, 12 (2010) 788-793.
- [10] S. Dhillon, Dinutuximab: first global approval, *Drugs*, 75 (2015) 923-927.
- [11] C. Ploessl, A. Pan, K.T. Maples, D.K. Lowe, Dinutuximab: An Anti-GD2 Monoclonal Antibody for High-Risk Neuroblastoma, *Ann Pharmacother*, 50 (2016) 416-422.
- [12] L. McGinty, J. Kolesar, Dinutuximab for maintenance therapy in pediatric neuroblastoma, *Am J Health Syst Pharm*, 74 (2017) 563-567.
- [13] E. Barker, B.M. Mueller, R. Handgretinger, M. Herter, A.L. Yu, R.A. Reisfeld, Effect of a chimeric anti-ganglioside GD2 antibody on cell-mediated lysis of human neuroblastoma cells, *Cancer Res*, 51 (1991) 144-149.

- [14] M.F. Ozkaynak, P.M. Sondel, M.D. Krailo, J. Gan, B. Javorsky, R.A. Reisfeld, K.K. Matthay, G.H. Reaman, R.C. Seeger, Phase I study of chimeric human/murine anti-ganglioside G(D2) monoclonal antibody (ch14.18) with granulocyte-macrophage colony-stimulating factor in children with neuroblastoma immediately after hematopoietic stem-cell transplantation: a Children's Cancer Group Study, *J Clin Oncol*, 18 (2000) 4077-4085.
- [15] A.L. Gilman, M.F. Ozkaynak, K.K. Matthay, M. Krailo, A.L. Yu, J. Gan, A. Sternberg, J.A. Hank, R. Seeger, G.H. Reaman, P.M. Sondel, Phase I Study of ch14.18 With Granulocyte-Macrophage Colony-Stimulating Factor and Interleukin-2 in Children With Neuroblastoma After Autologous Bone Marrow Transplantation or Stem-Cell Rescue: A Report From the Children's Oncology Group, *J Clin Oncol*, 27 (2009) 85-91.
- [16] R. Handgretinger, P. Baader, R. Dopfer, T. Klingebiel, P. Reuland, J. Treuner, R.A. Reisfeld, D. Niethammer, A phase I study of neuroblastoma with the anti-ganglioside GD2 antibody 14.G2a, *Cancer Immunol Immunother*, 35 (1992) 199-204.
- [17] N. Siebert, D. Seidel, C. Eger, D. Brackrock, D. Reker, M. Schmidt, H.N. Lode, Validated detection of anti-GD2 antibody ch14.18/CHO in serum of neuroblastoma patients using anti-idiotypic antibody ganglidiomab, *J Immunol Methods*, 398-399 (2013) 51-59.
- [18] G. Soman, X. Yang, H. Jiang, S. Giardina, G. Mitra, Comparison of GD2 binding capture ELISA assays for anti-GD2-antibodies using GD2-coated plates and a GD2-expressing cell-based ELISA, *J Immunol Methods*, 373 (2011) 181-191.
- [19] A.V. Desai, E. Fox, L.M. Smith, A.P. Lim, J.M. Maris, F.M. Balis, Pharmacokinetics of the chimeric anti-GD2 antibody, ch14.18, in children with high-risk neuroblastoma, *Cancer Chemother Pharmacol*, 74 (2014) 1047-1055.
- [20] M. El Amrani, M.P. van den Broek, C. Gobel, E.M. van Maarseveen, Quantification of active infliximab in human serum with liquid chromatography-tandem mass spectrometry using a tumor necrosis factor alpha -based pre-analytical sample purification and a stable isotopic labeled infliximab bio-similar as internal standard: A target-based, sensitive and cost-effective method, *J Chromatogr A*, 1454 (2016) 42-48.
- [21] P.M. Ladwig, D.R. Barnidge, M.A.V. Willrich, Mass Spectrometry Approaches for Identification and Quantitation of Therapeutic Monoclonal Antibodies in the Clinical Laboratory, *Clin Vaccine Immunol*, 24 (2017).
- [22] E.M. Agency, Guideline on bioanalytical method validation, in: C.f.M.p.f.H.U. (CHMP) (Ed.), EMA, [ema.europa.eu](http://ema.europa.eu), 2011.
- [23] FDA, Clinical Pharmacology and Biopharmaceutics Review, in: C.f.D.E.a. Research (Ed.), 2014.

- [24] B. An, M. Zhang, R.W. Johnson, J. Qu, Surfactant-aided precipitation/on-pellet-digestion (SOD) procedure provides robust and rapid sample preparation for reproducible, accurate and sensitive LC/MS quantification of therapeutic protein in plasma and tissues, *Anal Chem*, 87 (2015) 4023-4029.
- [25] J.Y. Zhou, G.P. Dann, T. Shi, L. Wang, X. Gao, D. Su, C.D. Nicora, A.K. Shukla, R.J. Moore, T. Liu, D.G. Camp, 2nd, R.D. Smith, W.J. Qian, Simple sodium dodecyl sulfate-assisted sample preparation method for LC-MS-based proteomics applications, *Anal Chem*, 84 (2012) 2862-2867.
- [26] M.A. Willrich, D.L. Murray, D.R. Barnidge, P.M. Ladwig, M.R. Snyder, Quantitation of infliximab using clonotypic peptides and selective reaction monitoring by LC-MS/MS, *Int Immunopharmacol*, 28 (2015) 513-520.
- [27] Y.H. Chang, Z.R. Gregorich, A.J. Chen, L. Hwang, H. Guner, D. Yu, J. Zhang, Y. Ge, New mass-spectrometry-compatible degradable surfactant for tissue proteomics, *J Proteome Res*, 14 (2015) 1587-1599.
- [28] E. Siddall, M. Khatri, J. Radhakrishnan, Capillary leak syndrome: etiologies, pathophysiology, and management, *Kidney Int*, 92 (2017) 37-46.
- [29] H. Li, R. Ortiz, L.T. Tran, H. Salimi-Moosavi, J. Malella, C.A. James, J.W. Lee, Simultaneous analysis of multiple monoclonal antibody biotherapeutics by LC-MS/MS method in rat plasma following cassette-dosing, *AAPS J*, 15 (2013) 337-346.
- [30] X.Y. Peng, B.N. Liu, Y.T. Li, H. Wang, X. Chen, H.Z. Guo, Q.C. Guo, J. Xu, H. Wang, D.P. Zhang, J.X. Dai, S. Hou, Y.J. Guo, Development and Validation of LC-MS/MS Method for the Quantitation of Infliximab in Human Serum, *Chromatographia*, 78 (2015) 521-531.
- [31] W.S. Law, J.C. Genin, C. Miess, G. Treton, A.P. Warren, P. Lloyd, S. Dudal, C. Krantz, Use of generic LC-MS/MS assays to characterize atypical PK profile of a biotherapeutic monoclonal antibody, *Bioanalysis*, 6 (2014) 3225-3235.
- [32] O. Heudi, S. Barteau, D. Zimmer, J. Schmidt, K. Bill, N. Lehmann, C. Bauer, O. Kretz, Towards absolute quantification of therapeutic monoclonal antibody in serum by LC-MS/MS using isotope-labeled antibody standard and protein cleavage isotope dilution mass spectrometry, *Anal Chem*, 80 (2008) 4200-4207.
- [33] K. Shibata, T. Naito, J. Okamura, S. Hosokawa, H. Mineta, J. Kawakami, Simple and rapid LC-MS/MS method for the absolute determination of cetuximab in human serum using an immobilized trypsin, *J Pharm Biomed Anal*, 146 (2017) 266-272.



# Chapter 5

# **A ‘no-touch’ antibody-staining method of adherent cells for high-throughput flow cytometry in 384-well microplate format for cell-based drug library screening**

---

Annelisa M. Cornel<sup>1</sup>, Celina L. Szanto<sup>1</sup>, Niek P. van Til<sup>1</sup>, Jeroen van Velzen<sup>1</sup>, Jaap-Jan Boelens<sup>2</sup>, Stefan Nierkens<sup>1,3</sup>

<sup>1</sup> Center for Translational Immunology, University Medical Center Utrecht, Utrecht University, Utrecht, The Netherlands

<sup>2</sup> Stem Cell Transplantation and Cellular Therapies Program, Department of Pediatrics, Memorial Sloan Kettering Cancer Center, New York, United States

<sup>3</sup> Princess Máxima Center for Pediatric Oncology, Utrecht University, Utrecht, The Netherlands

*Cytometry Part A. 2019 Dec 26. Epub ahead of print*

## **Abstract**

In the last decade, screening compound libraries on live cells has become an important step in drug discovery. The abundance of compounds in these libraries requires effective high-throughput (HT) analyzing methods. Although current cell-based assay protocols are suitable for HT analyses, the analysis itself is often restrained to simple, singular outcomes. Incorporation of HT samplers on flow cytometers has provided an interesting approach to increase the number of measurable parameters and increase the sensitivity and specificity of analyses. Nonetheless, to date, the labor intensive and time-consuming strategies to detach and stain adherent cells before flow cytometric analysis has restricted use of HT flow cytometry (HTFC) to suspension cells. We have developed a universal 'no touch' HTFC antibody staining protocol in 384-well microplates to bypass washing and centrifuging steps of conventional flow cytometry protocols. Optimizing culture conditions, cell-detachment and staining strategies in 384-well microplates resulted in an HTFC protocol with an optimal stain index with minimal background staining. The method has been validated using six adherent cell lines, and simultaneous staining of four parameters. This HT screening protocol allows for effective monitoring of multiple cellular markers simultaneously, thereby increasing informativity and cost-effectiveness of drug screening.

## Introduction

The new era of biologicals used in anti-cancer therapy shifts the focus of therapeutic intervention from achieving cell death to (immune) cell modulation, thereby making cells more susceptible to other compounds or immune clearance. Cell-based screening of drug libraries has become an important approach in discovering new drugs against these targets of interest. Biochemical assays are more and more replaced by cell-based assays, as they enable studying underlying cellular mechanisms (1). Many cell-based assays have been developed in recent years, including functional-, reporter-, and phenotypic assays. Nonetheless, high-throughput (HT) cell-based screening is still limited by labor-intensive, expensive, and throughput limiting analyzing methods.

Equipment of flow cytometers with HT samplers (both 96- and 384-well format) has made otherwise low-throughput flow cytometry more suitable as a HT analyzing strategy (2). In this way, whole 96-well microplates can be analyzed in as little as 15 minutes. One of the most favorable aspects of flow cytometry is the opportunity to multiplex the measurement of protein expression on the surface or in the cytosol of individual cells. In this way, multiple effects or the underlying mechanisms of drugs can be studied in more detail, contributing to the informativity of drug screens.

The application of HT flow cytometry (HTFC) multiparameter analysis may, however, still be compromised due to labor intensive and time-consuming staining protocols, especially when analyzing adherent cell types. As a result, HT microscopy (HTM) is currently recommended as the method of choice when analyzing adherent cells (3). It is important to note that different research questions can be answered with HTM compared to HTFC. A major advantage of HTM analysis is that cells can be analyzed in their natural shape and effects of compounds on morphology can be assessed. Disadvantages of HTM are the requisite of multiple wash steps, causing cell loss, the fact that HTM output files are typically 10-100 times bigger and less straightforward to analyze, as well as the restricted potential to multiplex protein expression measurements when compared to HTFC (3). This clearly indicates the potential of a 'no touch' antibody staining protocol to efficiently use HTFC to analyze protein expression on adherent cells.

A limited number of studies reports the preparation of adherent cells for HTFC (4-10). The published protocols either involve one or more washing steps or use trypsin/EDTA to generate single cell suspensions (4-7). Washing steps may cause loss of cells, thereby hampering HT screening protocols, whereas trypsin is reported to potentially cause loss of surface antigen expression

(8;9). A recent article by Kaur & Esau (10) describes a two-step protocol to prepare adherent cells for HTFC. They show that the use of EDTA as a cell detachment reagent bypasses the need of washing, enzymatic inactivation, centrifugation, and transfer between plates, reducing cell loss and labor-intensity of the protocol (10). Even though the report shows the 384-well protocol is compatible with several commercially available dyes to measure for instance apoptosis and production of reactive oxygen species, there is no data on the use of antibody staining to detect the dynamics of protein expression within or on the surface of the 384-well microplate seeded cells. The here described universal protocol allows for antibody staining in 384-well format and is validated with six adherent cell lines, including neuroblastoma-, cervical-, hepatocellular-, and breast cancer lines. We demonstrate that there is no difference in staining effectiveness between single and multiplex stained samples, showing the potential of adherent-cell HTFC to increase the informativity of HT screening protocols.

## Material and Methods

### Cell lines and reagents.

MCF-7 (human breast adenocarcinoma; ATCC HTB-22), SKBR3 (human breast adenocarcinoma; ATCC HTB30), HepG2 (human hepatocellular carcinoma; ATCC HB-8065), HeLa (human cervical adenocarcinoma; ATCC CCL-2), and HEK-293T (human embryonic kidney; ATCC CRL-3216) cells were obtained from ATCC (Manassas, VA). The GIMEN neuroblastoma cell line was obtained from the Academic Medical Center of Amsterdam. GIMEN NFkB reporter cells were generated as previously described (11). SKBR3 cells were maintained in RPMI 1640 GlutaMAX supplement medium (Life Technologies, Carlsbad, CA), supplemented with 10% FCS (Sigma-Aldrich, Steinheim, Germany) and 1% penicillin/streptomycin (50 U/mL, Life Technologies). GIMEN, HeLa and HEK-293T were maintained in Dulbecco's Modified Eagle Medium (DMEM) GlutaMAX supplement medium (Life Technologies), supplemented with 10% FCS (Sigma-Aldrich) and 1% penicillin/streptomycin (50 U/mL, Life Technologies).

### Cell plating and compound addition.

Cells were cultured in T75 flasks until 80% confluency, detached with 0.05% Trypsin/EDTA (Life Technologies) and counted using the Countess automated cell counter (Life Technologies). Optimal seeding density was determined. Cells were plated in a culture volume of 15  $\mu$ L in a low flange, polystyrene, tissue culture treated, flat bottom 384-well tissue-culture treated microplate (stock number: 3764, lot: 22017037, Corning, New York) using a multidrop combi reagent dispenser (Life Technologies). Cells were cultured for 16-24h under standard culturing conditions (5% CO<sub>2</sub>, 37°), after which 5  $\mu$ L of compound library would normally have been

added to the cells using a liquid handling system, e.g. the Sciclone G3 liquid handling system (PerkinElmer, Waltham, MA). As a proof of principle for this paper, we added TNF- $\alpha$  and IFN- $\gamma$  as a positive control for upregulation of the markers of interest (11). TNF- $\alpha$  was added at a final concentration of 50 ng/  $\mu$ L (Miltenyi Biotec, Bergisch Gladbach, Germany), IFN- $\gamma$  at a final concentration of 1000 U/mL (R&D, Abingdon, UK). Cells were incubated in presence of compounds for 16-24 hours (5% CO<sub>2</sub>, 37°) after which the effect on the protein(s) of interest was measured with HTFC.

### Sample preparation for HTFC.

EDTA (Life Technologies) was diluted with deionized H<sub>2</sub>O (pH=6.14), after which the optimal EDTA concentration was determined. Addition of 5  $\mu$ L 15 mM EDTA per well resulted in an optimal EDTA concentration of 3 mM per well. EDTA was added to the plate and after shaking at 1000 RPM with an orbital shaker (Heidolph Titramax 1000, Schabwach, Germany) for 30 seconds, incubated at 37° for 45 minutes to allow detachment of the cells. Plates were shaken again at 1000 RPM for 30 seconds, after which 5  $\mu$ L antibody, diluted in serum-free medium, was added in the concentration established with titration. The following monoclonal antibodies have been used: AlexaFluor-647-labeled mouse-anti-human HLA-ABC (W6/32, Biolegend, London, UK), FITC-labeled mouse-anti-human HLA-ABC (W6/32, Sony Biotechnology, Weybridge, UK), APC-labeled mouse-anti-human CD274 (PD-L1) (Clone MIH1, Life Technologies), and PE-labeled mouse-anti-human CD54 (ICAM-1) (MEM-111, Exbio, London, UK). The nucleic acid dye 7-AAD (BD Biosciences, Eysins, Switzerland) was used for exclusion of non-viable cells. Gating was based on unstained samples and verified using conventional flow cytometry. Cell viability has been validated with the mitochondrial membrane potential dye Tetramethylrhodamine (TMRM) at a concentration of 50 nM (Sigma Aldrich). Addition of 50  $\mu$ M Carbonyl cyanide-4-(trifluoromethoxy)phenylhydrazone (FCCP), a mitochondrial oxidative phosphorylation uncoupler (Sigma Aldrich) was used as a negative control for TMRM staining. Cells were incubated for 20 minutes on an orbital shaker at 4° to allow for antibody staining (300 RPM). Subsequently, 50  $\mu$ L of PBS supplemented with 2% FCS and 2  $\mu$ M EDTA was added per well using the multidrop combi reagent dispenser to dilute the samples. Plates are kept on ice until analysis.

### Flow Cytometry and analysis.

Cells were acquired on the FACSCanto II HT sampler (BD Biosciences), by measuring a fixed volume of 50  $\mu$ L sample per well at a flow rate of 3  $\mu$ L/second. Analysis of a full 384-well plate will take about 100 minutes. Fluorescent labelled beads (CS&T beads, Becton Dickinson) were used to check the performance and verify optical path and stream flow of the flow cytometer. This procedure enables controlled standardized results and allows the determination of long-term

drifts and incidental changes within the flow cytometer. No changes were observed which could affect the results. Shown data is a representation of at least six independent experiments. The Stain Index (SI) was used to reflect the ratio of separation between the positive and the negative population divided by two times the standard deviation (SD) of the negative population (12). Data was analyzed using FACS Diva Version 8.0.1 (BD Bioscience), FlowJo version 10.1, and Graphpad Prism version 7.

### Statistical analysis.

The non-parametric Mann-Whitney U-test was performed for statistical testing between single cell counts before and after optimization. P-values <0.05 are considered significant. A Z-score was calculated to define the difference in fluorescent intensity between medium-treated and cytokine-treated samples (n=8 per group) using the following equation:

$$Z = \frac{X - \mu}{\sigma}$$

In which X is the mean Mean Fluorescent Intensity (MFI) of the cytokine treated group,  $\mu$  is the mean MFI of the medium control group, and  $\sigma$  is the standard deviation of the medium control group. All data shown  $\pm$  SD.

## Results

### Optimization of cell seeding density, EDTA concentration, and cell density during analysis results in a 12-fold increase in single cell retrieval.

The first goal in the development of this HTFC protocol was to find a strategy to optimise reproducible cell retrieval, using the adherent GIMEN neuroblastoma cell line. Initially, we adapted the cell detachment protocol of Kaur & Esau to a 384-well format (10), but were unable to achieve sufficient and reproducible cell retrieval (**Figure 1A, before optimisation**).

First, cell seeding density was evaluated by seeding increasing numbers of cells per well. As expected, cell retrieval markedly improved when more cells were plated (**Figure 1B**). However, reproducibility of cell retrieval decreased when seeding density exceeded 5000 cells/well, as observed by an increase in SD. Based on these data, it was concluded that a cell seeding density of 4500 cells/well was optimal. Second, microscopic evaluation of the cell suspensions after different lengths of incubation periods with increasing EDTA concentrations revealed a minimum incubation time of 45 minutes and a minimum EDTA concentration of 3 mM (data not shown). Further increase of the EDTA concentration to 3.2 and 3.4 mM did not result in further improvement of cell retrieval (**Figure 1C**). Finally, we assessed the effect of sample dilution prior

to flow cytometric analysis. Dilution of the samples with 50  $\mu$ L PBS supplemented with 2% FCS + 2  $\mu$ M EDTA resulted in a 3.8-fold increase in cell retrieval (**Figure 1D**). Optimal cell seeding density, EDTA cell detachment concentration and incubation times, and final cell suspension density of the flow cytometry sample per well resulted in an over 12-fold increase in single cell retrieval (**Figure 1A**). More than 90% of the non-debris cell population were single cells and flow rate was constant. 7-AAD and TMRM staining confirmed the cells were alive (**Supplement 1**).

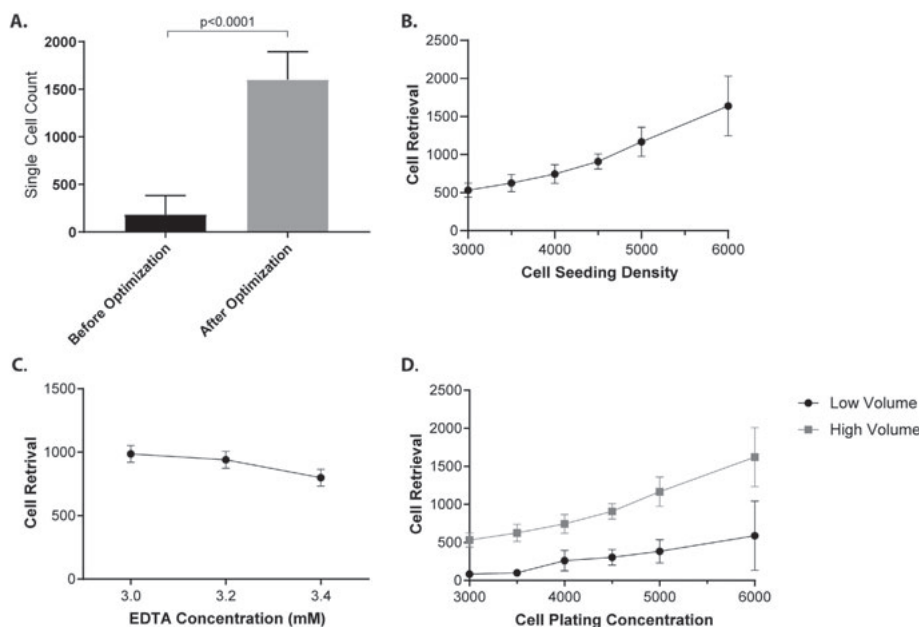


**Figure 1** – Optimization of flow cytometric cell retrieval using GIMEN cells. An over 12-fold increase in single cell retrieval is observed upon sample preparation optimization. **(A)** Bar graph representing average single cell retrieval prior to and after optimization. Before optimization:  $n=60$ , after optimization:  $n=7153$ . **(B)** Graphical display of flow cytometric cell retrieval when increasing cell seeding density. **(C)** Graphical display of cell retrieval after incubation with increasing EDTA concentrations at a seeding density of 4500 cells/well,  $n=2$  per group. **(D)** Cell retrieval when well volume is 30  $\mu$ L (low volume) or 80  $\mu$ L (high volume). Graphs: Dots reflect mean, error bars reflect SD between samples,  $n=6$  per group unless otherwise indicated. Mann-Whitney U-test was performed,  $p<0.05$  was considered significant. SD = standard deviation.

The reproducibility of the cell numbers retrieved with the protocol can be concluded from a HTFC compound screen we have performed utilizing this protocol, in which over 10,000 wells were analyzed with an average retrieval of 1600 ( $\pm$  SD 294) alive single cells/well. This corresponds to 74% alive single cell retrieval when corrected for sampled volume.

### **Optimised antibody staining allows for (multiplexed) staining with minimal non-specific background signal.**

Elimination of all washing steps from the HTFC protocol contributes to the HT nature of the protocol by decreasing the labor intensity, while minimizing cell loss inherent to washing. On the other hand, elimination of these steps also clearly indicates the need for antibody concentration titration. TNF- $\alpha$  and IFN- $\gamma$  are involved in upregulation of cell surface protein expression of MHC-I (11), CD54 (ICAM-1) (13;14), and CD274 (PD-L1) (15) in several tumor cell types. Effects of these cytokines on protein expression have been validated for all utilized cell lines using conventional flow cytometry (shown for GIMEN; **Figure 2A** and **Supplement 2**).

Decreasing the antibody concentration caused a clear decrease in background staining in medium-treated HLA-ABC stained MHC-I lacking GIMEN cells (**Figure 2B**). However, a marked decrease in the stain index between untreated and TNF- $\alpha$  + IFN- $\gamma$  treated samples was observed when decreasing the antibody concentration (**Figure 2C**). This indicates a delicate balance between non-specific background staining and discriminative ability of the antibody staining. Titration showed that HLA-ABC antibody concentration was optimal at a concentration of 8 ng/well (final concentration of 0.27 ng/ $\mu$ L). The HTFC staining protocol allows for distinct discrimination between HLA-ABC expression in untreated versus TNF- $\alpha$ -treated ( $Z=49$ ), and versus TNF- $\alpha$  + IFN- $\gamma$  treated cells ( $Z=94$ ) ( $n=8$  per group), comparable with results from a typical conventional staining protocol (**Figure 2A**). The same effect is observed for the other utilized antibodies (**Supplement 2**).

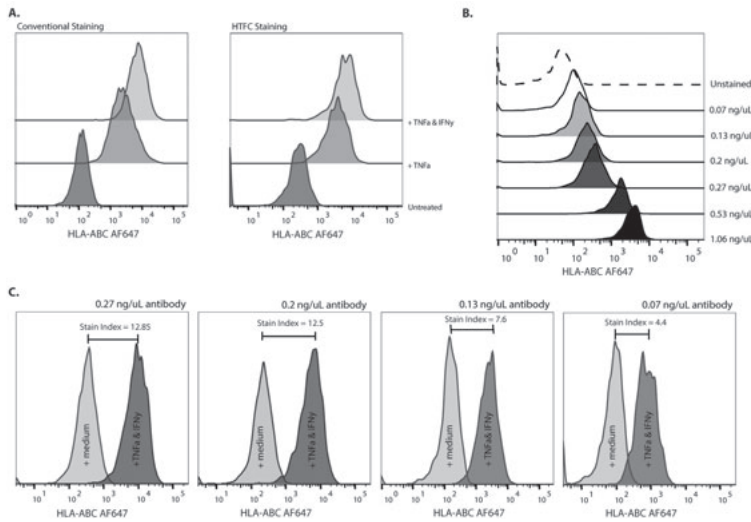


**Figure 2** – Antibody staining optimization in GIMEN cells. **(A)** The optimized HTFC staining protocol (right) shows similar expression patterns to a typical conventional staining protocol (left). Z-score of expression in untreated versus TNF- $\alpha$  treated cells is 49 ( $X = 1911$ ,  $\mu = 217$ ,  $\sigma = 35$ ), and 94 ( $X = 3466$ ,  $\mu = 217$ ,  $\sigma = 35$ ) in TNF- $\alpha$  + IFN- $\gamma$  treated cells ( $n=8$  per group). **(B)** HLA-ABC background staining decreases when antibody concentration (ng/mL) decreases. The dashed line represents the unstained control. **(C)** Histograms depicting HLA-ABC MFIs of untreated and TNF- $\alpha$  + IFN- $\gamma$  treated samples with diluting antibody concentrations. The stain index decreases when antibody concentration is reduced. Data shown are from a representative experiment using the HTFC protocol on GIMEN neuroblastoma cells. MFI = Mean Fluorescent Intensity.

A unique aspect of flow cytometry is the opportunity to multiplex expression analysis of proteins on/in the same cell. Combining this aspect with HTS allows for an opportunity to increase the possibilities and informativity of HTS analysis. Combining antibody staining of HLA-ABC with the nucleic acid dye 7-AAD, and antibody staining against PD-L1 and ICAM-1 revealed no noticeable differences in individual staining efficacy of the HTFC protocol, as shown for HLA-ABC antibody staining (**Figure 3A**).

We previously generated a GIMEN NF $\kappa$ B reporter cell line and found that TNF- $\alpha$  upregulates MHC-I expression in an NF $\kappa$ B dependent manner, whereas IFN- $\gamma$ -induced MHC-I upregulation is independent of NF $\kappa$ B (11). Utilizing our HTFC protocol combining HLA-ABC antibody staining with evaluation of the intrinsic NF $\kappa$ B reporter expression confirmed NF $\kappa$ B (in)dependency of the observed MHC-I upregulations (**Figure 3B**). This shows that the protocol is also suitable to study the effects of compounds on intracellular transcription factors using reporter cell lines.

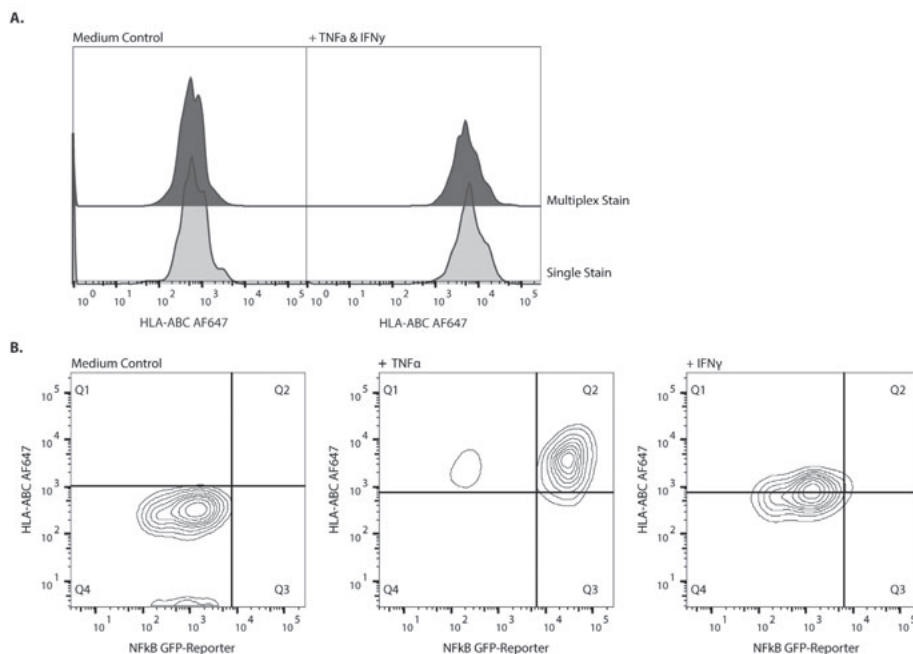


**Figure 3** – Multiplexed antibody staining in GIMEN cells. Multiplexing antibody staining using the HTFC protocol is technically feasible and as effective as singular staining. **(A)** HLA-ABC MFI in untreated controls (left) and TNF- $\alpha$  + IFN- $\gamma$  treated cells (right). Top graphs show the MFI in multiplex stained samples, lower graphs show MFIs in single stained samples. **(B)** Nf $\kappa$ B-GFP-reporter x HLA-ABC. Treatment of GIMEN Nf $\kappa$ B GFP reporter cells with TNF- $\alpha$  or IFN- $\gamma$  shows dependence of TNF- $\alpha$  induced upregulation of MHC-I, and independence of IFN- $\gamma$  induced upregulation. Left graph: untreated control, middle graph: TNF- $\alpha$  treated cells, right graph: IFN- $\gamma$  treated cells. Data shown are from a representative experiment using the HTFC protocol on GIMEN neuroblastoma cells. MFI = Mean Fluorescent Intensity

### The staining protocol is translatable to multiple cell lines without any modifications

The optimized HTFC protocol was subsequently performed using five additional cell lines, including breast cancer-, cervical cancer-, hepatocellular cancer, and human embryonal kidney cells. Retrieved single cell counts were lower (HepG2), comparable (MCF-7, SKBR3) or superior (HeLa, HEK293T) to the counts obtained in GIMEN neuroblastoma cells (**Supplement 3**). Individual and multiplex HTFC staining was performed and validated with conventional flow cytometry staining (data not shown). The HepG2 and MCF-7 cell lines were selected based on their trypsinization resistant nature. The MCF-7 line shows sufficiently high and reproducible cell retrieval, even though we do observe more doublets, which were excluded from analysis (**Supplement 3A**). In contrast, the slower growing, clumping HepG2 cells showed decreased cell counts, with an average single cell retrieval of 814 ( $n=44$ , 2 individual experiments), but the counts were still sufficiently high and reproducible for reliable results (**Supplement 3E**). This indicates the potential to translate the HTFC protocol universally to other adherent cell lines of interest, contributing to the versatility of the protocol.

## Discussion & Conclusion

HT cell-based screening of drug libraries is currently still limited by labor-intensive, time-consuming, expensive, and throughput limiting analyzing methods. The new era of biologicals used in anti-cancer therapy, including (immune) cell modulating biologicals, asks for novel, more delicate HT analysing protocols to screen for effects beyond cell death. Cell surface expression of proteins is often key in treatment response to (immuno)therapies in cancer (11;16-21). Screening for compounds affecting expression of these proteins may contribute to therapy efficacy in the future. For example, neuroblastoma immunotherapy efficacy is hampered by low MHC-I expression and requires upregulation (11), for which potential compounds can be selected by a compound screen. Similarly, novel compounds may affect immune checkpoint regulator expression as expression is correlated with poor survival in multiple cancers (16-21). Here we report the development of a universal 'no touch' HTFC antibody staining protocol in 384-well microplate format for adherent cells in which we are able to bypass washing and centrifuging steps of conventional flow cytometry protocols.

We have adapted a protocol from Kaur & Esau, in which the potential of EDTA as a non-enzymatic cell detachment agent in 'no touch' HTFC was demonstrated (10). Using EDTA instead of enzymatic detachment agents bypasses the need of indispensable wash steps to wash away the fetal calf serum and to neutralise the enzymatic activity to decrease cell toxicity and potential antigen loss (4-9). Bypassing washing steps not only contributes to the HT format of the protocol, it also contributes to the cell retrieval by preventing cell loss, which is especially a problem when working with small cell numbers. Even though Kaur & Esau show their 384-well protocol is compatible with several commercially available dyes, they have not optimized the 384-well format protocol in combination with (multiplexed) antibody staining (10). Furthermore, they show a clear need for cell line specific optimization of their protocol, limiting the throughput potential of the protocol.

Based on our data, decreasing the cell density prior to flow cytometric analysis markedly increased cell retrieval (3.8-fold). This indicates that cell density during analysis is a crucial factor in this protocol: when cell density is too high, the EDTA cannot avoid the tendency of cells to clump, thereby affecting (reproducibility of) cell retrieval. This also explains the reduction in reproducibility of the protocol when exceeding a seeding density of 5000 cells/well. The fact that cell density rather than other cellular parameters is so critical in this protocol also emphasizes the universal potential of this protocol.

Analysis of the very slow growing and clumping HepG2 cell line with our protocol showed decreased cell retrieval when compared to the other cell lines. We believe this can be explained by the extreme adherent nature of the cells, as well as by the slow growth rate. This was further confirmed by an ~1.5-fold increase in average cell retrieval (average single cell count = 1115 ( $\pm$  SD = 236) (n=9)), without a marked increase in variability between wells when increasing the plating density to 5000 cells/well. Even though the unmodified protocol still gave sufficient cell retrieval, these results indicate that the protocol might benefit from cell plating density titration when analyzing slow-growing cell lines. However, the extreme clumping nature of the HepG2 line makes its suitability questionable for flow cytometry analysis in general, and alternative hepatocyte cell lines may be preferred.

It has been reported that EDTA could have a significant impact on antibody binding capacity (22), especially when the structure of the epitope depends on ions, such as calcium. It is therefore of importance to compare conventional and high throughput protocol staining for every newly utilized antibody. Furthermore, more general, we recommend to include appropriate controls for every utilized antibody on every HTS plate to be able to monitor basal protein expression and antibody staining efficiency.

To our knowledge, we are the first to report a universal 'no touch' HTFC antibody staining protocol for adherent cell lines in 384-well microplate format. We show that our protocol allows for multiplexing antibody staining and addition of reporter gene analysis, thereby improving the output of cell-based screening of drug libraries in a cost-efficient manner.

## **Author Contributions**

CS, SN, and AC designed the study, and AC wrote the manuscript. CS and AC performed the experiments and AC analyzed the data with critical comments from CS, JvV, NvT, SN, and JJB. All authors read and approved the manuscript.

## **Acknowledgement**

This work was supported by the Villa Joep Foundation.

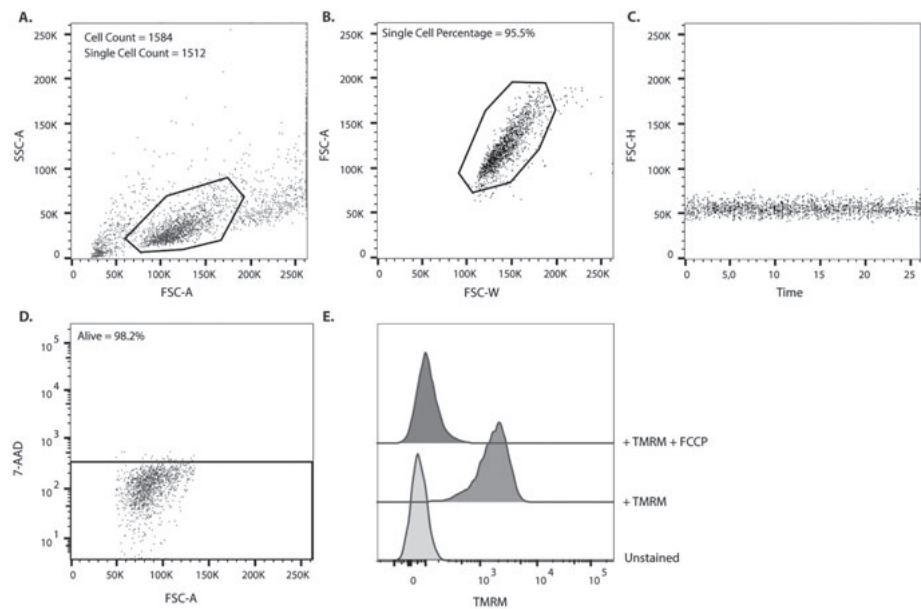
## References

1. An WF, Tolliday N. Cell-Based Assays for High-Throughput Screening. *Molecular Biology* 2010;45;180-186. DOI: 10.1007/s12033-010-9251-z
2. Picot J, Guerin CL, Kim CLV, Boulanger CM. Flow Cytometry: retrospective, fundamentals and recent instrumentation. *Cytotechnology* 2012;64(2);109-130. DOI: 10.1007/s10616-011-9415-0
3. Black CB, Duensing TD, Trinkle LS, Dunlay RT. Cell-Based Screening Using High-Throughput Flow Cytometry. *Technology Reviews* 2011;9(1);13-20. DOI: 10.1089/adt.2010.0308
4. Haynes MK, Strouse JJ, Waller A, Leitao A, Curpan RF, Bologa C, Oprea TI, Prossnitz ER, Edwards BS, Sklar LA *et al.* Detection of Intracellular Granularity Induction in Prostate Cancer Cell Lines by Small Molecules Using the HyperCyt® High- Throughput Flow Cytometry System. *Journal of Biomedical Screening* 2009;14;596-609. DOI: 10.1177/1087057109335671
5. Young SM, Bologa CM, Fara D, Bryant BK, Strouse JJ, Arterburn JB, Ye RD, Oprea TI, Prossnitz ER, Sklar LA *et al.* Duplex High Throughput Flow Cytometry Screen Identifies Two Novel Formylpeptide Receptor Family Probes. *Cytometry A*;75;253-263. DOI: 10.1002/cyto.a.20645
6. Glazer ES, Massey KL, Curley SA. A protocol to effectively create single cell suspensions of adherent cells for multiparameter high-throughput flow cytometry. *In vitro cellular & developmental Biology* 2010;46(2);97-101 DOI: 10.1007/s11626-009-9256-8
7. Martinez EM, Klebanoff SD, Secrest S, Romain G, Haile ST, Emtage PCR, Gilbert AE. High-Throughput Flow Cytometric Method for the Simultaneous Measurement of CAR-T Cell Characterization and Cytotoxicity against Solid Tumor Cell Lines. *SLAS Discovery* 2018;23(7);603-612. DOI: 10.1177/2472555218768745
8. Tsuji K, Ojima M, Otabe K, Horie M, Koga H, Sekiya I, Menuta T. Effects of Different Cell-Detaching Methods on the Viability and Cell Surface Antigen Expression of Synovial Mesenchymal Stem Cells. *Cell Transplant* 2017;26(6);1089-1102. DOI: 10.3727/096368917X694831
9. Huang HL, Hsing HW, Lai TC, Chen YW, Lee TR, Chan HT, Lyu PC, Wu CL, Lu YC, Lin ST *et al.* Trypsin-induced proteome alteration during cell subculture in mammalian cells. *Journal of Biomedical Sciences* 2010;17(1);36. DOI: 10.1186/1423-0127-17-36
10. Kaur M, Esau L. Two-step protocol for preparing adherent cells for high-throughput flow cytometry. *Biotechniques* 2015;59;119-126. DOI: 10.2144/000114325

11. Spel L, Nieuwenhuis J, Haarsma R, Stickel E, Bleijerveld OB, Altelaar M, Boelens JJ, Brummelkamp TR, Nierkens S, Boes M. Nedd4 Binding Protein 1 (N4BP1) and TNFAIP3 Interacting Protein 1 (TNIP1) control MHC-1 display in neuroblastoma. *Cancer Research* 2018; epub ahead of print. DOI: 10.1158/0008-5472.CAN-18-0545
12. Maecker HT, Frey T, Nomura LE, Trotter J. Selecting fluorochrome conjugates for maximum sensitivity. *Cytometry A* 2004;62(2);169-173. DOI: 10.1002/cyto.a.20092
13. Chang YJ, Holtzman MJ, Chen CC. Interferon- $\gamma$ -induced Epithelial ICAM-1 Expression and Monocyte Adhesion. *The Journal of Biological Chemistry* 2002;277(9);7118-7126. DOI: 10.1074/jbc.M109924200
14. Ren G, Zhao X, Zhang L, Zhang J, L'Huillier A, Ling W, Roberts AI, Le AD, Shi S, Shao C *et al.* Inflammatory Cytokine-Induced Intercellular Adhesion Molecule-1 and Vascular Cell Adhesion Molecule-1 in Mesenchymal Stem Cells Are Critical for Immunosuppression. *The Journal of Immunology* 2010;184;2321-2328. DOI: 10.4049/jimmunol.0902023
15. Dondero A, Pastorino F, Della Chiesa M, Corrias MV, Morandi F, Pistoia V, Olive D, Bellora F, Locatelli F, Castellano A *et al.* PD-L1 expression in metastatic neuroblastoma as an additional mechanism for limiting immune surveillance. *Oncoimmunology* 2016;5(1);e1064578. DOI: 10.1080/2162402X.2015.1064578
16. Hino R, Kabashima K, Kato Y, Yagi H, Nakamura M, Honjo T, Okazaki T *et al.* Tumor cell expression of programmed cell death-1 ligand 1 is a prognostic factor for malignant melanoma. *Cancer* 2010;116(7);1757-1766. DOI: 10.1002/cncr.24899
17. Taube JM, Klein A, Brahmer JR, Xu H, Pan X, Kim JH, Chen L. Association of PD-1, PD-1 ligands, and other features of the tumor immune microenvironment with response to anti-PD-1 therapy. *Clinical Cancer Research* 2014;20(19);5064-5074. DOI: 10.1158/1078-0432.CCR-13-3271
18. Pistillo MP, Tazzari PL, Palmisano GL, Pierri I, Bolognesi A, Ferlito F, Capanni P *et al.* CTLA-4 is not restricted to the lymphoid cell lineage and can function as a target molecule for apoptosis induction of leukemic cells. *Blood* 2003;101(1);202-209 DOI: 10.1182/blood-2002-06-1668
19. Paulsen EE, Thomas KK, Rakaee M, Richardsen E, Hald SM, Andersen, S, Busund LT *et al.* CTLA-4 expression in the non-small cell lung cancer patient tumor microenvironment: diverging prognostic impact in primary tumors and lymph node metastases. *Cancer Immunology & Immunotherapy* 2017;66(11);1449-1461. DOI: 10.1007/s00262-017-2039-2
20. Zaretsky JM, Garcia-Diaz A, Shin DS, Escuin-Ordinas H, Hugo W, Hu-Lieskovan S, Torrejon DY *et al.* Mutations Associated with Acquired Resistance to PD-1 Blockade in Melanoma. *New England Journal of Medicine* 2016;375(9);819-829. DOI: 10.1056/NEJMoa1604958

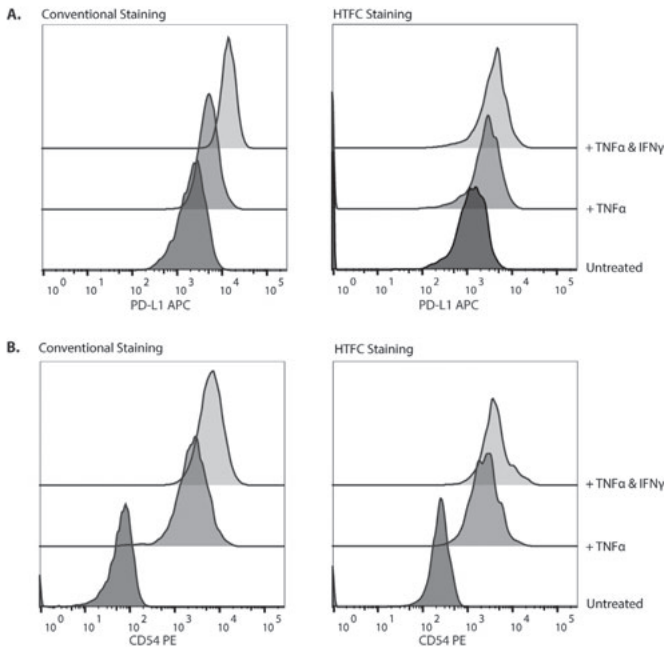
21. Pfirschke C, Engblom C, Rickelt S, Cortez-Retamozo V, Garriss C, Pucci F, Yamazaki T *et al.* Immunogenic chemotherapy sensitizes tumors to checkpoint blockade therapy. *Immunity* 2016;44(2);343-354. DOI: 10.1016/j.immuni.2015.11.024
22. Giroux M & Denis F. Influence of Calcium Ions in the Flow Cytometric Analysis of Human CD8-Positive Cells. *Cytometry A* 2004;62;61-64. DOI: 10.1002/cyto.a.20084
23. Pfirschke C, Engblom C, Rickelt S, Cortez-Retamozo V, Garriss C, Pucci F, Yamazaki T *et al.* Immunogenic chemotherapy sensitizes tumors to checkpoint blockade therapy. *Immunity* 2016;44(2);343-354. DOI: 10.1016/j.immuni.2015.11.024

# Supplementary Figures



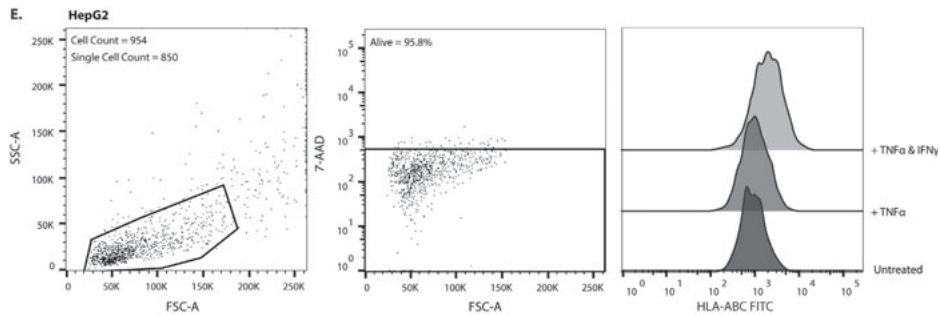
**Supplement 1** – Flow cytometric characteristics of GIMEN cells after protocol optimization.

**(A)** FSC/SSC after optimization, gate reflects the non-debris population ((total cell retrieval = 1584, single cell retrieval = 1512); **(B)** FSC-W/FSC-A graph of the non-debris population. Gate contains the single cell population (95.5% of non-debris population is single cell). **(C)** FSC-H/time were plotted against each other to detect potential drifts. Flow rate is constant. **(D)** 7-AAD staining of single cell population. The gate contains the alive cell population (98.2% of the single cells are alive). **(E)** TMRM staining of single cell population. TMRM staining intensity in unstained cells (bottom), TMRM-stained cells (middle), and TMRM stained cells to which the mitochondrial oxidative phosphorylation uncoupler FCCP is added (top). Data shown are from a typical experiment using the HTFC protocol on GIMEN neuroblastoma cells and is representative of at least six independent experiments.



**Supplement 2** – PD-L1 and CD54 staining using the conventional and HTFC protocol show similar results.

The optimized HTFC staining protocol shows similar PD-L1 (**A**) and CD54 (**B**) expression patterns (right) to a typical conventional staining protocol (left). Z-score of PD-L1 expression in untreated versus TNF- $\alpha$  treated cells is 14 ( $X = 3453$ ,  $\mu = 978$ ,  $\sigma = 175$ ), and 23 ( $X = 5081$ ,  $\mu = 978$ ,  $\sigma = 175$ ) in TNF- $\alpha$  + IFN- $\gamma$  treated cells ( $n=3$  per group). Z-score of CD54 expression between untreated versus TNF- $\alpha$  treated cells is 151 ( $X = 2511$ ,  $\mu = 205$ ,  $\sigma = 15$ ), and 236 ( $X = 3817$ ,  $\mu = 205$ ,  $\sigma = 15$ ) between TNF- $\alpha$  + IFN- $\gamma$  treated cells ( $n=3$  per group). Data shown are from a representative experiment using the HTFC protocol on GIMEN neuroblastoma cells.



**Supplement 3** – Cell retrieval & HLA-ABC antibody staining of additional analyzed cell lines analyzed with the unmodified HTFC staining protocol.

Left: FSC/SSC of MCF-7 (**A**), SKBR3 (**B**), HEK-293T (**C**), HeLa (**D**), and HepG2 (**E**) cell lines, gate reflects the non-debris population. Single cell retrieval is based on exclusion via FSC-W/FSC-A characteristics (data not shown). Cells outside the non-debris gate are confirmed to be doublets. Middle: Viability of MCF-7 (**A**), SKBR3 (**B**), HEK-293T (**C**), and HeLa (**D**), and HepG2 (**E**) cell lines. Gating is based on unstained controls of the respective cell lines. Right: HLA-ABC staining intensity in untreated controls (bottom), TNF- $\alpha$  (middle) or TNF- $\alpha$  + IFN- $\gamma$  (top) treated MCF-7 (**A**), SKBR3 (**B**), HEK-293T (**C**), HeLa (**D**), and HepG2 (**E**) cell lines. Data shown are from a representative experiment using the HTFC protocol on the respective cell line.





# Part 2

**Immune monitoring in pediatric patients receiving allogeneic HCT**

---



# Chapter 6

# **Adequate CD4+ T-cell reconstitution enhances survival probability after acute Graft-versus-Host-Disease**

---

Coco C.H. de Koning<sup>1</sup>, Celina L. Szanto<sup>1</sup>, Jurgen B. Langenhorst<sup>1</sup>, Caroline A. Lindemans<sup>2</sup>, Stefan Nierkens<sup>1,2†</sup>, Jaap Jan Boelens<sup>2,3†</sup>

<sup>1</sup> Center for Translational Immunology, University Medical Center Utrecht, Utrecht University, Utrecht, The Netherlands

<sup>2</sup> Princess Máxima Center for Pediatric Oncology, Utrecht University, Utrecht, The Netherlands

<sup>3</sup> Stem Cell Transplantation and Cellular Therapies Program, Department of Pediatrics, Memorial Sloan Kettering Cancer Center, New York, United States

† These authors contributed equally to this work.

*Manuscript in preparation*

## Abstract

### Background

Acute Graft-versus-Host-Disease (aGvHD) is a major cause of morbidity and mortality after allogeneic hematopoietic (stem) cell transplantation (HCT). Studies evaluating the relation between immune reconstitution (IR) and aGvHD are largely lacking. We previously showed that successful CD4+ IR strongly predicts event-free survival chances. Therefore, we studied how CD4+ IR post-HCT influences survival chances in patients suffering from aGvHD.

### Methods

Pediatric patients receiving their first allogeneic HCT between 2004 and 2018 were included. Blood samples and outcome data were collected and registered prospectively. The main outcomes of interest were 5-year overall survival (OS) and 5-year non-relapse mortality (NRM), stratified for aGvHD (grade II-IV) and for the presence or absence of adequate CD4+ IR (twice  $>50 \times 10^6$  CD4+CD3+ cells/L) prior to aGvHD onset. For this, we applied a time-to-event multivariate Log-rank test with HCT-source; cord blood transplantation, and bone marrow or peripheral blood transplantation, as covariates.

### Results

276 pediatric patients with a median age of 7.06 years (range 0.16-22.74), were included; 73 (26.4%) had moderate-severe aGvHD (grade II-IV) and 29 (10.5%) had severe aGvHD (grade III-IV). Adequate early CD4+ IR before diagnosis of aGvHD grade II-IV was associated with higher 5-year OS probability (77% versus 48%,  $p < 0.001$ ) and lower 5-year NRM (34% versus 18%,  $p = 0.006$ ), which was comparable to patients without aGvHD (76% OS;  $p = 0.6$ , 18% NRM;  $p = 0.635$ ). For grade III-IV aGvHD differences were even more striking with only 24% 5-year OS and 74% NRM in patients having no CD4+ IR compared to patients having CD4+ IR prior to diagnosis (78% OS;  $p < 0.001$ , 12% NRM;  $p = 0.006$ ), the latter of which had comparable survival chances as patients without aGvHD (76% OS;  $p = 0.56$ , 18% NRM;  $p = 0.506$ ).

### Interpretation

Adequate CD4+ IR prior to aGvHD onset protects against increased mortality risk after aGvHD in HCT. These findings provide insight in the importance of adequate IR in HCT patients in surviving severe aGvHD. Patients with inadequate CD4+ T-cells prior to aGvHD onset might have insufficient development of regulatory processes and are more at risk for viral infections. As such, these patients may benefit from personalized (anti-viral / immune suppressive) treatment to improve survival chances.

## Introduction

Acute Graft-versus-Host-Disease (aGVHD) is a life-threatening complication causing high mortality after allogeneic hematopoietic (stem) cell transplantation (HCT). To limit the risk for aGVHD, standard HCT protocols may contain serotherapy for *in vivo* T-cell depletion (e.g. ATG).<sup>1-5</sup> In addition, prophylactic immunosuppressive therapies (e.g. cyclosporine A, prednisolone, methotrexate) are often given after HCT to further limit aGVHD risk.<sup>5</sup> Alternative strategies are *ex-vivo* T cell depletion strategies, such as CD34+ selection and the more recent alpha-beta TCR depletion. However, aGVHD is still common and affects 40-60% of patients receiving an allogeneic HCT,<sup>6</sup> causing high mortality risk when aGVHD treatment strategies fail. Currently, aGVHD still accounts for 10-20% of deaths after allogeneic HCT.<sup>7</sup> Major hurdles in limiting aGVHD risk and improving survival after aGVHD are; the fact that factors that increase aGVHD risk are only partly known, and the current inability to identify patients who are more likely to die from aGVHD once it occurs. This highlights the need for identification of factors that can predict severity of aGVHD, treatment response and -related mortality. This may help guiding aGVHD treatment and prophylaxis in these patients.

The immune system has a major role in the pathobiology of aGVHD following allogeneic HCT. A balanced immune reconstitution (IR), especially of T-cells; consisting of both effector T-cells and regulatory CD4+ T-cells (Tregs), is thought to limit aGVHD development or severity. Early recovery of Tregs has been related to a reduced aGVHD risk and better prognosis.<sup>8,9</sup> Furthermore, we previously identified that CD4+ T-cell reconstitution (CD4+ IR) overcomes virus-induced aGVHD after HCT, a risk factor for aGVHD development.<sup>10</sup> However, studies evaluating the relation between CD4+ IR, aGVHD, and subsequent survival, are lacking. In this report, we evaluated the effect of adequate CD4+ IR prior to aGVHD on survival probability after aGVHD.

## Materials and Methods

### Patients and blood samples

Pediatric patients receiving their first allogeneic HCT between 2004 and 2018 within the pediatric transplantation program at the Wilhemina Children's Hospital at the UMC Utrecht (2004-2017) and/or Princess Máxima Center for Pediatric Oncology (from 2018), in Utrecht, The Netherlands, who had CD4+ T-cell data available, were included in this study. Immune monitoring data and clinical outcome data were collected and registered prospectively. Patients were enrolled and data were collected only after written informed consent in accordance with the Helsinki Declaration. The study was approved by the local ethical committee (trial numbers 05-143 and 11-063k).

## Procedures

Patients were treated in high-efficiency, particle-free, air-filtered, positive-pressure isolation rooms. Conditioning regimens were applied according to (inter-)national protocols. Patients received gut decontamination and infection prophylaxis. GvHD-prophylaxis consisted of cyclosporin A (CsA; targeted at trough levels of 200-250 µg/L for all patients), combined with either prednisolone 1 mg/kg (cord blood) or methotrexate 10 mg/m<sup>2</sup> (on day +1, +3, and +6; unrelated donor). CsA was continued for at least 3 months after HCT. Prednisolone was tapered after 28 days.

## Immune-monitoring

Absolute numbers of CD4+ T-cells (CD3+CD4+CD8-) were measured by using TruCOUNT tubes (BD Biosciences, Erembodegem, Belgium) / Sapphire (Abbott), in EDTA-treated whole blood only after reaching a leukocyte count of at least  $0.4 \times 10^9$  cells/L, as standard immune monitoring after HCT. Blood CD4+ T-cell reconstitution was measured at least every other week up to twelve weeks post-HCT and monthly thereafter up to six months, followed by every 3 months until 1 year, and twice in the 2<sup>n</sup> year after HCT. GvHD was classified according to the Glucksberg and Shulman criteria.<sup>11,12</sup>

## Outcomes

Our outcomes of interest were 5-year overall survival (OS) and non-relapse mortality (NRM) probabilities, stratified for aGvHD (grade II-IV) and for the presence or absence of adequate CD4+ IR (twice  $>50 \times 10^6$  CD4+CD3+ cells/L) prior to aGvHD onset. 5-year OS was defined as time from transplantation to death or last follow-up at 5 years. 5-year NRM was defined as death due to a cause other than relapse of malignancy within 5 years of follow-up.

## Statistical analysis

Duration of the follow-up was defined as the time from HCT to death or the last assessment for surviving patients. For the clinical endpoints OS and NRM, CD4+ IR ((twice  $>50 \times 10^6$  CD4+CD3+ cells/L) was evaluated as predictor, and considered as time-varying variable. This threshold for CD4+ IR was chosen in line with previous findings.<sup>13-16</sup> The probability of OS was calculated using the Kaplan-Meier estimate; the two-sided log-rank test was used for univariate comparisons. For the endpoint NRM, Fine-Gray competing risk regressions were applied in cumulative incidence curves to calculate NRM probability. Statistical analyses were performed using R version 3.3.<sup>17</sup>

## Results

### Patients

276 Patients with a median age of 7.06 years (range 0.16-22.74) receiving their first allogeneic HCT within the pediatric transplantation program met the inclusion criteria. Detailed patient characteristics are depicted in Table 1. Of the patients, 73 (26.4%) had moderate-severe aGvHD (grade II-IV) and 29 (10.5%) had severe aGvHD (grade III-IV). After aGvHD (grade II-IV), 19 patients later developed chronic GvHD.

**Table 1:** Patient characteristics

	All patients
Number of patients (n)	276
Age at transplant (median; range)	7.06 (0.16-22.74)
Male/Female (n/n)	159/117
<b>Stem cell source (n)</b>	
Bone Marrow	100
Cord Blood	172
Peripheral blood stem cells	4
<b>Diagnosis (n)</b>	
Malignancy	139
Metabolic inborn error	53
Primary immune deficiency	52
Bone marrow failure	29
Autoimmune disease	3
<b>Acute GvHD incidence (n)</b>	
Grade I	51
Grade II	44
Grade III	19
Grade IV	10
Chronic GvHD incidence (n)	31
Serotherapy in conditioning (n)	198
Median time to grade II-IV aGvHD (days; range)	35 (6-514)
Follow-up (days; range)	1293 (14-5017)

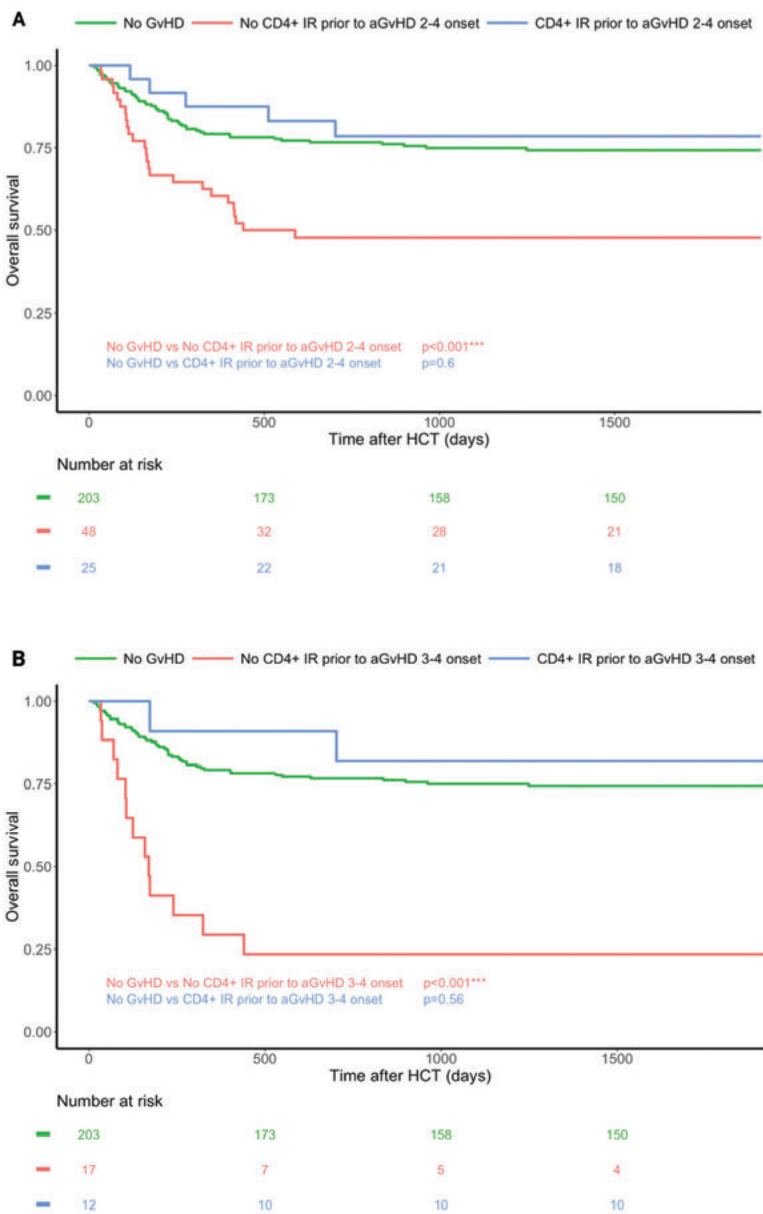


**Figure 1: 5-Year Overall Survival after moderate-severe aGvHD stratified for having adequate CD4+ IR prior to diagnosis.** Kaplan-Meier curves showing; (A) 5-Year OS was higher in patients having CD4+ IR (defined as  $\geq 50 \times 10^6$  CD4+ T-cells/L in 2 consecutive measurements after HCT) (blue, n=25) compared to patients having no CD4+ IR prior to aGvHD grade II-IV diagnosis (red, n=48,  $P<0.001$ ), and comparable to patients having no aGvHD (red, n=203,  $P=0.6$ ). (B) Patients having no CD4+ IR prior to aGvHD grade III-IV (red, n=17) had even more drastically lower 5-Year OS compared to no patient with prior CD4+ IR (blue, n=12,  $P<0.001$ ), the latter had comparable OS to patients having no aGvHD (green, n=203,  $P=0.56$ ). A multivariate 2-sided log-rank test was applied to calculate P-values.

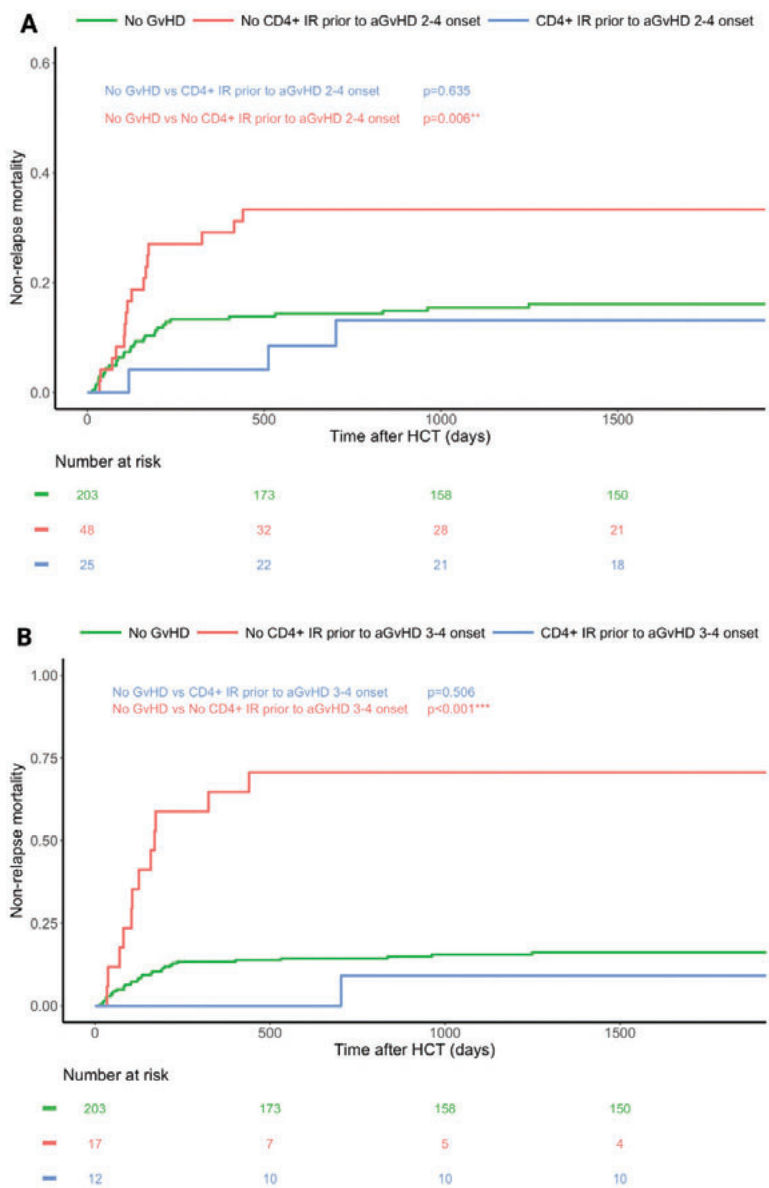


**Figure 2: 5-Year Non-Relapse Mortality after moderate-severe aGvHD stratified for having adequate CD4+ IR prior to diagnosis.** Cumulative incidence curves showing: (A) 5-Year NRM was higher in patients having CD4+ IR (defined as  $350 \times 10^6$  CD4+ T-cells/L in 2 consecutive measurements after HCT) (blue, n=25) compared to patients having no CD4+ IR prior to aGvHD grade II-IV diagnosis (red, n=48,  $P=0.006$ ), and comparable to patients having no aGvHD (red, n=203,  $P=0.635$ ). (B) Patients having no CD4+ IR prior to aGvHD grade III-IV (red, n=17) had even more drastically lower 5-Year NRM compared to no patient with prior CD4+ IR (blue, n=12,  $P<0.001$ ), the latter had comparable NRM to patients having no aGvHD (green, n=203,  $P=0.506$ ). A multivariate Gray's test was applied to calculate P-values.

Adequate early CD4+ IR before diagnosis of aGvHD grade II-IV was associated with increased OS probability ( $p<0.001$ ); 5-year OS was 77% with CD4+ IR prior to aGvHD onset (similar to no aGvHD; 76%,  $p=0.6$ ), while only 48% of the patients without adequate CD4+ IR prior to aGvHD survived (Figure 1A). 5-Year NRM was only 16% in patients having adequate CD4+ IR prior to aGvHD grade II-IV compared to 34% in patients without prior CD4+ IR ( $p=0.006$ ), which was comparable to 18% in patients having no aGvHD ( $p=0.635$ ; Figure 2A).

For aGvHD grade III-IV, differences were even more striking with only 24% 5-year OS without prior CD4+ IR compared to 78% in patients with adequate CD4+ IR prior to grade III-IV aGvHD ( $p<0.001$ ), which was comparable to 76% OS in patients without aGvHD ( $p=0.56$ ; Figure 1B). NRM was only 12% in patients who had adequate CD4+ IR prior to aGvHD grade III-IV diagnosis, comparable to 18% in patients without aGvHD ( $p=0.506$ ), but much lower compared to 74% in patients having no CD4+ IR ( $p<0.001$ ; Figure 2B).

## Discussion

In this short-report, we uniquely show that adequate CD4+ IR before aGvHD onset increases the probability of surviving this severe complication after allogeneic HCT. CD4+ IR at time of onset seems to be an interesting predictor for mortality in patients with moderate-severe aGvHD. This indicates that patients with  $<50 \times 10^6$  CD4+CD3+ cells/L who develop aGvHD might benefit from more intensive aGvHD treatment (e.g. higher dose, quicker after diagnosis) to improve survival chances. It would be of high interest to evaluate CD4+ IR as a predictive marker in a prospective study, especially since adequate CD4+ IR has also been related to lower risk of viral reactivations,<sup>10</sup> virus-related morbidity and mortality,<sup>10</sup> and relapse.<sup>16</sup>

Improving CD4+ IR probability after HCT can be an important strategy to enhance HCT success. Strategies to improve the chance of having adequate CD4+ IR lie in individualizing conditioning regimens to allow for better predictable IR. A major factor hampering CD4+ IR in the majority of patients is residual ATG exposure (or other serotherapy) after HCT<sup>18,19</sup>, which can be limited by targeted dosing.<sup>20–23</sup> In addition, Fludarabine has also recently been shown to affect CD4+ IR probability (Langenhorst et al, unpublished data), indicating CD4+ IR might further improve with individualized Fludarabine dosing.<sup>24</sup>

The most likely explanation of why adequate CD4+ IR protects against death after aGvHD is because of higher CD4+ Treg counts that dampen the allogeneic reaction in aGvHD. High Treg counts early after HCT have been related to higher T-cell receptor (TCR)-diversity, limiting aGvHD risk and severity,<sup>8,9,25–27</sup> and therefore possibly also mortality after severe aGvHD. An approach

to enhance expansion and regulation by CD4+ Tregs, might be low-dose IL-2 therapy,<sup>28–30</sup> or infusion of graft-derived or third-party Tregs,<sup>28–30</sup> in patients without spontaneous adequate CD4+ IR. Alternatively, sirolimus or other mTOR inhibitors might be useful as they can selectively suppress effector memory T-cells, while expanding Tregs, resulting in better immune regulation.<sup>31,32</sup>

For now it remains unknown what the exact biology is behind protection of early adequate CD4+ T-cell count against mortality after aGvHD. In further studies, we will evaluate Treg counts, and study the effect of TCR-diversity in Tregs and effector-memory T-cells in patients with and without aGvHD. Unraveling the biology why CD4+ IR predicts survival chance after moderate-severe aGvHD will provide us tools to further improve HCT outcomes.

## Acknowledgements

This work was supported by Foundation Children Cancerfree (KiKa) project number 142.

## Footnotes

### Contributors

SN, JJ, JL and CdK designed the study, and CdK and CS wrote the manuscript. JL analyzed the data. CL, JJ, and SN provided critical comments, and all authors read and approved the manuscript.

## References

1. Kröger N, Solano C, Wolschke C, et al. Antilymphocyte Globulin for Prevention of Chronic Graft-versus-Host Disease. *N. Engl. J. Med.* 2016;374(1):43–53.
2. Malilay GP, Sevenich EA, Condie RM, Filipovich AH. Prevention of graft rejection in allogeneic bone marrow transplantation: I. Preclinical studies with antithymocyte globulins. *Bone Marrow Transplant.* 1989;4(1):107–12.
3. Podgorny PJ, Ugarte-Torres A, Liu Y, et al. High Rabbit-Antihuman Thymocyte Globulin Levels Are Associated with Low Likelihood of Graft-vs-Host Disease and High Likelihood of Posttransplant Lymphoproliferative Disorder. *Biol. Blood Marrow Transplant.* 2010;16(7):915–926.
4. Lindemans CA, Te Boome LCJ, Admiraal R, et al. Sufficient Immunosuppression with Thymoglobulin Is Essential for a Successful Haplo-Myeloid Bridge in Haploidentical-Cord Blood Transplantation. 2015; 21(10):1839-45. doi: 10.1016/j.bbmt.2015.06.001.
5. Ruutu T, Gratwohl A, de Witte T, et al. Prophylaxis and treatment of GVHD: EBMT–ELN working group recommendations for a standardized practice. *Bone Marrow Transplant.* 2014;49(2):168–173.
6. Jagasia M, Arora M, Flowers MED, et al. Risk factors for acute GVHD and survival after hematopoietic cell transplantation. *Blood.* 2012;119(1):296–307.
7. D’Souza A, Fretham C. Current Uses and Outcomes of Hematopoietic Cell Transplantation (HCT): CIBMTR Summary Slides, 2017;23(9):1417-1421.
8. Magenau JM. Frequency of CD4(+)CD25(hi)FOXP3(+) regulatory T cells has diagnostic and prognostic value as a biomarker for acute graft-versus-host-disease. *Biol. Blood Marrow Transpl.* 2010;16:907–914.
9. Rezvani K. High donor FOXP3 -positive regulatory T-cell ( T reg ) content is associated with a low risk of GVHD following HLA-matched allogeneic SCT. *Blood.* 2006;108(4):1291–1294.
10. Admiraal R, de Koning CCH, Lindemans CA, et al. Viral reactivations and associated outcomes in the context of immune reconstitution after pediatric hematopoietic cell transplantation. *J. Allergy Clin. Immunol.* 2017;140(6):1643-1650.
11. Glucksberg H, Fefer A, et al SR. Clinical manifestations of graft-versus-host disease in human recipients of marrow from HL-A-matched sibling donors. *Transplantation.* 1974;18(4):295–304.
12. Shulman HM, Sullivan KM, Weiden PL, et al. Chronic graft-versus-host syndrome in man. A long-term clinicopathologic study of 20 Seattle patients. *Am. J. Med.* 1980;69(2):204–17.

13. Bartelink IH Knibbe CAJ, et al. BS V. Immune Reconstitution Kinetics as an Early Predictor for Mortality using Various Hematopoietic Stem Cell Sources in Children. *Biol Blood Marrow Transpl.* 2013;19(2):305–313.
14. Admiraal R. Association between anti-thymocyte globulin (ATG) exposure and CD4+ immune reconstitution predicting overall survival in paediatric haematopoietic cell transplantation: a multicentre retrospective pharmacodynamic cohort analysis. *Lancet Haematol.* 2015;2(5):e194-203. doi: 10.1016/S2352-3026(15)00045-9.
15. Admiraal R, de Koning C, Bierings MB, et al. Viral reactivations and associated outcomes in context of immune reconstitution after pediatric hematopoietic cell transplantation. 2017;140(6):1643-1650.e9. doi: 10.1016/j.jaci.2016.12.992.
16. Admiraal R, Chiesa R, Bierings M, et al. Early CD4+ Immune Reconstitution Predicts Probability of Relapse in Pediatric AML after Unrelated Cord Blood Transplantation: Importance of Preventing in Vivo T-Cell Depletion Using Thymoglobulin®. *Biol. Blood Marrow Transplant.* 2015;21(2):S206.
17. Team RC. R: A language and environment for statistical computing. 2017. Vienna, Austria. URL <https://www.R-project.org>
18. Admiraal R, Nierkens S, de Witte MA, et al. Association between anti-thymocyte globulin exposure and survival outcomes in adult unrelated haemopoietic cell transplantation: a multicentre, retrospective, pharmacodynamic cohort analysis. *Lancet Haematol.* 2017;4(4):e183–e191.
19. Willemsen L, Jol-Van Der Zijde CM, Admiraal R, et al. Impact of Serotherapy on Immune Reconstitution and Survival Outcomes After Stem Cell Transplantations in Children: Thymoglobulin Versus Alemtuzumab. *Biol. Blood Marrow Transplant.* 2015;21:473–482.
20. Admiraal R, Lindemans CA, van Kesteren C, Bierings MB, Versluijs B, Nierkens S B.J. Excellent T-cell Reconstitution and Survival Provided ATG exposure is low or Absen after Pediatric Cord Blood Transplantation. *Blood.* 2016;128(23):2734-2741.
21. Admiraal R, van Kesteren C, Jol-van der Zijde CM, et al. Population Pharmacokinetic Modeling of Thymoglobulin® in Children Receiving Allogeneic-Hematopoietic Cell Transplantation: Towards Improved Survival Through Individualized Dosing. *Clin. Pharmacokinet.* 2015;54(4):435–446.
22. Bouazza N, Urien S, Neven B, et al. Evaluation of antithymocyte globulin pharmacokinetics and pharmacodynamics in children. *J. Allergy Clin. Immunol.* 2016;137(1):306–309.e4.
23. De Koning C, Admiraal R, Nierkens S, Boelens JJ. Immune reconstitution and outcomes after conditioning with antithymocyte-globulin in unrelated cord blood transplantation; the good, the bad, and the ugly. *Stem Cell Investig.* 2017;7(6):4-38. doi: 10.21037/sci.2017.05.02.

24. Langenhorst JB, Dorlo TPC, van Maarseveen EM, et al. Population Pharmacokinetics of Fludarabine in Children and Adults during Conditioning Prior to Allogeneic Hematopoietic Cell Transplantation. *Clin. Pharmacokinet.* 2019;58(5):627-637. doi: 10.1007/s40262-018-0715-9.
25. Brunstein CG. Infusion of ex vivo expanded T regulatory cells in adults transplanted with umbilical cord blood: safety profile and detection kinetics. *Blood.* 2011;117:1061-1070.
26. Edinger M. CD4+CD25+ regulatory T cells preserve graft-versus-tumor activity while inhibiting graft-versus-host disease after bone marrow transplantation. *Nat. Med.* 2003;9:1144-1150.
27. Yew PY, Alachkar H, Yamaguchi R, et al. Quantitative characterization of T-cell repertoire in allogeneic hematopoietic stem cell transplant recipients. *Bone Marrow Transplant.* 2015;50(9):1227-1234.
28. Matsuoka K. Low-Dose Interleukin-2 Therapy Restores Regulatory T Cell Homeostasis in Patients with Chronic Graft-Versus-Host Disease. *Sci. Transl. Med.* 2013;5(179):43.
29. Koreth J. Interleukin-2 and regulatory T cells in graft-versus-host disease. *English J. Med.* 2011;365:2055-2066.
30. Kennedy-Nasser AA, Ku S, Castillo-Caro P, et al. Ultra low-dose IL-2 for GVHD prophylaxis after allogeneic hematopoietic stem cell transplantation mediates expansion of regulatory T cells without diminishing antiviral and antileukemic activity. *Clin. Cancer Res.* 2014;20(8):2215-25.
31. Chen Y-B, Efebera YA, Johnston L, et al. Increased Foxp3 + Helios + regulatory T cells and decreased acute graft-versus-host disease after allogeneic bone marrow transplantation in patients receiving sirolimus and RGI-2001, an activator of invariant natural killer T cells HHS Public Access. *Biol Blood Marrow Transpl.* 2017;23(4):625-634.
32. Pidala J, Kim J, Anasetti C. Sirolimus as Primary Treatment of Acute Graft-versus-Host Disease following Allogeneic Hematopoietic Cell Transplantation. *Biol Blood Marrow Transpl.* 2009;15(7):881-5. doi: 10.1016/j.bbmt.2009.03.020





# Chapter 7

# Predictors for autoimmune cytopenias after allogeneic hematopoietic cell transplantation in children

---

Celina L. Szanto<sup>1</sup>, Jurgen B. Langenhorst<sup>1</sup>, Coco C.H. de Koning<sup>1</sup>, Stefan Nierkens<sup>1,2</sup>, Marc B. Bierings<sup>2</sup>, Alwin D.R. Huitema<sup>3,4</sup>, Caroline A. Lindemans<sup>2†</sup> Jaap-Jan Boelens<sup>5†</sup>

<sup>1</sup> Center for Translational Immunology, University Medical Center Utrecht, Utrecht University, Utrecht, The Netherlands

<sup>2</sup> Princess Máxima Center for Pediatric Oncology, Utrecht University, Utrecht, The Netherlands

<sup>3</sup> Department of Clinical Pharmacy, University Medical Center Utrecht, Utrecht University, Utrecht, The Netherlands

<sup>4</sup> Department of Pharmacy & Pharmacology, Netherlands Cancer Institute, Amsterdam, The Netherlands

<sup>5</sup> Stem Cell Transplantation and Cellular Therapies Program, Department of Pediatrics, Memorial Sloan Kettering Cancer Center, New York, United States

† These authors contributed equally to this work.

*Biology of Blood and Marrow Transplantation. 2020 Jan; 26(1): 114-122.*

## Abstract

Development of autoimmune cytopenia (AIC) after allogeneic hematopoietic cell transplantation (HCT) is a serious complication requiring urgent intensification of immunosuppressive therapy. The pathophysiology and predictors of AIC are not completely understood. In this retrospective cohort analysis, including 380 pediatric patients, we evaluated the incidence, outcomes, and related various variables, including immune reconstitution markers to AIC.

A total of 380 patients (median age of 7.4 years; range 0.1-22.7) were included of which 30 patients (7.8%) developed AIC in 1 (n=6), 2 (n=6) or 3 (n=16) cell lineages at a median of 133 (46-445) days post HCT. Using multivariate analysis, we found that chemo-naivety prior to HCT, acute-graft-versus-host-disease (aGvHD) grade II-IV and serotherapy were associated with the development of AIC. Development of AIC was preceded by an increased levels of IgM, IgA, and IgG. Immune profiles of total absolute lymphocytes were very similar between AIC patients and controls. However, CD3-CD16+CD56+ natural killer cells, CD3+ T cells, CD3+CD4+ T cell subset and CD3+CD8+ T subset were lower in AIC patients. Overall survival (OS) was good, 83% (similar between AIC patients and controls).

In conclusion, we identified chemo-naivety prior to HCT, preceding aGvHD grade II-IV, and serotherapy as predictors for development of AIC. Increasing levels of IgM, IgA and IgG preceded AIC development. These data provide clues to further study the biology of AIC.

## Introduction

Allogeneic hematopoietic cell transplantation (HCT) is a potentially curative procedure to treat a variety of malignant and nonmalignant hematologic disorders. The development of autoimmune cytopenia (AIC) is a severe complication after HCT in 2% to 6% of pediatric patients<sup>1-5</sup>. AIC may be restricted to a single lineage of blood cells, such as autoimmune hemolytic anemia (AIHA), autoimmune thrombocytopenia (AIT), autoimmune neutropenia (AIN) or present in multiple lineages such as Evans' syndrome in which AIHA is associated with AIT and/or AIN<sup>6</sup>.

The management of AIC is challenging since not all patients respond to initial immunosuppressive therapy with steroids. Development of AIC after HCT has been associated with graft-versus-host-disease (GvHD), higher risk of relapse, T-cell depletion and HCT from unrelated donors suggesting that immune dysregulation or impaired immune reconstitution may be involved<sup>7-9,10</sup>. Other studies have reported age at transplantation, viral reactivations, HCT for nonmalignant indications, cord blood (CB) stem cell source, conditioning and interval time from primary diagnosis to HCT as predictors for AIC<sup>4,9,11,12,13</sup>. Furthermore, Kruizinga et al. and González-Vicent et al. studied the immune status at AIC diagnosis<sup>11,14</sup>. Kruizinga et al. found that cytokine profiles of patients at the time of AIC diagnosis were skewed toward a more pronounced T-helper 2 response compared to controls. González-Vicent et al. showed in a very large registry analysis (n>4000) that most patients at the time of AIC diagnosis were lymphopenic (median 882 lymphocytes/mL), including very low regulatory T cells (Tregs), suggesting that deep immune deficiency is a predictor. These associations with AIC might give more insight in the pathogenesis of AIC and may eventually help in early diagnosis and thus treatment of AIC. We are also interested in relating development of AIC to immune markers, including immunoglobulins. Therefore, we performed a retrospective cohort analysis in which we aimed to relate clinical data as well as data from 'in depth' immune monitoring (immunoglobulins and variety of lymphocyte subsets) from our cohort to the development of AIC.

## Methods

### Study design and Patients

All patients receiving their first allogeneic HCT between January 2004 and February 2018 at the University Medical Center in Utrecht, The Netherlands, were included. The conditioning regimen and source of hematopoietic stem cells were based on indication and availability according to (inter)national protocols/guidelines. The minimum follow-up for surviving patients was 1 month in this study. Data were collected prospectively in a local clinical database. Written informed consent was obtained from the parents before enrollment in accordance with the Declaration of Helsinki. The study was approved by the local ethical committee through trial numbers 05/143 and 11/063-k.

## Procedures

GvHD-prophylaxis consisted of cyclosporine A (CsA; targeted at trough levels of 150-250 mg/L for all patients) combined with prednisone 1 mg/kg (cord blood [CB]) or methotrexate (on day +1, +3, +6). CsA was administered for a minimum of 3 months (malignant disease) or 6 months (non-malignant disease) after HCT. Prednisone was tapered in 2 weeks starting 4 weeks post-HCT in benign disorders, and in one week after engraftment in malignant disorders. CB recipients were treated with filgrastim from day +7 after HCT until neutrophils were above 2000 cells/ml. Erythrocytes were transfused to maintain a minimal hemoglobin level of 4.3 mmol/L and platelets were administered in patients with evidence of mucosal bleeding. All patients received antiviral prophylaxis using acyclovir, gut decontamination and pneumocystis jiroveci prophylaxis according to local protocols. Patients were monitored weekly after HCT for adenovirus (AdV), cytomegalovirus (CMV), Epstein-Barr virus (EBV) and human herpesvirus 6 (HHV6) reactivation by PCR screening techniques. Viral reactivation was defined as having a viral load above 1000 copies/mL. Starting from 2012 onwards, EBV and CMV viral loads were measured in IU/mL. Therefore, the threshold for EBV and CMV was set at 5000 and 500 IU/ml, respectively, following the conversion factor used in the same viral laboratory.

Lymphocyte subsets consisting of CD3+ T cells, CD3+CD4+CD8- T-helper cells, CD3+CD8+CD4- cytotoxic T cells, CD19+ B cells, and CD3-CD16+CD56+ natural killer (NK) cells were measured every other week up to 12 weeks after HCT, thereafter monthly using flow cytometry. Absolute counts were acquired by the use of TruCount technology. At the same time points immunoglobulin levels (IgA, IgG and IgM) were monitored. Patients received a dose of intravenous immunoglobulin (IVIg) immediately after HCT or in the early post-HCT period only in case of IgG < 4 g/L.

## AIC definitions and diagnosis

AIHA was defined by a positive direct agglutinin test (DAT), testing for both IgG and C3 detection of specific (irregular antibodies against known RBC antigens) or nonspecific antibodies and/or a rapid decrease in erythrocytes combined with markers of hemolysis such as an increased reticulocyte level, elevated serum bilirubin, reduced plasma haptoglobin and raised serum lactic dehydrogenase. If the DAT was positive, the eluate was examined for antibodies against specific RBC antigens. If IgG was detected and there was hemolysis but no specificity against RBC could be determined it was booked as "aspecific antibodies". In case of a negative or unknown DAT, all patients were included if they showed a rapid decrease of erythrocytes combined with increased reticulocytes, elevated serum bilirubin, reduced plasma haptoglobin and raised serum lactic dehydrogenase. Further, we evaluated carefully the possibility of any non-immune

hemolytic cause (such as microangiopathy or paroxysmal nocturnal hemoglobinuria). We excluded patients with fragmentocytes and patients with GVHD symptoms or infections at onset of AIC. If patients did not have these above mentioned conditions and were responsive to immunosuppressive therapy, patients were defined with AIHA. AIT and AIN were defined by a rapid decrease in thrombocytes (below  $100 \times 10^9/L$ ) and neutrophils ( $1.0 \times 10^9/L$ ), respectively, with or without detection of antibodies against thrombocytes and neutrophils, and when other causes of cytopenia were excluded. For antibody testing, the platelet immunofluorescence test (PIFT) and the monoclonal immobilization of platelet antigen assay were used to detect reactive autoantibodies for AIT and an indirect immunofluorescent test and indirect monoclonal immobilization of granulocyte antigen assay were used to detect reactive autoantibodies for AIN. In addition, when antibody detection against thrombocytes and neutrophils was negative, patient's response to immunosuppressive treatment was key for the diagnosis of AIT and AIN. In none of the patients, the clinical symptoms could be explained by any other diagnosis than AIHA, AIT and AIN.

## Treatment

In a step-up treatment protocol AIC patients were treated with prednisone 1-2 mg/kg, while CsA (trough levels of 150-250 ug/L) or tacrolimus (8-15 mg/L) were continued or reinstated. When not directly responsive, refractory, or when tapering was not possible, often additional therapy with mycophenolate mofetil and sirolimus (trough levels 5-10 mg/ml) was combined with B cell reduction therapy with rituximab ( $375 \text{ mg/m}^2$ , once a week for 3 weeks). In case of rituximab treatment, IVIG every three weeks was started as IgG substitution therapy, according to our local treatment procedure.

## Outcomes

Main outcome of interest was development of AIC after HCT, defined as a rapid decrease of erythrocytes, thrombocytes and/or neutrophils as described above.

## Statistical analysis

Duration of the follow up was defined as the time from HCT to the occurrence of a complication, last assessment for surviving patients or death. Variables considered in the analysis consisted of donor specific variables (HLA disparity and CMV status), recipient specific variables (age at transplantation, sex, CMV status) and transplantation specific variables (conditioning regimen, stem cell source, use of serotherapy and chemo-naivety prior to HCT [defined as no chemotherapy or B-cell therapy prior to the conditioning phase]). We also considered immune events (e.g. aGvHD, viral reactivation) as time dependent variables. For univariate analysis, cumulative

incidence curves were computed for AIC, taking the following competing risks into account: treatment related mortality (TRM), relapse and death caused by other causes than AIC. P-values were calculated using Gray's test. For multivariate analysis, the risk factors significant ( $p < 0.05$ ) in univariate analysis were imputed in a Cox regression model via backward selection and p-values were calculated using Wald's test.

Immune reconstitution markers were considered as time varying factors and therefore evaluated as time-dependent variables. These variables were evaluated specifically prior to the development of AIC. As the onset of AIC varied between patients, immune reconstitution markers were aligned between patients by setting the time point of AIC development at time zero (index time). To compare immune reconstitution to patients that did not develop AIC, a control group was created by comparison to a random selection of minimal 12 controls for each AIC patient. For these controls the time point of immune reconstitution markers was aligned with the time of AIC development in patients (e.g. if patient A developed AIC at 133 days after HCT, immune reconstitution markers in the 12 randomly selected controls were studied up to 133 days by setting day 133 at zero). Loess-smoothed regression lines were generated to compare both groups. Due to the heterogeneity of the data (unstructured repeated measurements with variable index time) no further statistical testing was performed, hence these analyses were considered exploratory. Cross-sectional analysis of different immune reconstitution markers in the period before the index date were considered, but due to the heterogeneity in available samples before the index date, this proved to be not feasible. Acute and chronic GvHD were classified according to the Glucksberg<sup>15</sup> and Shulman<sup>16</sup> criteria. Statistical analysis was performed using R version 3.3.2.

## Results

### Patient demographics and baseline characteristics

A total of 380 patients with a median age of 7.4 years (range 0.1-22.7 years) were included (Table 1). The majority of the patients were transplanted for a malignant disease ( $n=196$ , 52%), followed by metabolic/inborn errors ( $n=66$ , 17%), immunodeficiency ( $n=62$ , 16%), bone marrow failure ( $n=52$ , 14%) and autoimmune diseases ( $n=4$ , 1%). Most patients received chemotherapy-based conditioning (86%), in which busulfan in combination with fludarabine was most frequently used (36%). Serotherapy was administered to 272 patients (72%), of which 264 patients (97%) received ATG (Genzyme) and 8 patients (3%) received alemtuzumab. The majority of the patients received a HCT from a HLA identical donor (57%, of which 61% was unrelated and 39% related). Of the 289 patients (76%) with an unrelated donor, 72% was transplanted with CB. Post HCT

viral reactivation occurred in 24 (6.2%), 48 (12.4%), 42 (10.9%) and 93 (24.5%) patients for EBV, CMV, AdV and HHV6 respectively. The median follow-up time was 35 months (1.0-168.8). Of all patients, 30 patients (7.8%) developed AIC at a median time of 133 days (range, 46-445 days) post HCT (1-year CI 7.1% and 5-year CI 7.8%). All AIC patients had complete donor chimerism at onset of AIC. Acute GvHD grade II-IV occurred in 15 patients before AIC development with a median duration between aGvHD and AIC of 75.5 days. Characteristics of patients that developed AIC are shown in Table 2.

**Table 1.** Patient characteristics

	No AIC (n = 350)	AIC (n = 30)
Male, n (%)	196 (56)	21 (70)
Median age at HCT (range), y	7 (0.1-22.7)	4 (0.2-18)
<b>Diagnosis, n (%)</b>		
Malignant	187 (53.4)	9 (30)
Non-malignant	163 (46.6)	21 (70)
Chemotherapy prior to HCT, n (%)	179 (51.1)	7 (23.3)
<b>Stem cell source, n (%)</b>		
CB	189 (54)	23 (76.7)
BM	154 (44)	6 (20)
PBSCs	7 (2)	1 (3.3)
<b>Conditioning regimen, n (%)</b>		
Radiation based	50 (14.3)	0
Chemotherapy based	300 (85.7)	30 (100)
Bu-Flu	120 (34.3)	18 (60)
Bu-Flu-Clo	77 (22)	5 (16.7)
Bu-Cy	47 (13.4)	5 (16.7)
Bu-Mel-Cy	15 (4.3)	0
Flu-Cy	23 (6.6)	2 (6.7)
Flu-thiotepa	7 (2)	0
Bu-Flu-Cy	5 (1.4)	0
Cy	4 (1.1)	0
Flu-Mel	1 (0.3)	0
Flu	1 (0.3)	0
Serotherapy, n (%)	242 (69.1)	30 (100)
<b>Ablative*, n (%)</b>		
Yes	327 (93.4)	30 (100)
No	23 (6.6)	0
<b>HLA mismatch, n (%)</b>		
0	202 (57.7)	16 (53.3)

**Table 1.** Patient characteristics

	No AIC (n = 350)	AIC (n = 30)
1	104 (29.7)	10 (33.3)
2	37 (10.6)	4 (13.3)
> 2	4 (1.1)	0
Unknown	3 (0.9)	0
<b>ABO-incompatibility, n (%)</b>		
<b>Mismatch</b>	224 (64)	16 (53.3)
Of which major		5 (16.7)
Of which minor		7 (23.3)
Of which major and minor		4 (13.3)
<b>Match</b>	126 (36)	14 (46.6)
<b>Viral reactivation, n (%)</b>		
EBV reactivation	20 (5.7)	4 (13.3)
CMV reactivation	41 (11.7)	7 (23.3)
AdV reactivation	37 (10.6)	4 (13.3)
HHV6 reactivation	87 (24.9)	7 (23.3)
<b>Donor type, n (%)</b>		
Related	90 (25.7)	1 (3.3)
Unrelated	260 (74.3)	29 (96.7)
<b>aGVHD, n (%)</b>		
aGVHD grade I	61 (17.4)	4 (13.3)
aGVHD grade II-IV	82 (23.4)	15 (50)
<b>cGVHD, n (%)</b>		
cGVHD limited	15 (4.3)	4 (13.3)
cGVHD extensive	17 (4.9)	5 (16.7)
Median follow up OS (range), mo	35 (1.0-168.8)	41 (3.8-148.6)

\* Fanconi conditioning considered ablative in the context of this disease; BM, bone marrow; Bu, busulfan; Clo, Clofarabine; Cy, Cyclophosphamide; Flu, Fludarabine; HLA, human leukocyte antigen; Mel, Melphalan; OS, overall survival; TBI, total body irradiation

**Table 2.** Characteristics of patients with AIC

Patient	Primary disease	Stem cell source	Sex	Time to AIC (days)	Conditioning regimen	Chemotherapy prior to HCT	AIC	DAT	Antibodies	Identified antibodies	Outcome
1	CID	BM	M	289	Bu-Cy	No	AIHA	IgG+C3+	Pos	Warm, auto-antibodies	Alive
2	WAS	CB	M	136	Bu-Flu	No	AIHA, AIT, AIN	IgG+C3+	Pos	Cold, warm, aspecific auto-antibodies	Alive
3	ALL	CB	F	267	Bu-Flu-Clo	Yes	AIHA, AIN	IgG+C3+	Pos	Warm, aspecific auto-antibodies	Alive
4	CGD	CB	M	63	Bu-Flu	No	AIHA, AIT, AIN	IgG+C3+	Pos	Cold, Warm, aspecific auto-antibodies, HNA-1a	Death: Invasive fungal infection
5	MDS	PBSC	M	80	Bu-Cy	No	AIHA, AIT, AIN	C3+	Pos	Warm, aspecific auto-antibodies, HNA-1a and HNA-1b	Death: Relapse
6	Hurler	CB	M	314	Bu-Flu	No	AIHA, AIT, AIN	IgG+C3+	Pos	Warm, aspecific auto-antibodies, IgM	Alive
7	WAS	CB	M	336	Bu-Flu	No	AIHA, AIT, AIN	IgG+C3+	Pos	Cold, Warm, aspecific auto-antibodies	Alive
8	CNL	BM	M	105	Bu-Flu-Clo	Yes	AIHA, AIT, AIN	IgG+C3+	Pos	Cold, Warm, aspecific auto-antibodies, anti-D	Alive
9	Hurler	CB	F	171	Bu-Flu	No	AIHA, AIT	IgG+C3+	Pos	Cold, Warm, aspecific auto-antibodies	Alive
10	ALL	BM	M	119	Bu-Cy	Yes	AIHA, AIN	Neg	Pos	Autoantibodies against granulocytes	Death: BM and kidney failure
11	CGD	CB	M	229	Bu-Flu	No	AIT	Neg	Not reported	Not reported	Alive
12	CGD	CB	M	115	Bu-Flu	No	AIHA, AIT, AIN	C3+	Pos	IgM class auto-antibodies targeting granulocytes	Death: Lung injury
13	SCID	CB	M	153	Bu-Flu	No	AIHA, AIT, AIN	Pos	Pos	Cold, Warm, aspecific auto-antibodies	Alive
14	MLD	CB	F	271	Bu-Flu	No	AIHA, AIT, AIN	IgG+C3+	Pos	Autoantibodies pan-FcR1Ib specificity against granulocytes	Alive
15	Fanconi	CB	M	479	Flu-Cy	No	AIT, AIN	Not reported	Pos	Cold, aspecific auto-antibodies	Alive

Table 2. Characteristics of patients with AIC

Patient	Primary disease	Stem cell source	Sex	Time to AIC (days)	Conditioning regimen	Chemotherapy prior to HCT	AIC	DAT	Antibodies	Identified antibodies	Outcome
16	MPSVI	CB	M	46	Bu-Flu	No	AIHA, AIT	Neg	Pos	autoantibodies against thrombocytes	Alive
17	Hurler	CB	F	71	Bu-Flu	No	AIHA, AIT, AIN	IgG+C3+	Pos	Cold, Warm, aspecific auto antibodies, autoantibodies against thrombocytes and granulocytes	Alive
18	ALL	BM	F	131	Bu-Flu-Clo	Yes	AIT	Neg	Not reported	Not reported	Alive
19	MLD	CB	M	445	Bu-Cyclo	No	AIHA, AIT, AIN	IgG+C3+	Pos	Warm, aspecific antibodies	Alive
20	Fanconi	CB	M	374	Bu-Flu	No	AIHA, AIT, AIN	Pos	Pos	autoantibodies against thrombocytes	Alive
21	ALL	BM	M	226	Bu-Flu-Clo	Yes	AIHA, AIT, AIN	Neg	Neg	Not reported	Alive
22	AML	CB	M	58	Bu-Flu	Yes	AIHA, AIT	IgG+C3+	Pos	Warm, aspecific antibodies, HNA-2	Death: Multiple organ failure
23	CGD	CB	M	55	Bu-Flu	No	AIHA, AIT, AIN	IgG+C3+	Pos	Warm, specific allo antibodies, anti-A, HNA-1a	Alive
24	Hurler	CB	F	81	Bu-Flu	No	AIT	Pos	Not reported	Not reported	Alive
25	Hurler	CB	M	72	Bu-Flu	No	AIHA, AIT	IgG+C3+	Pos	Warm, specific auto antibodies, anti-e	Alive
26	CID	CB	M	104	Bu-Flu	No	AIHA, AIT, AIN	IgG+C3+	Pos	Warm, aspecific antibodies, HNA-1b	Alive
27	ALL	CB	M	178	Bu-Flu-Clo	Yes	AIHA, AIT, AIN	Neg	Pos	autoantibodies against thrombocytes	Alive
28	Hurler	CB	F	162	Bu-Cy	No	AIHA, AIT	C3+	Pos	Warm, aspecific antibodies	Alive
29	MDS	BM	F	98	Bu-Flu	No	AIT	Neg	Neg	Not reported	Alive
30	Fanconi	CB	F	122	Flu-Cy	No	AIT	Not reported	Not reported	Not reported	Alive

ALL, acute lymphoblastic leukemia; AML, acute myeloid leukemia; Bu, Busulfan; CGD, chronic granulomatous disease; CID, combined immune deficiency; CNL, chronic neutrophilic leukemia; Cy, cyclophosphamide; Flu, fludarabine; HNA, human neutrophil antigens; MDS, myelodysplastic syndrome; MLD, metachromatic leukodystrophy; Pos, positive; SCID, severe combined immunodeficiency; Unk, unknown; WAS, Wiskott-Aldrich syndrome

## Outcomes

Twenty-five out of 30 patients with AIC were alive at last follow up. Two patients died because of TRM (one patient died of bone marrow [BM] and kidney failure and one patient died of lung injury). In addition, one patient died of relapse. Overall, survival was good for AIC patients (83%) and controls (70%), however, due to inherent immortal time bias this could not further be tested.

Sixteen patients (53%) developed AIC in which three cell types were affected resulting in AIHA, AIT and AIN. Five patients (17%) developed AIHA in combination with AIT, two patients (7%) developed AIHA in combination with AIN, one patient developed only AIHA (3%), one patient developed AIT in combination with AIN and 5 patients (17%) developed AIT. Of the 24 patients with AIHA, 19 patients had a positive DAT with IgG and/or C3 polyspecific antibodies and 22 patients had increased reticulocytes. In four patients with AIHA the DAT was negative and in one patient no DAT was performed.

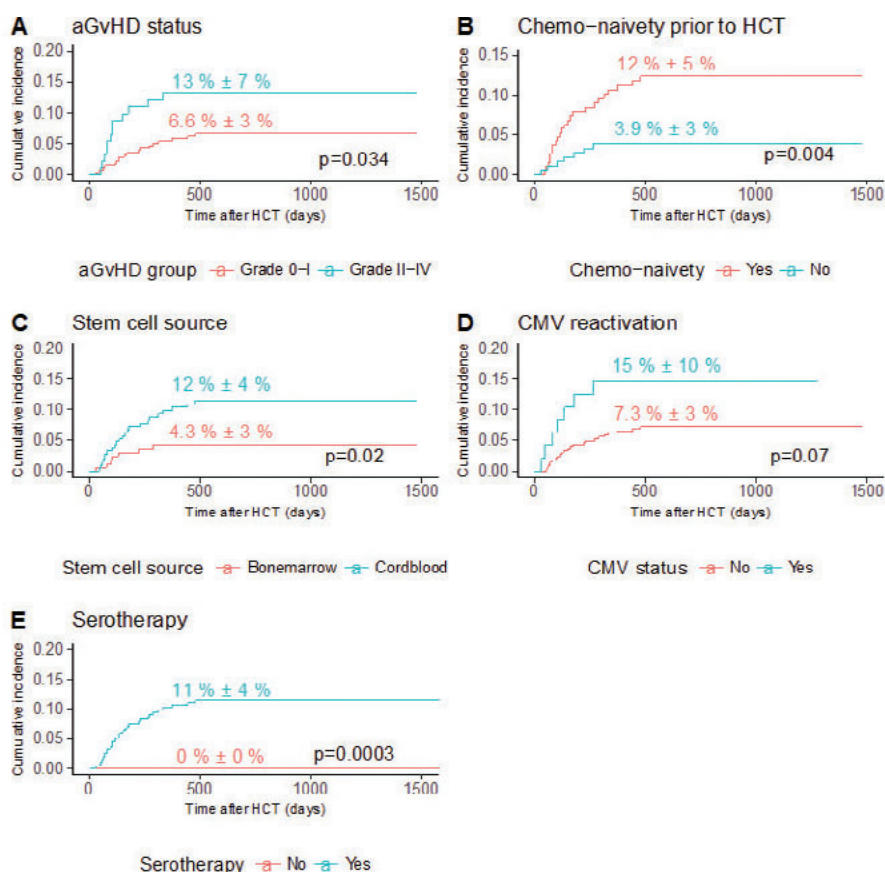


**Figure 1.** Cumulative incidence curves of AIC development

Depicted p-values are results of univariate analysis. (A) Patients with aGvHD grade 0-I compared to patients with aGvHD grade II-IV prior to AIC. (B) Patients with chemotherapy prior to HCT compared to patients without chemotherapy (chemo-naïve patients). (C) Patients transplanted with CB compared to patients transplanted with BM (including peripheral blood stem cells). (D) Patients with CMV reactivation compared to patients without CMV reactivation after HCT. (E) Patient with serotherapy compared to patients without serotherapy.

Cumulative incidence curves of potential predictors for AIC development are depicted in Figure 1. In multivariate Cox regression analysis, aGvHD grade II-IV (hazard ratio [HR] 2.45, 95% cumulative incidence [CI] 1.18-5.09,  $p=0.0167$ ), chemo-naïvety prior to HCT (HR 2.36, 95% CI 1.00-5.57,  $p=0.0499$ ) and serotherapy (HR 8.00, 95% CI 1.05-61.04,  $p=0.045$ ) were independent predictors for AIC development. Taken together these 3 predictors showed that patients treated with serotherapy, without chemotherapy prior to HCT (chemo-naïve) and who developed aGvHD grade II-IV prior to AIC development have a 22% chance to develop AIC (Figure 2). CB was not significant in multivariate analysis ( $p=0.0813$ , HR 2.14 95% CI 0.91-5.01), however, given the relatively high HR this effect might be relevant. Univariate analysis can be found in supplementary table 1.

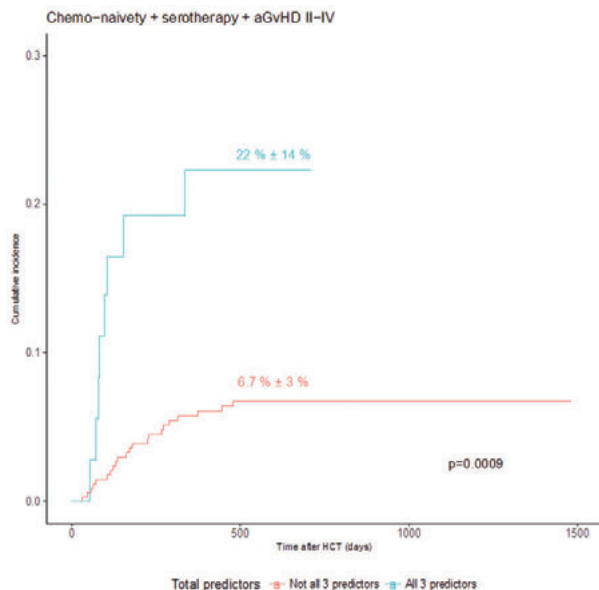


**Figure 2.** Cumulative incidence curve of AIC development

Patients treated with serotherapy, without chemotherapy prior to HCT (chemo-naïve) and who developed aGvHD grade II-IV prior to AIC development are compared to patients that did not have all 3 predictors.

All AIC patients started with prednisone, as first line therapy. This treatment was sufficient in 4 patients (13%). The other 26 patients received additional therapy with mycophenolate mofetil (15 patients; 50%) and/or sirolimus (12 patients; 40%) and/or rituximab (19 patients; 63%); Six of these patients received only 1 treatment modality (mycophenolate mofetil, 2 patients; sirolimus, 1 patient; rituximab, 3 patients). In addition, all patients that received rituximab received IgG substitution therapy. Overall, all patients responded to additional immunosuppressive therapy.

### Immune marker analysis

To explore the immune status in the period leading up to AIC development, immune profiles were generated of total lymphocyte counts, NK cells, B cells, immunoglobulin levels and T cell populations. Immune profiles of each AIC patient were matched to profiles of 12 controls and LOESS-smoothed regression lines were generated to compare both groups.

Immune profiles of total lymphocytes were very similar, but CD3-CD16+CD56+ natural killer cells, CD3+ T cells, CD3+CD4+ T cell subset and CD3+CD8+ T subset profiles showed more variability. Despite this high variability, AIC patients tend to show lower levels of these cell subsets compared to controls at corresponding time points (Figure 3). CD19+ B cell levels did not differ between AIC patients and controls at corresponding time points. After AIC diagnosis patients were treated with immunosuppressive therapy and rituximab, resulting in a strong decrease in B cell levels compared to controls (Figure 4).

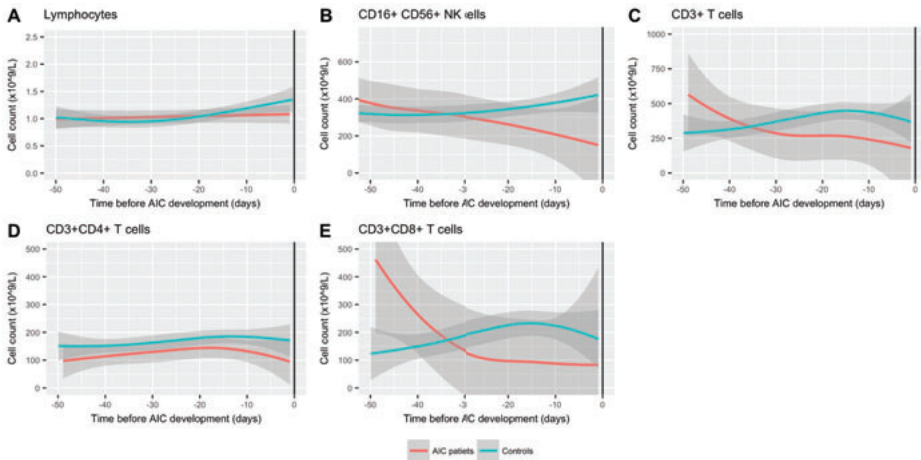


**Figure 3. Immune profiles prior to the development of AIC.** The solid lines represent a loess curve model and 95% confidence intervals are depicted in light gray. Lines represent averages of immune profiles of individual patients. AIC development is indicated with a black line at day 0. (A) Absolute lymphocyte count in AIC patients and controls. (B) Absolute NK cell (CD3-CD16+CD56+) count in AIC patients and controls. (C) Absolute CD3+ T cell count in AIC patients and controls. (D) Absolute CD3+CD4+ T cell count in AIC patients and controls. (E) Absolute CD3+ CD8+ T cell count in AIC patients and controls.

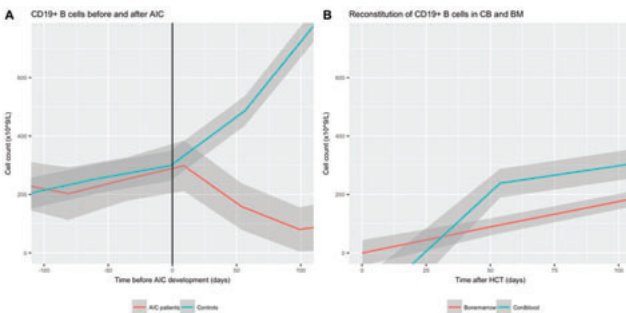


**Figure 4. B cell levels after HCT.** The solid lines represent a loess curve model and 95% confidence intervals are depicted in light gray. Lines represent averages of immune profiles of individual patients. AIC development is indicated with a black line at day 0. CD19+ B cell profiles 100 days before and 100 days after the development of AIC.

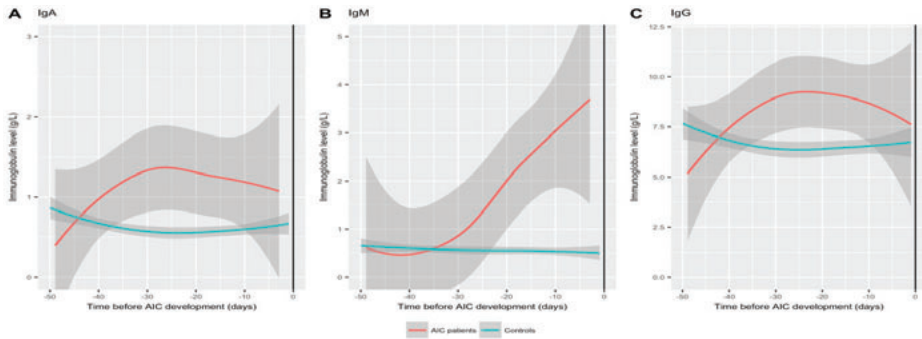


**Figure 5. Immunoglobulin levels prior to the development of AIC.**

The solid lines represent a loess curve model and 95% confidence intervals are depicted in light gray. Lines represent averages of immune profiles of individual patients. AIC development is indicated with a black line at day 0. (A) IgA profiles of AIC patients and controls before the development of AIC. (B) IgM profiles of AIC patients and controls before the development of AIC. (C) IgG profiles of AIC patients and controls before the development of AIC.

Immunoglobulin profiles showed that AIC patients, compared to controls, have increased levels of IgA, IgM and IgG between 30-40 days prior to AIC (Figure 5).

## Discussion

In this single center retrospective cohort analyses we showed that aGvHD grade II-IV, chemo-naivety prior to HCT procedure and serotherapy are predictors for development of AIC. In addition, we also identified an increase of IgM, IgG and IgA as potential immune predictors for development of AIC.

Especially early after HCT allo-reactivity may be responsible for hemolysis (due to ABO-incompatibility). However, in our cohort, all AIC patients have complete donor chimerism and AIC onset is relatively late suggesting autoimmunity.

We report an incidence of AIC after HCT of 7.8%. 53% was diagnosed with a pancytopenia. These numbers are higher than previous studies in similar patient populations, which report incidences of 1.5 – 4.6% for AIC<sup>1,3,4,17</sup>, and 0 - 38% for pancytopenia<sup>2,13,14</sup>. These high numbers can be explained by a multitude of factors, such as our strong interest in metabolic disease transplantation, in the development of AIC in CB transplanted patients, broader inclusion criteria and a possible underestimation in other studies, as AIC can sometimes be hard to discern from other pathologies. Differences in definition of AIC between the described cohorts influence the observed different incidences of AIC. As such, the increased minimum neutrophil levels in combination with other AIC supporting symptoms (in our paper set at  $1.0 \times 10^9/L$  instead of  $0.5 \times 10^9/L$  in comparative literature) may be in part contributing to the higher incidence of

pancytopenia. Lastly we have included patients who had, by exclusion, no alternative explanation for the cytopenia and who responded to steroids. In a prospective study we would aim to interrogate these patients further with alternative testing for instance DAT negative AIHA<sup>18</sup>.

We identified chemo-naivety prior to HCT as a predictor for AIC development. Most chemo-naïve patients received a HCT for a non-malignant indication. Non-malignancy has been described before as risk factor<sup>2,14</sup>. However in these studies chemo-naivety was not taken into account. In our study chemo-naivety showed a stronger relationship ( $p=0.004$ ) than “non-malignant indication” ( $p=0.02$ ), indicating that the therapy itself is more likely involved in the development of AIC rather than the disease indication. Although WAS ( $n=2$ ) and CID patients ( $n=1$ ) had autoimmune phenomena prior to HCT so did some of the patients that did not develop AIC. Actually the patients with refractory autoimmune disease did not develop AIC, probably because of intensive immune suppressive therapy prior to the HCT procedure. The main indication for chemotherapy prior to HCT is for treatment of malignant disease, aimed to kill tumor cells. In this setting, it is possible that this chemotherapy prior to the HCT procedure removes AIC-initiating regulatory lymphocytes (Tregs, innate lymphoid cells), or not fully matured B cell populations (antibody producing plasma cells), which would otherwise survive after HCT conditioning.

Also adding serotherapy to the conditioning (in our study mainly Anti-Thymocyte Globulin [ATG]) was found to be associated with the development of AIC, as reported previously<sup>2,4,12,14</sup>. In a recent study were all patients received serotherapy, no effect of the conditioning regimen could be found, suggesting the importance of serotherapy in AIC development<sup>10</sup>. Profound lympho-depletion can inhibit the mechanisms of tolerance, by depleting Tregs leading to expansion of autoreactive naïve and/or memory T cells. The fact that T cell reconstitution is slower in patients with AIC suggests a role for serotherapy in developing AIC. The highly variable pharmacokinetics (as described by various groups, including our group<sup>19,20</sup>) make some patients more vulnerable for AIC than others. Individualizing ATG dosing may therefore also influence the probability of developing AIC.

We found that preceding aGvHD grade II-IV was a significant risk factor for the development of AIC. The association between GvHD and autoimmunity has been described before, although not in a similar setting<sup>21</sup>. During aGvHD antigen presenting cells (APCs) activate donor T cells and give rise to an inflammatory reaction. These T cells might also be autoreactive. Although we did not define if the T cells present were autoreactive, we hypothesize that these cells could be involved in the pathogenesis of AIC. In line with this, although not statistically significant ( $p=0.07$ ) in this analysis, CMV (and viral reactivation) could also be of possible influence to the

development of AIC. Viral reactivations may either be a trigger for dysregulating T cells or an expression of bad immune defense.

CB has been mentioned as a risk factor for AIC before<sup>1,3</sup> although most studies have not performed a predictor analysis in a cohort where CB has been used in a wide range of diseases, malignant and non-malignant. CB grafts differ from BM grafts as the lymphocytes within the CB grafts are more immature and mostly naïve, and nearly always from unrelated donors<sup>15</sup>. Although 76.6% of AIC patients were transplanted with CB (univariate  $p=0.02$ ), CB did not remain a predictor for AIC development in multivariate analysis. This can be explained by the fact that CB transplantation itself is not a risk factor for AIC development but the treatment and indication related to CB transplantation. González-Vicent et al.<sup>11</sup> report CB as risk factor for AIC development, but they did not test it in multivariate analysis. Page et al.<sup>3</sup> suspected that the increase of AIC in CB patients was caused by immune dysregulation associated with GVHD prophylaxis, leading to aberrant immune ontogeny.

Normal levels of IgM are usually measurable between 3-6 months post HCT. IgG levels normalize between 1-2 years post HCT and IgA levels can take up to 5 years<sup>22</sup>. In line with these findings it has been reported that early onset AIC is associated with cold antibodies and late onset AIC is associated with warm antibodies reflecting immune reconstitution post HCT<sup>23</sup>. The strong increase in IgM, IgA and IgG levels prior to AIC in our study was independent of onset of AIC diagnosis, and might indicate the start of the development of AIC weeks before the diagnosis. As the rise occurs in all three, and most specifically in IgM by no means this is explained by IVIG administration. If proven and validated in future studies monitoring IgM, IgG and/or IgA after HCT, may be a trigger for clinicians to monitor carefully and not taper immune-suppressants at that time.

The findings in this study come with some limitations: its retrospective nature, relative small numbers and patients with different AICs treated for their primary disease under several different treatment protocols. Limited antibody specificity tests were performed to confirm if the antibodies present are real auto-antibodies or establish the donor versus patient origin (if even possible). However, it is also possible that donor lymphocytes activate recipients or donor plasma cells to produce immune antibodies.

In conclusion, we found various predictors for the development of AIC and potential biomarkers. The IgM, IgG and IgA increase prior to AIC development suggest plasma cell development to be key in the pathophysiology. The newly found predictors of chemo-naivety prior to HCT confirms

this and points towards a possible role for both the autologous and the donor immune system. Potentially, for chemo-naïve patients receiving serotherapy a prophylaxis strategy such as early rituximab can be a potentially effective preventive strategy. Also individualizing serotherapy (e.g. ATG) resulting in better predictable immune reconstitution may influence probability of developing AIC. Future, confirmative studies, preferably multicenter prospective ones, should be undertaken.

## **Acknowledgements**

The authors thank Charlotte van Kesteren for her expert advice on analyzing the data. In addition we thank all clinical doctors involved in caring for these patients.

## **Authorship Contributions**

CL, JJB, SN and CS designed the study, and CS wrote the manuscript. CS performed the experiments and CS and JL analyzed the results with critical comments from AH. CL, JJB, SN, CdK, MB and AH provided critical feedback, and all authors read and approved the manuscript.

## References

1. Daikeler T, Labopin M, Ruggeri A, et al. New autoimmune diseases after cord blood transplantation: A retrospective study of EUROCORD and the autoimmune disease working party of the European group for blood and marrow transplantation. *Blood*. 2013;121(6):1059-1064. doi:10.1182/blood-2012-07-445965.
2. Faraci M, Zecca M, Pillon M, et al. Autoimmune hematological diseases after allogeneic hematopoietic stem cell transplantation in children: an Italian multicenter experience. *Biol Blood Marrow Transplant*. 2014;20(2):272-278. doi:10.1016/j.bbmt.2013.11.014.
3. Page KM, Mendizabal AM, Prasad VK, et al. Posttransplant autoimmune hemolytic anemia and other autoimmune cytopenias are increased in very young infants undergoing unrelated donor umbilical cord blood transplantation. *Biol Blood Marrow Transplant*. 2008;14(10):1108-1117. doi:10.1016/j.bbmt.2008.07.006.
4. O'Brien TA, Eastlund T, Peters C, et al. Autoimmune haemolytic anaemia complicating haematopoietic cell transplantation in paediatric patients: High incidence and significant mortality in unrelated donor transplants for non-malignant diseases. *Br J Haematol*. 2004;127(1):67-75. doi:10.1111/j.1365-2141.2004.05138.x.
5. Wang M, Wang W, Abeywardane A, et al. Autoimmune hemolytic anemia after allogeneic hematopoietic stem cell transplantation: Analysis of 533 adult patients who underwent transplantation at king's college hospital. *Biol Blood Marrow Transplant*. 2015;21(1):60-66. doi:10.1016/j.bbmt.2014.09.009.
6. Miano M. How I manage Evans Syndrome and AIHA cases in children. *Br J Haematol*. 2016;172(4):524-534. doi:10.1111/bjh.13866.
7. Drobyski WR, Potluri J, Sauer D, Gottschall JL. Autoimmune hemolytic anemia following T cell-depleted allogeneic bone marrow transplantation. *Bone Marrow Transplant*. 1996;17(6):1093-1099. doi: 10 1038/sj.bmt.1703206
8. Sevilla J, González-Vicent M, Madero L, Díaz MA. Acute autoimmune hemolytic anemia following unrelated cord blood transplantation as an early manifestation of chronic graft-versus-host disease. *Bone Marrow Transplant*. 2001;28(1):89-92. doi:10.1038/sj.bmt.1703087.
9. Sanz J, Arango M, Carpio N, et al. Autoimmune cytopenias after umbilical cord blood transplantation in adults with hematological malignancies: A single-center experience. *Bone Marrow Transplant*. 2014;49(8):1084-1088. doi:10.1038/bmt.2014.107.
10. Scordo M, Hsu M, Jakubowski AA, et al. Immune Cytopenias After Ex-Vivo CD34+ Selected Allogeneic Hematopoietic Cell Transplantation. *Biol Blood Marrow Transplant*. 2019;25(6):1136-1141. doi:https://doi.org/10.1016/j.bbmt.2018.12.842.

11. González-Vicent M, Sanz J, Fuster JL, et al. Autoimmune hemolytic anemia (AIHA) following allogeneic hematopoietic stem cell transplantation (HSCT): A retrospective analysis and a proposal of treatment on behalf of the Grupo Español De Trasplante de Medula Osea en Niños (GETMON) and the Grupo Español. *Transfus Med Rev.* 2018;pii: S0887-7963(17)30164-5. doi:<https://doi.org/10.1016/j.tmr.2018.02.005>.
12. Sanz J, Arriaga F, Montesinos P, et al. Autoimmune hemolytic anemia following allogeneic hematopoietic stem cell transplantation in adult patients. *Bone Marrow Transplant.* 2007;39(9):555-561. doi:10.1038/sj.bmt.1705641.
13. Deambrosis D, Lum SH, Hum RM, et al. Immune cytopenia post-cord transplant in Hurler syndrome is a forme fruste of graft rejection. *Blood Adv.* 2019;3(4):570-574. doi:10.1182/bloodadvances.2018026963.
14. Kruizinga MD, van Tol MJD, Bekker V, et al. Risk factors, treatment and immune dysregulation in autoimmune cytopenia following allogeneic hematopoietic stem cell transplantation in pediatric patients. *Biol Blood Marrow Transplant.* 2018;24(4):772-778. doi: 10.1016/j.bbmt.2017.12.782.
15. Glucksberg, H; Storb, R; Fefer, A; Buckner, C.D. ; Neiman, Paul; Clift, R.A.; Lerner, K.G.; Thomas E. Clinical manifestations of graft-versus-host disease in human recipients of marrow from HL-A-matched sibling donors. *Transplantation.* 1974;18(4):295-304. doi:10.1097/00007890-197410000-00001.
16. Shulman HM, Sullivan KM, Weiden PL, et al. Chronic graft-versus-host syndrome in man: A long-term clinicopathologic study of 20 seattle patients. *Am J Med.* 1980;69(2):204-217. doi:[https://doi.org/10.1016/0002-9343\(80\)90380-0](https://doi.org/10.1016/0002-9343(80)90380-0).
17. Ahmed I, Teruya J, Murray-Krezan C, Krance R. The incidence of autoimmune hemolytic anemia in pediatric hematopoietic stem cell recipients post-first and post-second hematopoietic stem cell transplant. *Pediatr Transplant.* 2015;19(4):391-398. doi:10.1111/petr.12455.
18. Segel GB, Lichtman MA. Direct antiglobulin ("Coombs") test-negative autoimmune hemolytic anemia: A review. *Blood Cells, Mol Dis.* 2014;52(4):152-160. doi:<https://doi.org/10.1016/j.bcmd.2013.12.003>.
19. Admiraal R, van Kesteren C, Jol-van der Zijde CM, et al. Population Pharmacokinetic Modeling of Thymoglobulin® in Children Receiving Allogeneic-Hematopoietic Cell Transplantation: Towards Improved Survival Through Individualized Dosing. *Clin Pharmacokinet.* 2015;54(4):435-446. doi:10.1007/s40262-014-0214-6.

20. Admiraal R, van Kesteren C, Jol-van der Zijde CM, et al. Association between anti-thymocyte globulin exposure and CD4+ immune reconstitution in paediatric haemopoietic cell transplantation: a multicentre, retrospective pharmacodynamic cohort analysis. *Lancet Haematol*. 2015;2(5):e194-e203. doi:[https://doi.org/10.1016/S2352-3026\(15\)00045-9](https://doi.org/10.1016/S2352-3026(15)00045-9).
21. Tivol E, Komorowski R, Drobyski WR. Emergent autoimmunity in graft-versus-host disease. *Blood*. 2005;105(12):4885-4891. doi:10.1182/blood-2004-12-4980.
22. Series TM, Cell ONB, In S. Translational Mini-Review Series on B cell subsets in disease . Reconstitution after haematopoietic stem cell transplantation – revelation of B cell developmental pathways and lineage phenotypes. *Clin Exp Immunol*. 2012; 167(1): 15–25. doi: 10.1111/j.1365-2249.2011.04469.x
23. Chen FE, Owen I, Savage D, et al. Late onset haemolysis and red cell autoimmunisation after allogeneic bone marrow transplant. *Bone Marrow Transplant*. 1997;19(5):491-5.



# Chapter 8

# Identifying early immune predictors for alloimmune-lung disease after hematopoietic cell transplantation (HCT) in children

---

Celina L. Szanto<sup>1</sup>, Birgitta Versluys<sup>2</sup>, Caroline A. Lindemans<sup>2</sup>, Coco C.H. de Koning<sup>1</sup>, Marc B. Bierings<sup>2</sup>, Jurgen B. Langenhorst<sup>1</sup>, Alwin D.R. Huitema<sup>3,4</sup>, Jaap-Jan Boelens<sup>2,5</sup>, Stefan Nierkens<sup>1,2</sup>

<sup>1</sup> Center for Translational Immunology, University Medical Center Utrecht, Utrecht University, Utrecht, The Netherlands

<sup>2</sup> Princess Máxima Center for Pediatric Oncology, Utrecht University, Utrecht, The Netherlands

<sup>3</sup> Department of Clinical Pharmacy, University Medical Center Utrecht, Utrecht University, Utrecht, The Netherlands

<sup>4</sup> Department of Pharmacy & Pharmacology, Netherlands Cancer Institute, Amsterdam, The Netherlands

<sup>5</sup> Stem cell transplantation and cellular therapies program, Department Pediatrics, Memorial Sloan Kettering Cancer Center, New York, United States

*Manuscript in preparation*

## Abstract

Development of allo-immune lung syndromes (Allo-LS) after allogeneic hematopoietic cell transplantation is a life-threatening complication. Predictors for Allo-LS after HCT are lacking. This study aimed to evaluate potential clinical and biological predictors for Allo-LS. In a retrospective cohort analysis, incidence, outcomes, and immune reconstitution markers were related to Allo-LS. Using multivariate analysis, significant risk factors in univariate analyses were imputed in a Cox regression model via backward selection. Of the 380 patients (median age, 7.4 years; range 0.1-22.7), 22 developed bronchiolitis obliterans (BO) and 27 developed idiopathic pneumonia syndrome (IPS) at a median of 98.5 (range, 21-694) and 52 (range, 4-114) days after HCT respectively. Multivariate analysis showed that chemo-naivety (HR=1.78; 95% CI 0.98-3.23,  $p=0.04$ ) and plasma reactivation of adenovirus were predictors for Allo-LS (HR=1.75; 95% CI 1.26-2.44,  $p=0.0008$ ). In the IPS subgroup, non-malignant indication (HR=4.4; 95% CI 1.66-11.65,  $p=0.003$ ) and adenovirus (HR=4.05; 95% CI 1.81-9.03,  $p=0.0006$ ) were predictors. No independent predictors were identified for BO patients. We found a strong increase of EASIX scores, a marker for endothelial damage and transplant related thrombotic microangiopathy, shortly before the development of IPS. In addition, development of IPS was preceded by increased neutrophil levels. In BO patients, immune profiles were similar to controls (HCT patients without BO). Overall survival was worse in Allo-LS patients (59% for BO patients and 41% for IPS patients) compared to control patients (72%).

In conclusion, we identified chemo-naivety, adeno virus and non-malignant indication as predictors for development of Allo-LS. In addition, increased EASIX scores and neutrophils preceded IPS development. These immune profiles provide new directions to study the pathophysiology of Allo-LS.

## Introduction

Allogeneic hematopoietic cell transplantation (HCT) is a potentially curative procedure to treat a variety of malignant and nonmalignant hematologic disorders. Despite advances in HCT, non-infectious pulmonary complications can occur post HCT, which have been associated with mortality rates of 50-80 %. Idiopathic pneumonia syndrome (IPS), an early onset pulmonary complication, has an incidence of 2-12 % after HCT<sup>1,2</sup>. Bronchiolitis obliterans syndrome (BOS), a late onset pulmonary complication, has a highly variable incidence rate of 0-48 % after HCT, depending on transplantation setting<sup>3-6</sup>. Both complications are defined as Allo-immune lung syndromes (Allo-LS) as the incoming donor immune system appears to play a critical role (according to Versluys et al. 2010<sup>7</sup>). Respiratory virus (RV) in BAL might trigger alloreactivity in Allo-LS<sup>8</sup>. Additional endothelial and/or tissue damage caused e.g. by direct toxicity of used drugs, could accelerate the influx of donor-derived alloreactive T cells. Thrombotic microangiopathy (TMA), contributing to endothelial damage, may have a central role in the development of Allo-LS. However, the role of the activated alloimmune system and which immune and host tissue cells are most involved in the etiology of Allo-LS remains unclear.

We aimed to identify early immune predictors for Allo-LS and relate biological data from immune monitoring (leukocyte and lymphocyte populations, markers for endothelial damage) to the development of Allo-LS.

## Material and Methods

### Study design and Patients

All patients receiving their first allogeneic HCT between January 2004 and February 2018 at the University Medical Center in Utrecht, The Netherlands, were included. The conditioning regimen and source of hematopoietic stem cells were based on indication and availability according to (inter)national protocols/guidelines. The minimum follow-up for surviving patients was one month in this study. Data were collected prospectively in a local clinical database. Written informed consent was obtained from all participants and/or their parents before enrollment in accordance with the Declaration of Helsinki. The study was approved by the local ethical committee through trial numbers 05/143 and 11/063-k.

### Procedures

Graft-versus-host-disease (GvHD) prophylaxis consisted of cyclosporine A (CsA; targeted at trough levels of 150-250 mg/L for all patients) combined with prednisone 1 mg/kg (cord blood [CB]) or methotrexate (on day +1, +3, +6; unrelated donor). CsA was administered for a

minimum of 3 months (malignant disease) or 6 months (non-malignant disease) after HCT. Prednisone was tapered in 2 weeks starting 4 weeks post-HCT in benign disorders, and in one week after engraftment in malignant disorders. CB recipients were treated with filgrastim from day +7 after HCT until neutrophils were above 2000 cells/ml. Erythrocytes were transfused to maintain a minimal hemoglobin level of 4.3 mmol/L and platelets were administered in patients with evidence of mucosal bleeding or a hemoglobin level < 4.0 mmol/L. All patients received antiviral prophylaxis using acyclovir, gut decontamination and pneumocystis jiroveci prophylaxis according to local protocols. Patients were monitored weekly after HCT for adenovirus (AdV), cytomegalovirus (CMV), Epstein-Barr virus (EBV) and human herpesvirus 6 (HHV6) reactivation by PCR screening techniques. Viral reactivation was defined as having a viral load above 1000 copies/mL. Lymphocyte subsets consisting of CD3+ T cells, CD19+ B cells, and CD16+CD56+ NK cells were measured every other week up to 12 weeks after HCT and monthly thereafter using flow cytometry. Absolute cell counts were measured using TruCount technology.

### **Endothelial activation and stress index**

Endothelial activation and stress index (EASIX) scores, a biomarker for transplant associated microangiopathy were calculated using: LDH (U/l) \*Creatinine (mg/dL)/thrombocytes (nL). Pre-EASIX scores were defined as the EASIX score prior to conditioning and HCT. EASIX scores of Allo-LS patients were compared to EASIX scores of patients without Allo-LS at matching time points as described below.

### **IPS and BO definitions and diagnosis**

IPS was defined as the following definition, according to the American Thoracic Society: the evidence of widespread lung injury by clinical symptoms and radiological abnormalities, in the absence of active lower respiratory infection and other factors explaining pulmonary dysfunction (like cardiac dysfunction, fluid overload or renal failure). BO was defined according to the National Institutes of Health Consensus Criteria on Chronic GvHD disease 2014 as forced expiratory volume in 1 second (FEV1)/Forced Vital Capacity (FVC) < 0.7, FEV1 < 75%, evidence of air trapping (on pulmonary function tests [PFT] or high-resolution computed tomography [HRCT]) in the absence of respiratory tract infection. We adjusted these definitions with RV positivity in patients diagnosed with Allo-LS, as we previously found that these viruses in BAL and nasopharyngeal aspirate (NPA) were already present prior to HCT, and that there was no difference in therapeutic response to corticosteroid therapy in patients with or without RV present.

When Allo-LS was suspected (e.g. new onset respiratory signs or unforeseen worsening of respiratory condition, with a normal temperature and laboratory parameters unsuspecting

for infection) patients underwent the following work up: PFT (if feasible), chest HRCT, and NPA or BAL. PFT included at least spirometry (FEV1 and FVC), and in some cases body-box measurements (Residual volume, Total Lung Capacity) and CO-diffusion tests were done. Chest HRCTs were routinely reviewed by the radiologist, looking for signs of infiltrations, air trapping, pleural effusion, pneumothorax etc. A second radiologist examined all the scans to calculate the HRCT composite- and Allo-score as described by our group before. BAL and NPA were tested for bacteria (by GRAM stain and culture), fungi (by culture and Aspergillus antigen testing) and respiratory viruses (RV) (by PCR).

### **RV screening**

From 2008 onwards, all patients were screened following the pre-HCT pulmonary screening protocol, as described previously. This protocol includes microbial screening in BAL and NPA, HRCT of the lungs and pulmonary function tests (PFT) in children over 5 years of age. Microbial screening included bacterial cultures, PCR for RV panel, fungal cultures and Aspergillus antigen testing. Based on the screening, patients at risk for developing IPS or BO received prolonged GvHD prophylaxis, as we have shown a protective effect of immunosuppressive therapy on the incidence of Allo-LS in RV positive patients.

### **Treatment**

First line treatment of Allo-LS consisted of methylprednisolone (MP) 10 mg/kg/day iv for 3 days and 2 mg/kg/day thereafter, tapering by 25% per week to 0.5 mg/kg/day. MP pulses were repeated monthly until recovery, up to a maximum of 6 pulses. Recovery was defined as normalization of PFT and/or resolved symptoms. In between subsequent MP pulses prednisone 0.5mg/kg/day was given. For poor responders to MP-pulse therapy our protocol prescribed second line therapy of 3 weekly cycles of fludarabine 30 mg/m<sup>2</sup>/dose.

Other immunosuppressive agents (e.g. cyclosporine) were continued. In addition, azathioprine was given because of its suggested immune modulatory effect. In BO patients, imatinib was added for its known antifibrotic effects. Supportive care was provided with extra oxygen and mechanical ventilation when necessary. Furthermore, because of increased and prolonged immunosuppressive treatment, antifungal prophylaxis (voriconazol) was initiated if not already given.

### **Outcomes**

The main outcome of interest was the development of Allo-LS after HCT. Other outcomes of interest were early predictors/biomarkers related to the development of Allo-LS and overall survival related to Allo-LS.

## Statistical analysis

Duration of the follow up was defined as the time from HCT to the occurrence of Allo-LS, last assessment for surviving patients or death. For univariate analysis, cumulative incidence curves were computed for Allo-LS, taking the following competing risks into account: relapse and death caused by other causes than Allo-LS. P-values were calculated using Gray's test. For multivariate analysis, the risk factors significant ( $p < 0.05$ ) in univariate analysis were imputed in a Cox regression model via backward selection and p-values were calculated using Wald's test.

Immune reconstitution markers after transplantation were evaluated as time-dependent variables, specifically prior to the development of IPS and BO, to explore whether markers could be identified preceding clinical symptoms. As the onset of Allo-LS varied between patients, immune reconstitution markers were aligned between patients by setting the time point of Allo-LS development at time zero (index time). To compare immune reconstitution to patients that did not develop Allo-LS, a control group was created by comparison to a random selection of minimal 6 controls for each Allo-LS patient. For these controls the time point of immune reconstitution markers was aligned with the time of Allo-LS development in patients (e.g. if patient A developed IPS at 50 days after HCT, immune reconstitution markers in the 6 randomly selected controls were studied up to 50 days by setting day 50 at zero). Loess-smoothed regression lines were generated to compare both groups. Due to the heterogeneity of the data (unstructured repeated measurements with variable index time) no further statistical testing was performed, hence these analyses were considered exploratory. Acute and chronic GvHD were classified according to the Glucksberg<sup>9</sup> and Shulman<sup>10</sup> criteria. Statistical analysis was performed using R version 3.3.2.

## Results

### Patient characteristics

Three hundred eighty patients with a median of 7.4 years (range 0.1 to 22.7) were included (Table 1). Most patients were transplanted for malignant disease ( $n=196$ , 52%), followed by metabolic/inborn errors ( $n=66$ , 17.4%), immune deficiency ( $n=62$ , 16.3%), bone marrow failure ( $n=52$ , 13.7%) and autoimmune diseases ( $n=4$ , 1%). The majority of patients received chemotherapy-based conditioning (86%), in which busulfan in combination with fludarabine was most frequently used (36%). Serotherapy was administered in 272 patients (72%). 186 patients (49%) received chemotherapy prior to HCT. The median follow-up time was 35 months (range, 1.0-168.8). Of all patients, 49 (12.9%) developed Allo-LS at a median time of 74 days (range, 4-694) post-HCT. Of these 49 cases, 22 patients were diagnosed with BO (median time of diagnosis 98.5 days, range 21-694) and 27 patients with IPS (median time of diagnosis 52 days, range 4-114 ).

**Table 1.** Patient Characteristics

	No allo-LS (n = 331)	Allo-LS (n = 49)	
		IPS (n=27)	BO (n=22)
<b>Male, n (%)</b>	148 (45)	13 (48)	11 (50)
<b>Median age at HCT (range), y</b>	7 (0.1-22.7)	3 (0.2-17.0)	10 (0.2-17.1)
<b>Diagnosis, n (%)</b>			
<b>Malignant</b>	177 (53.4)	5 (19)	14 (64)
<b>Non-malignant</b>	154 (46.6)	22 (81)	8 (36)
<b>Chemotherapy prior to HCT, n (%)</b>	169 (51.1)	5 (19)	12 (44)
<b>Stem cell source, n (%)</b>			
<b>CB</b>	185 (56)	18 (67)	9 (41)
<b>BM</b>	138 (42)	9 (33)	13 (59)
<b>PBSCs</b>	8 (2)	0	0
<b>Conditioning regimen, n (%)</b>			
<b>Radiation based</b>	48 (14.5)	2 (7.4)	0
<b>Chemotherapy based</b>	283 (85.5)	25 (92.6)	22 (100)
<b>Busulfan-based</b>	247 (74.6)	23 (85.2)	22 (100)
<b>Non Busulfan-based</b>	36 (10.9)	2 (7.4)	0
<b>Serotherapy, n (%)</b>	242 (69.1)	21 (77.7)	11 (50)
<b>Ablative*, n (%)</b>			
<b>Yes</b>	310 (93.7)	25 (92.6)	22 (100)
<b>No</b>	21 (6.3)	2 (7.4)	0
<b>HLA mismatch, n (%)</b>			
<b>matched</b>	193 (58.3)	11 (40.7)	13 (59.1)
<b>mismatch</b>	136 (41.1)	16 (59.3)	8 (36.4)
<b>unknown</b>	2 (0.1)	0	1 (4.5)
<b>Donor type, n (%)</b>			
<b>Related</b>	78 (23.6)	5 (18.5)	8 (36.4)
<b>Unrelated</b>	253 (76.4)	22 (81.5)	16 (63.6)
<b>aGVHD, n (%)</b>			
<b>Grade II-IV</b>	88 (26.6)	7 (25.9)	3 (13.6)
<b>Viral reactivation, n (%)</b>			
<b>CMV</b>	71 (21)	7 (25.9)	3 (13.6)
<b>EBV</b>	47 (14.1)	8 (29.6)	5 (22.7)
<b>Adeno</b>	58 (17.5)	7 (25.9)	3 (13.6)
<b>HHV-6</b>	99 (29.9)	12 (44.4)	10 (45.5)
<b>Median pre-EASIX scores, range</b>	236 (11.26-30550)	479.5 (15.45-31017.56)	122.54 (22.50-23481)

## Outcomes

Cumulative incidence curves of potential predictors for Allo-LS are depicted in Figure 1. In multivariate Cox regression analysis chemo-naivety before HCT (HR=1.78; 95% CI 0.98-3.23, p=0.04) and viral reactivation of adenovirus (HR=1.75; 95% CI 1.26-2.44, p=0.0008) were independent predic-

tors for Allo-LS development. Chemo-naivety was defined as no chemotherapy or B cell therapy before the conditioning phase. In the IPS subgroup, non-malignant indication (HR=4.4; 95% CI 1.66-11.65,  $p=0.003$ ) and viral reactivation of adenovirus (HR=4.05; 95% CI 1.81-9.03,  $p=0.0006$ ) were predictors. In the BO subgroup, no predictors were identified in multivariate analysis.

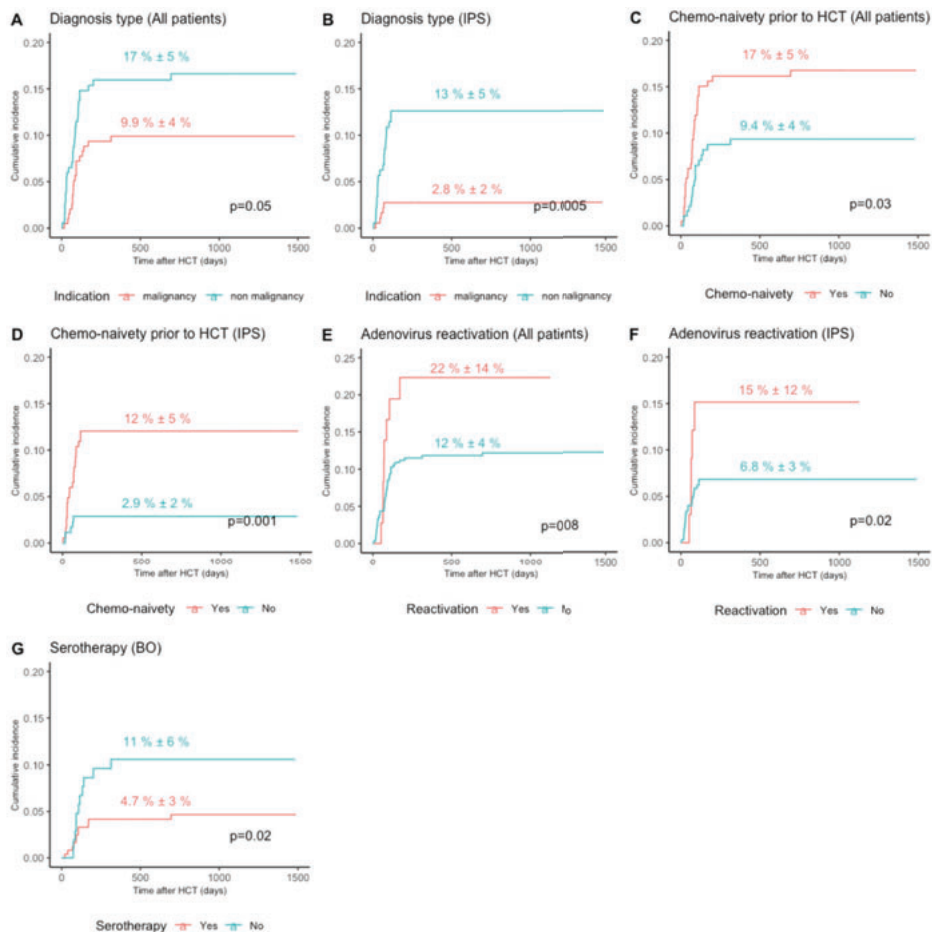


**Figure 1.** Cumulative incidence curves of Allo-LS development. Depicted p values are results of univariate analysis. A) Patients with malignant of nonmalignant disease indication (BO and IPS taken together). B) Patients with malignant of nonmalignant disease indication (IPS patients). C) Patients with chemotherapy before HCT compared with patients without chemotherapy (chemo-naïve patients, BO and IPS taken together). D) Patients with chemotherapy before HCT compared with patients without chemotherapy (IPS patients). E) Patients with adenovirus reactivation compared with patients without adenovirus reactivation after HCT (BO and IPS taken together). F) Patients with adenovirus reactivation compared with patients without adenovirus reactivation after HCT (IPS patients). G) Patients with serotherapy compared with patients without serotherapy (BO patients).

## Immune marker analysis

Immune profiles for total lymphocytes, NK cells and CD3+ CD4+ T cells, CD19+ B cells, CD3+ T cells were similar between Allo-LS patients and controls (Figure 3). A similar analysis was performed separately for IPS and BO, but due to the low number of patients and low number of observations, no relevant conclusions could be drawn (data not shown). IPS patients showed higher levels of neutrophils just before the diagnosis of Allo-LS compared to controls at corresponding time points (Figure 4). When stratifying these patients into RV positive and negative subgroups, RV+ IPS patients showed higher neutrophil counts than RV-IPS patients and RV+ or RV- controls. Neutrophil levels between BO patients and controls remained similar. EASIX scores were increased in IPS patients before the development of IPS compared to controls that did not develop IPS. No difference was noted for BO patients. Pre-treatment EASIX scores were no predictor for Allo-LS (Figure 2).

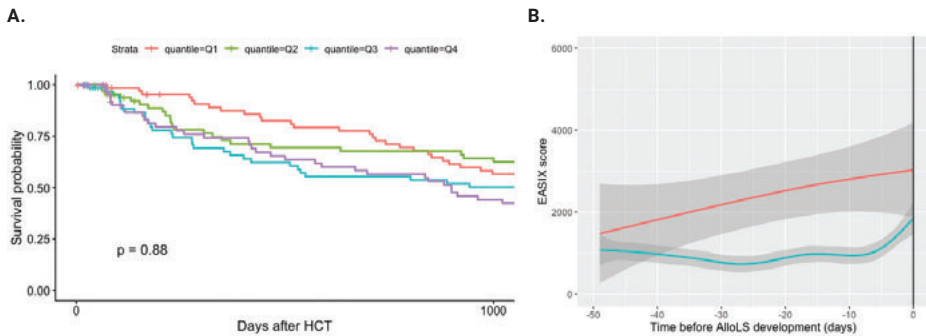


**Figure 2.** EASIX scores before HCT and before the development of IPS. A) Patients are stratified into 4 quartiles referring to pre-EASIX scores (Q1 = lowest EASIX scores, Q4 = highest EASIX scores). B) EASIX score in IPS patients (red) and controls (blue). The solid lines represent a Loess curve model, and 95% CI are depicted in light gray. Lines represent averages of EASIX score of individual patients.

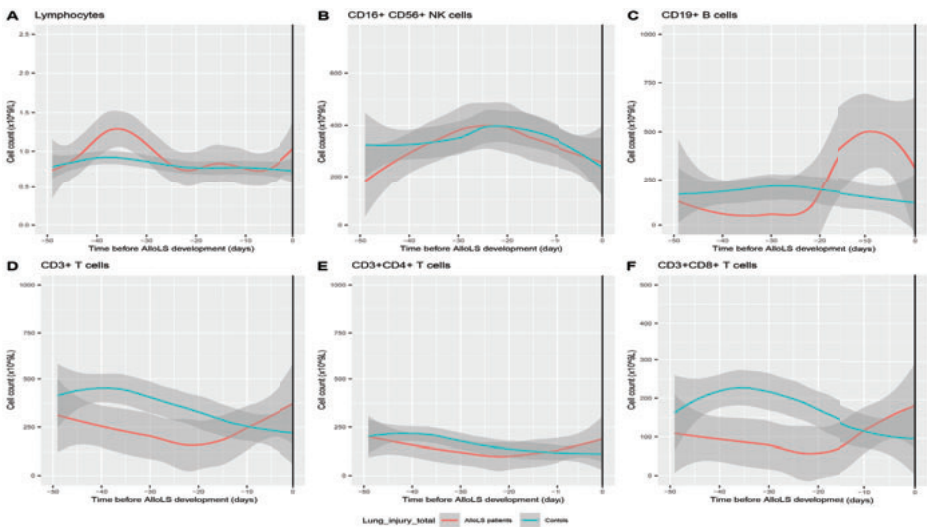


**Figure 3.** Immune profiles before the development of Allo-LS. The solid lines represent a Loess curve model, and 95% CI are depicted in light gray. Lines represent averages of immune counts of individual patients. A) Lymphocytes; B) CD16+CD56+ NK cells; C) CD19+ B cells; D) CD3+ T cells; E) CD3+ CD4+ T cells; F) CD3+ CD8+ T cells. Allo-LS patients are depicted in red and controls in blue.

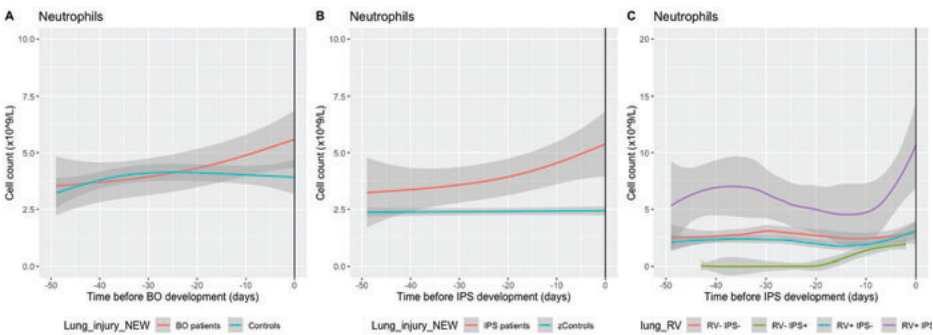


**Figure 4.** Neutrophil counts before the development of Allo-LS. The solid lines represent a Loess curve model, and 95% CI are depicted in light gray. Lines represent averages of EASIX score of individual patients. A) Neutrophil counts in BO patients (red) and controls (blue). B) Neutrophil counts in IPS patients (red) and controls (blue). C) Neutrophil counts in RV+ IPS patients (purple), RV- IPS patients (green), RV+ controls (blue) and RV- controls (red).

## Discussion

In this single center retrospective analysis, we showed that chemo-naivety and reactivation of adenovirus are predictors for Allo-LS. The main indication for chemotherapy before HCT is the treatment of malignant disease, aimed to kill tumor cells. Nonmalignant disease was an independent predictor for IPS, which was previously described in univariate analysis as a predictor for Allo-LS<sup>7</sup>. However, chemo-naivety was not taken into account in that study. Patients that did not receive chemotherapy prior to HCT were most often patients with nonmalignant disease indication. It remains to be studied

why chemo-naïve patients and patients with nonmalignant disease are more at risk to develop Allo-LS. One hypothesis could be that nonmalignant diseases cause more tissue damage to the lungs than malignant diseases.

Adenovirus reactivation prior to the development of Allo-LS was a predictor in the present study. Adenovirus reactivation was described previously as a risk factor in univariate analysis, but not in multivariate analysis<sup>7</sup>. It is possible that adenovirus reactivation triggers an inflammatory response at time of immune reconstitution. These parameters were not identified as predictors for BO. It is possible that the small numbers of patients and the retrospective nature of the previous study complicated the detection of predictors.

We showed an increase of EASIX scores before the clinical onset of IPS suggesting a relation with transplantation associated microangiopathy. To our knowledge, this is the first analysis exploring EASIX scores over time. In recent literature, EASIX scores predicted overall survival after GvHD and non-relapse mortality<sup>11</sup>, survival in lower-risk MDS and mortality after HCT<sup>12,13</sup>. This score combines three routine parameters (creatinine, lactate dehydrogenase, and thrombocyte counts) that have been associated with endothelial damage and transplant-associated thrombotic microangiopathy (TMA). In murine models, endothelial cell activation and injury have been associated with the development of IPS<sup>14</sup>. In pre-mortem long biopsy samples, pathological evidence of cell damage has been found<sup>15</sup>. We did not find any correlation between BO development and increased EASIX scores. To our knowledge, no other studies investigated the correlation between endothelial damage and BO. Our study shows that endothelial cell activation injury might underlie the pathology of IPS. Increased neutrophils preceded the development of IPS, but not BO. In mouse IPS models, neutrophils have been detected in BAL fluid and have been associated with increased levels of TNF- $\alpha$  and LPS<sup>16,17</sup>. In patients with ARDS, an abundance of neutrophil products (elastase, myeloperoxidase, metalloproteinases, and oxidants) in BAL fluid have been noticed, that might contribute to endothelial cell damage<sup>18</sup>.

Together, these data suggest that IPS and BO are distinct complications with a distinct pathology. Although the exact pathophysiology of Allo-LS remains unclear, present data suggest that endothelial damage plays a role in IPS.

In conclusion, we identified chemo-naivety and adenovirus reactivation as predictors for the development of Allo-LS. In addition, we identified non-malignant disease and adenovirus reactivation as predictor for IPS. The increase of EASIX scores before the development of IPS suggests that endothelial damage is involved in the pathophysiology of IPS. Potentially, this damage results in the influx of donor allo-reactive T cells. These results should be validated in a larger, preferable multicenter cohort.

## References

1. Ahya VN. Noninfectious Acute Lung Injury Syndromes Early After Hematopoietic Stem Cell Transplantation. *Clin Chest Med*. 2017. doi:<https://doi.org/10.1016/j.ccm.2017.07.002>.
2. Yanik GA, Grupp SA, Pulsipher MA, et al. TNF-receptor inhibitor therapy for the treatment of children with idiopathic pneumonia syndrome. a joint pediatric blood and marrow transplant consortium and children's oncology group study (ASCT0521). *Biol Blood Marrow Transplant*. 2015. doi:10.1016/j.bbmt.2014.09.019.
3. Sakaguchi H, Takahashi Y, Watanabe N, et al. Incidence, clinical features, and risk factors of idiopathic pneumonia syndrome following hematopoietic stem cell transplantation in children. *Pediatr Blood Cancer*. 2012. doi:10.1002/pbc.23298.
4. Duncan CN, Buonanno MR, Barry E V., Myers K, Peritz D, Lehmann L. Bronchiolitis obliterans following pediatric allogeneic hematopoietic stem cell transplantation. *Bone Marrow Transplant*. 2008. doi:10.1038/bmt.2008.19.
5. Park M, Koh KN, Kim BE, Im HJ, Seo JJ. Clinical features of late onset non-infectious pulmonary complications following pediatric allogeneic hematopoietic stem cell transplantation. *Clin Transplant*. 2011. doi:10.1111/j.1399-0012.2010.01357.x.
6. Keates-Baleeiro J, Moore P, Koyama T, Manes B, Calder C, Frangoul H. Incidence and outcome of idiopathic pneumonia syndrome in pediatric stem cell transplant recipients. *Bone Marrow Transplant*. 2006. doi:10.1038/sj.bmt.1705436.
7. Versluys AB, Rossen JWA, van Ewijk B, Schuurman R, Bierings MB, Boelens JJ. Strong Association between Respiratory Viral Infection Early after Hematopoietic Stem Cell Transplantation and the Development of Life-Threatening Acute and Chronic Alloimmune Lung Syndromes. *Biol Blood Marrow Transplant*. 2010. doi:10.1016/j.bbmt.2009.12.534.
8. Versluys B, Bierings M, Murk JL, et al. Infection with a respiratory virus before hematopoietic cell transplantation is associated with alloimmune-mediated lung syndromes. *J Allergy Clin Immunol*. 2018. doi:10.1016/j.jaci.2017.03.055.
9. Glucksberg, H; Storb, R; Fefer, A; Buckner, C.D. ; Neiman, Paul; Clift, R.A.; Lerner, K.G.; Thomas E. Clinical manifestations of graft-versus-host disease in human recipients of marrow from HL-A-matched sibling donors. *Transplantation*. 1974. doi:10.1097/00007890-197410000-00001.
10. Shulman HM, Sullivan KM, Weiden PL, et al. Chronic graft-versus-host syndrome in man: A long-term clinicopathologic study of 20 seattle patients. *Am J Med*. 1980. doi:[https://doi.org/10.1016/0002-9343\(80\)90380-0](https://doi.org/10.1016/0002-9343(80)90380-0).

11. Luft T, Benner A, Jodele S, et al. EASIX in patients with acute graft-versus-host disease: a retrospective cohort analysis. *Lancet Haematol*. 2017. doi:10.1016/S2352-3026(17)30108-4.
12. Merz A, Germing U, Kobbe G, et al. EASIX for prediction of survival in lower-risk myelodysplastic syndromes. *Blood Cancer J*. 2019. doi:10.1038/s41408-019-0247-z.
13. Luft T, Benner A, Terzer T, et al. EASIX and mortality after allogeneic stem cell transplantation. *Bone Marrow Transplant*. 2019. doi:10.1038/s41409-019-0703-1.
14. Cooke KR, Jannin A, Ho V. The Contribution of Endothelial Activation and Injury to End-Organ Toxicity following Allogeneic Hematopoietic Stem Cell Transplantation. *Biol Blood Marrow Transplant*. 2008. doi:10.1016/j.bbmt.2007.10.008.
15. Altmann T, Slack J, Slatter MA, et al. Endothelial cell damage in idiopathic pneumonia syndrome. *Bone Marrow Transplant*. 2018. doi:10.1038/s41409-017-0042-z.
16. Cooke KR, Kobzik L, Martin TR, et al. An experimental model of idiopathic pneumonia syndrome after bone marrow transplantation: 1. The roles of minor H antigens and endotoxin. *Blood*. 1996. doi:10.1182/blood.v88.8.3230.bloodjournal8883230.
17. Cooke KR, Hill GR, Gerbitz A, et al. Tumor necrosis factor- $\alpha$  neutralization reduces lung injury after experimental allogeneic bone marrow transplantation. *Transplantation*. 2000. doi:10.1097/00007890-200007270-00006.
18. Yanik G, Hellerstedt B, Custer J, et al. Etanercept (Enbrel) administration for idiopathic pneumonia syndrome after allogeneic hematopoietic stem cell transplantation. *Biol Blood Marrow Transplant*. 2002. doi:10.1053/bbmt.2002.v8.pm12171486.



# Chapter 9

## General Discussion

---

Discussion

The immune system is a complex and dynamic system. HCT and immunotherapy further challenge this system, making understanding of the functional dynamics during and after the interventions even more complex. Particularly in pediatric patients, immune monitoring has been limited to studies with small patient numbers without longitudinal sampling, phenotyping of immune subsets/markers and confirmation of immune cell function. The questions arising from this thesis are described below in combination with the most important lessons learned.

Part 1 – Immune monitoring in high-risk neuroblastoma patients

In neuroblastoma patients, immune monitoring is largely lacking (Chapter 2). In part 1 new methods for immune monitoring before and after autologous HCT in high-risk neuroblastoma patients are described (Figure 1).

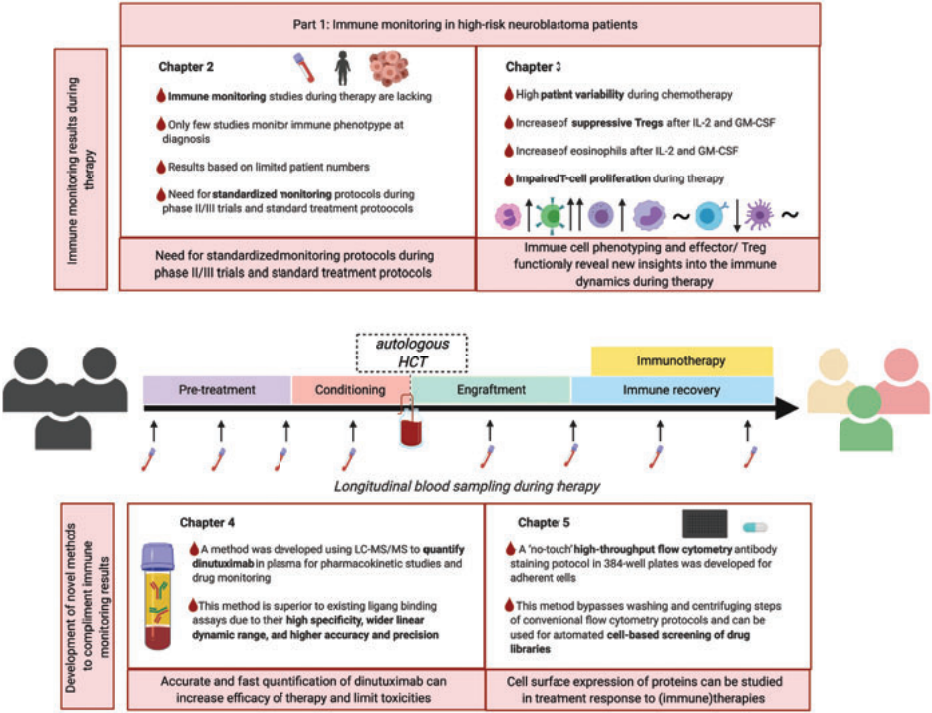


Figure 1: Key findings of Chapter 2-5 in Part 1 of this thesis. Created with BioRender.com

Despite intensive therapy, many children suffer from refractory and relapse of disease. Immune phenotyping in high-risk neuroblastoma patients demonstrated large patient variability (Chapter 3). Sample size was too small to combine clinical parameters with dynamic insights. Immune monitoring aimed to explore the functional dynamics of the immune system before and during

therapy. Standardized immune monitoring in larger patient groups is required to be able to relate the variability in numbers and function of immune cells to treatment efficacy. However, functional assays studying Treg and T-cell effector function showed more homogenous results. A strong increase (5-fold) of suppressive regulatory T cells (suppression confirmed in functional assays) and eosinophils in peripheral blood after IL-2 and GM-CSF treatment was identified. Interestingly, T cell proliferation (assessed after isolation of peripheral blood T cells) was impaired during therapy. It remains debatable if impaired T cell proliferation after HCT is caused by the tumor or by the intensive treatment regimen. To determine which specific pathways of T cell proliferation are impaired, and if they could be modulated, needs to be investigated.

The timing of immune monitoring related to (immune)therapy is important to capture the dynamics of the biological process. The dosage and half-life of the drugs (therapy) and the life span of immune parameters detectable in blood should be taken into account. In case of dinutuximab beta (anti-gd2 antibody ch14.18/CHO, Chapter 4), pharmacokinetic (PK) and pharmacodynamic (PD) properties can be studied. The dose and timing of dinutuximab beta can be adjusted for each patient to investigate if this can lead to optimal exposure and limited toxicities. For IL-2, a high (4.5 MIU/m<sup>2</sup>/day) and low dose (1-3 MIU/ m<sup>2</sup>/day) are administered during immunotherapy potentially having distinct effects on immune dynamics. In healthy adults, Tregs are 7-10 times more sensitive to IL-2 than NK cells and memory T cells indicating that low dose IL-2 will mainly expand Tregs<sup>8</sup>. In autoimmunity, IL-2 has been used for its favorable effect on Treg expansion. In neuroblastoma high levels of Tregs were observed in blood that suppress effector cells *in vitro* (Chapter 3). This increase of suppressive Tregs was temporarily after IL-2 administration, as levels normalized at subsequent sampling points. Without frequent sampling around IL-2 administration, Treg increase would have been missed. Whether this is a relevant predictor for outcome is currently unknown. We hypothesize that suppressive Tregs might hamper anti-neuroblastoma immune responses. If the effect of drugs is unknown on immune parameters, more frequent sampling during the first treatment cycle may be warranted. The timing of sampling also depends on the measured parameter. For instance, tumor-infiltration and persistence by T-cells or induction of T-cell proliferation develops over a few days, while receptor expression changes rapidly upon stimulation<sup>9</sup>.

Part 2 – Immune monitoring in pediatric patients receiving allogeneic HCT

In part 2 risk factors for non-infectious complications and the value of immune monitoring after allogeneic HCT were investigated (Figure 2).

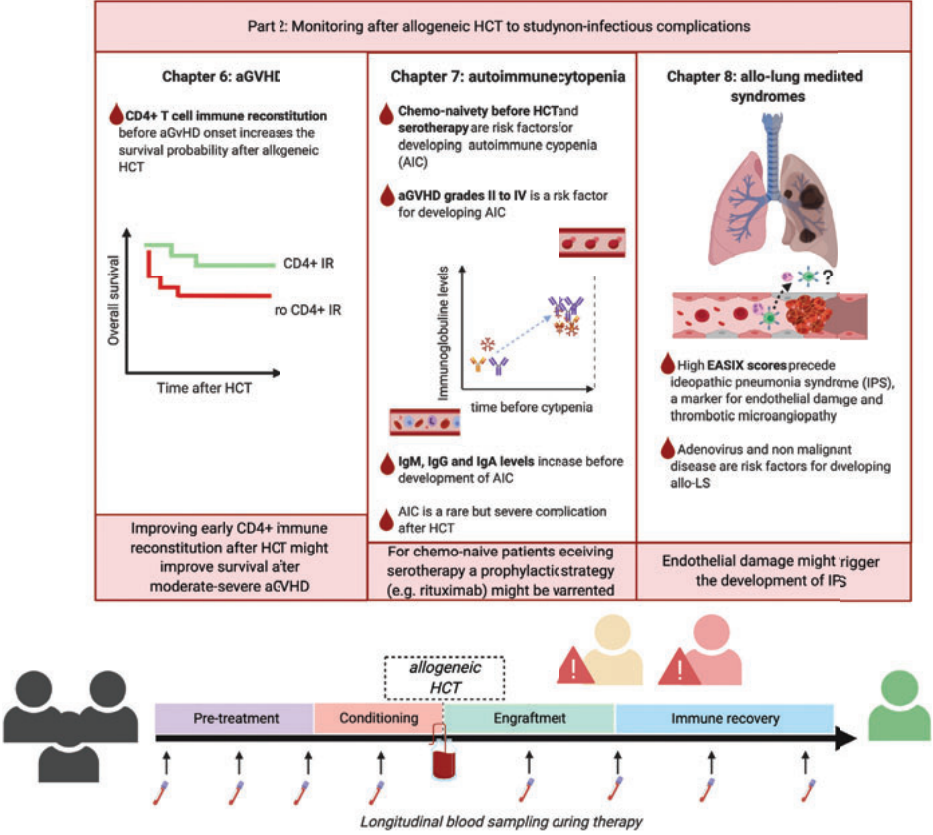


Figure 2: Key findings of Chapter 6-8 in Part 2 of this thesis. Created with BioRender.com

When immune monitoring aims to predict complications after HCT, early and frequent blood sampling may be warranted. In the single-center pediatric cohort studied in part 2 of this thesis, lymphocyte subsets and immunoglobulin levels were monitored every other week up to 12 weeks after HCT and monthly thereafter. This frequent blood monitoring enabled the study of immune profiles weeks before the onset of complications.

Implementing immune monitoring into daily clinical practice is still far from being achieved. Studies are limited by small patient numbers, rare diseases, and lack of harmonization of monitoring and treatment protocols<sup>1</sup>. In addition, the recognition of rare complications after HCT might be difficult and defined differently between treatment centers. Most studies associate 'static' clinical parameters (disease indication, treatment regimen, complications such as GvHD,

viral reactivation) to survival and incidence of complications. However, immune response to therapy and the risk of complications in the months after HCT are 'dynamic' processes. Immune monitoring after HCT showed that patients with CD4+ T cell reconstitution had lower risk of GvHD-associated death (Chapter 6), lower relapse risk, better overall survival, lower risk of viral reactivations, lower virus-induced death and virus related GvHD<sup>2-5</sup>. It is hypothesized that patients with CD4+ T cell reconstitution have higher regulatory T cell (Treg) counts that suppress the allogeneic reaction in aGvHD. Unfortunately, Treg data was lacking. Further it is possible that CD4+ T cell counts vary less in blood than other immune cells resulting in a parameter that is easy to relate to HCT. Early CD4+ T cell reconstitution might reflect a healthy balanced immune system with large TCR-diversity. However, improving CD4+ T cell immune reconstitution after HCT could enhance the success of HCT.

No association was found between CD4+ T cell reconstitution and autoimmune cytopenia (AIC), however increase of immunoglobulins preceded AIC (Chapter 7). Although no increase in total absolute B-cells was observed, it is hypothesized that the production of autoantibodies by plasma B cells is involved in the pathogenesis of AIC. If residual autologous plasma cells are responsible for the dysregulated antibody production, therapies targeting these cells such as daratumumab or bortezomib may be warranted. Chemo-naivety before HCT and treatment with serotherapy (mainly antithymocyte globulin [ATG]) were predictors for AIC. Lymphodepletion by ATG could inhibit the mechanisms of tolerance by depleting regulatory T cells and leading to expansion of autoreactive naive and/or memory T cells. Individualizing the dose of ATG may therefore reduce the probability of developing AIC<sup>6</sup>. Chemotherapy before HCT might also remove AIC initiating regulatory lymphocytes such as Tregs and innate lymphoid cells or antibody-producing plasma cells that would otherwise survive after HCT conditioning. These results suggest that in chemo-naïve patients treated with serotherapy a prophylactic treatment strategy could be initiated when immunoglobulin levels increase and before symptoms of AIC develop.

The potential additive value of predictive scores for complications after HCT combining different biological predictors is worth exploring. In patients with idiopathic pneumonia syndrome (IPS), an increase of the endothelial activation and stress index (EASIX) score preceded the clinical onset of IPS (Chapter 8). This score, combining the three routinely measured parameters creatinine, lactate dehydrogenase and thrombocyte counts, predicted overall survival after GvHD and non-relapse mortality<sup>7,8</sup>. A higher EASIX score preceding the onset of IPS might imply that IPS development is associated with endothelial damage and transplant-associated thrombotic microangiopathy. Potentially, endothelial damage might result in the influx of donor allo-reactive T cells.

The results of part 2 of this thesis show the potential of combining clinical predictors with dynamic insights of the immune system to generate new hypotheses on the pathogenesis of complications after HCT. Eventually, this may lead to a feasible intervention to prevent these complications.

*Value of peripheral blood monitoring and correlation to the tumor microenvironment/targeted organs*

Immune monitoring in peripheral blood is most attractive as sample collection is easy and longitudinal sampling is feasible. However, the question arises what the relevance is of peripheral blood monitoring and if it reflects the tumor microenvironment (in case of malignancy) or effected organ(s) (in case of non-infectious complications). In the studies described in this thesis, immune monitoring was performed longitudinally and unstructured (i.e. no predefined timepoints for sampling). The analysis of these dataset is challenging given the heterogeneous nature of the collected data. In the future, advanced mathematical techniques like mixed effects modelling could be employed to fully unravel the dynamics of the different immune markers.

Despite the small number of patients, longitudinal sampling and in depth immune cell phenotyping and functional analyses revealed new insights into the immune dynamics of neuroblastoma patients. Whether these findings translate to the tumor microenvironment and clinical outcome remains to be studied.

## **Conclusion**

In this thesis, the potential of immune monitoring before and after HCT in pediatric patients was described. Immune monitoring has the ability to generate new hypotheses on the pathogenesis and mechanisms of disease. In addition, identification of predictors potentially aid to stratify responders and non-responders to therapy. Standardization of the design of immune monitoring protocols within clinical trials will enable comparison between trials and increase patient numbers. As each patient is unique, immune monitoring can facilitate future personalized treatment. These efforts may maximize clinical efficacy and minimize toxicities. Our results identified several factors that might be important for the success and outcome of HCT. The field is only at the beginning of critically evaluating the clinical utility of immune monitoring approaches, some of which involve novel assays. Immune monitoring will facilitate the 'switch' from a 'one-size fits-all' approach to a more detailed patient stratification and future personalized treatment.

1. Nierkens S, Lankester AC, Egeler RM, et al. Challenges in the harmonization of immune monitoring studies and trial design for cell-based therapies in the context of hematopoietic cell transplantation for pediatric cancer patients. *Cytotherapy*. 2015;17(12):1667-1674. doi:10.1016/j.jcyt.2015.09.008.
2. Admiraal R, Koning CCH De, Lindemans CA, Bierings MB. Translational and clinical immunology Viral reactivations and associated outcomes in the context of immune reconstitution after pediatric hematopoietic cell transplantation. *J Allergy Clin Immunol*. 2017;140(6):1643-1650.e9. doi:10.1016/j.jaci.2016.12.992.
3. Admiraal R, van Kesteren C, Jol-van der Zijde CM, et al. Association between anti-thymocyte globulin exposure and CD4+ immune reconstitution in paediatric haemopoietic cell transplantation: a multicentre, retrospective pharmacodynamic cohort analysis. *Lancet Haematol*. 2015;2(5):e194-e203. doi:https://doi.org/10.1016/S2352-3026(15)00045-9.
4. Admiraal R, Lindemans CA, Van Kesteren C, et al. Excellent T-cell reconstitution and survival depend on low ATG exposure after pediatric cord blood transplantation. *Blood*. 2016;128 (23): 2734-2741. doi:10.1182/blood-2016-06-721936.
5. Admiraal R, Chiesa R, Bierings M, et al. Early CD4+ Immune Reconstitution Predicts Probability of Relapse in Pediatric AML after Unrelated Cord Blood Transplantation: Importance of Preventing in Vivo T-Cell Depletion Using Thymoglobulin®. *Biol Blood Marrow Transplant*. 2015;21(2):S206. doi:10.1016/j.bbmt.2014.11.315.
6. Admiraal R. Individualizing dosing of serotherapy in allogeneic hematopoietic cell transplantation – a delicate balance. PhD dissertation, University Leiden, 2017.
7. Luft T, Benner A, Jodele S, et al. EASIX in patients with acute graft-versus-host disease: a retrospective cohort analysis. *Lancet Haematol*. 2017;4(9):e414-e423. doi:10.1016/S2352-3026(17)30108-4.
8. Luft T, Benner A, Terzer T, et al. EASIX and mortality after allogeneic stem cell transplantation. *Bone Marrow Transplant*. 2020;55(3):553-651. doi:10.1038/s41409-019-0703-1.
9. Yu A, Snowwhite I, Vendrame F, et al. Selective IL-2 responsiveness of regulatory t cells through multiple intrinsic mechanisms supports the use of low-dose IL-2 therapy in type 1 diabetes. *Diabetes*. 2015;64(6):2172-83. doi:10.2337/db14-1322.





# Appendices

**Nederlandse samenvatting**

**Dankwoord**

**Curriculum vitae**

**List of publications**

---

## **Immuun monitoring in de context van hematopoietische stamceltransplantatie in kinderen**

Hematopoietische (stam)celtransplantatie (HCT) is een potentieel levensreddende behandeling voor ernstig zieke patiënten met maligniteiten of niet-maligne ziektes zoals immuundeficiënties, metabole ziektes en beenmergfalen. Deze behandeling draagt verschillende risicofactoren met zich mee. Na de transplantatie met cellen afkomstig van een donor (allogeen) is het mogelijk dat er een afweerreactie ontstaat van de patiënt tegen de donor (afstoting) of van de donor tegen de patiënt. In dit laatste geval spreken we van transplantatieziekte, oftewel Graft-versus-Host-Disease. Deze kan acuut of chronisch zijn. Naast transplantatieziekte, is de patiënt vatbaar voor levensbedreigende complicaties die infectieus of niet-infectieus van aard kunnen zijn. Ook is het mogelijk dat de oorspronkelijke ziekte terugkomt (relapse/recidief). Deze risicofactoren samen, resulteren in een hoge morbiditeit en mortaliteit na HCT.

De laatste jaren wordt autologe HCT vaker gecombineerd met aanvullende immuuntherapie. Dit gebeurt bijvoorbeeld bij kinderen met neuroblastoom. Zij worden na de autologe HCT behandeld met immuuntherapie. Immuuntherapie is een verzamelnaam voor verschillende behandelingen waarbij de natuurlijke afweerreactie tegen kankercellen wordt versterkt. Het is vaak niet bekend hoe het immuunsysteem van de patiënt reageert op deze medicijnen, na de zeer intensieve HCT. Ook zijn er nog te weinig factoren bekend die ernstige complicaties in een vroeg stadium kunnen voorspellen. Het monitoren van het immuunsysteem tijdens ziektebeloop en behandeling, kan mogelijk inzicht geven in het effect van (immuun)therapie.

De kennis, die via immuunmonitoring wordt verkregen, kan de ontwikkeling van nieuwe therapeutische strategieën bevorderen. Het monitoren van immuuncellen ten tijde van de diagnose kan nieuwe inzichten geven in het ziektemechanisme en risicofactoren correleren aan de ernst van de ziekte. Daarnaast kan immuunmonitoring helpen om toxische bijwerkingen zo veel mogelijk te voorkomen. Immuunmonitoring kan ook een rol spelen bij de ontwikkeling van gepersonaliseerde behandelingen, waarin behandelstrategieën worden geoptimaliseerd op basis van resultaten van immuunmonitoring.

Dit proefschrift bestaat uit twee delen. In deel 1 beschrijven we de resultaten van immuunmonitoring in kinderen met een hoog-risico neuroblastoom. In deel 2 beschrijven we de voorspellers van complicaties die na allogene HCT kunnen optreden.

## Deel 1 – Immunosmonitoring in patiënten met een hoog-risico neuroblastoom

Een neuroblastoom is een tumor van het sympathische of autonome zenuwstelsel. Bijna alle kinderen die neuroblastoom krijgen, zijn jonger dan 6 jaar. Aan de hand van bepaalde kenmerken worden patiënten met een neuroblastoom ingedeeld in risicogroepen. De behandeling is aangepast aan de risicogroep. Laag-risicopatiënten hebben een goede overlevingskans (5-jaarsoverleving van 90-95%), terwijl hoog-risicopatiënten een slechte prognose hebben (5-jaarsoverleving van 40-50%). Behandeling van hoog-risicopatiënten bestaat uit een combinatie van chemotherapie, het operatief verwijderen van de tumor indien mogelijk, een autologe HCT, radiotherapie en immuuntherapie. Immuuntherapie bestaat uit het toedienen van het antilichaam anti-GD2 in combinatie met de cytokine GM-CSF, isotretinoïne en tot voorkort de cytokine IL-2.

Patiënten reageren verschillend op immuuntherapie. Bij niet iedere patiënt leidt het tot het beoogde effect en soms moet de therapie vroegtijdig gestopt worden omdat er toxische bijwerkingen optreden. Het monitoren van het immuunsysteem tijdens therapie zou meer inzicht kunnen geven in de patiënten die wel of niet reageren op de therapie. In **hoofdstuk 2** wordt een overzicht gegeven van de beschikbare literatuur over immuunmonitoring in neuroblastoom patiënten. Literatuur over het fenotype en de frequentie van immuuncellen in het bloed, beenmerg of tumor voor en tijdens behandeling van neuroblastoom patiënten wordt besproken. Ook wordt besproken hoe deze bevindingen zich relateren aan het resultaat van de behandeling. Dit hoofdstuk laat zien, dat de resultaten van de beschreven studies vaak gebaseerd zijn op kleine patiëntengroepen (soms 3 tot 5 patiënten). Daarnaast ontbreken geharmoniseerde immuunmonitoring protocollen waardoor het moeilijk wordt om studies te vergelijken. Daarom geven we in dit hoofdstuk een voorbeeld van, hoe gestandaardiseerde immuunmonitoring protocollen geïmplementeerd kunnen worden in preklinische studies en klinische trials.

In **hoofdstuk 3** wordt een prospectieve studie beschreven waarin het fenotype en de frequentie van immuuncellen in het bloed van hoog-risico neuroblastoom patiënten gemonitord is gedurende therapie. In deze studie zijn 25 patiënten gemonitord ten tijde van chemotherapie, voor HCT, en tijdens immuuntherapie (na HCT). De resultaten van deze studie laten zien dat de dynamiek van immuuncellen in het bloed verschillend is tussen neuroblastoom patiënten onderling tijdens chemotherapie. Daarnaast wordt een stijging van regulerende T-lymfocyten (Tregs) waargenomen na IL-2 en GM-CSF-therapie. Ook nemen de eosinofiele granulocyten en monocyten toe na GM-CSF-therapie en stijgt de totale lymfocyten populatie en CD56+/CD16+ NK-cel populatie na IL-2 therapie. Naast het bestuderen van het fenotype en frequentie, is de

functie van deze immuuncellen bepaald in vitro. De Tregs waren in staat om in vitro effector T-cellen van gezonde donoren te onderdrukken. In tegenstelling tot de Tregs, was de proliferatie in vitro van effector T cellen afkomstig uit bloed van neuroblastoom patiënten verstoord na HCT. Deze bevindingen laten zien, dat immuunmonitoring tijdens therapie nieuwe inzichten kan geven in het effect van therapie op het immuunsysteem.

Het antilichaam anti-GD2, dat tijdens immuuntherapie wordt gegeven, herkent het glycolipide GD2 op de membraan van neuroblastoom cellen. Dit glycolipide is niet beperkt tot neuroblastoom cellen, maar komt ook tot expressie op centraal zenuwweefsel en perifere zenuwcellen. Dit leidt tot neuropathische pijn tijdens de therapie en in sommige gevallen tot het vroegtijdig stopzetten van de anti-GD2 behandeling. Er is weinig bekend over de effectiviteit en toxiciteit van anti-GD2 in relatie tot de toedieningsdosis. Door anti-GD2 te kwantificeren in plasma van patiënten kan mogelijk de toedieningsdosis geoptimaliseerd worden. In **hoofdstuk 4** wordt een meetmethode om anti-GD2 te kwantificeren door middel van LC-MS/MS beschreven. Deze methode is sneller, gemakkelijker te implementeren in geharmoniseerde immuunmonitoring protocollen, heeft een groter lineair bereik en hogere selectiviteit dan bestaande meetmethodes. Deze laatste methodes zijn gebaseerd zijn op antilichaam binding analyses.

Naast immuunmonitoring is de vraag naar nieuwe therapeutische strategieën groot. Neuroblastoom cellen kunnen het immuunsysteem ontwijken door de expressie van MHC-1 op het oppervlak te vermijden. Zonder MHC-1 is er geen antigeen presentatie en kunnen cytotoxische T-cellen de tumor niet herkennen. Er zijn eiwitten zoals IFN $\gamma$ , die MHC-1 weer tot expressie kunnen brengen. Om geschikte geneesmiddelen te vinden, die MHC-1 weer tot expressie brengen en eventueel gecombineerd kunnen worden met de huidige therapie, zijn geautomatiseerde technieken met een hoge doorvoercapaciteit (high-throughput screening) nodig. In **hoofdstuk 5** wordt een methode beschreven om adherente neuroblastoom cellijnen te screenen in 384-wells platen in combinatie met het uitlezen van de MHC-1 expressie met behulp van flowcytometrie.

## **Deel 2 – Immuunmonitoring in pediatrische patiënten die een allogene HCT ondergaan**

Bij een allogene HCT worden stamcellen van een donor getransplanteerd naar de patiënt. Stamcellen afkomstig van het beenmerg, het perifere bloed of het navelstrengbloed kunnen gebruikt worden. Na HCT kunnen verschillende complicaties optreden die invloed hebben op de kwaliteit van leven, morbiditeit en mortaliteit. Veel voorkomende complicaties zijn transplantatieziekte, virale re-activaties en terugkeer van de ziekte. Het is van belang om beter te

begrijpen hoe deze complicaties ontstaan, en het is van belang om het ontstaan van deze complicaties eerder te kunnen voorspellen. De complicaties, die moeilijk te behandelen zijn, worden besproken in deel 2 van dit proefschrift.

Een veelvoorkomende complicatie na allogene HCT is acute graft-versus-host-disease (GvHD). In **hoofdstuk 6** laat resultaat van immuunmonitoring zien dat kinderen met een snel CD4+ T-lymfocyt herstel een grotere kans hebben om zeer ernstige acute GvHD te overleven vergeleken met kinderen met een traag CD4+ T-lymfocyt herstel na HCT.

Een andere complicatie die minder vaak voorkomt, maar zeer ernstig kan zijn als er niet tijdig wordt ingegrepen met immuun onderdrukkende medicatie, is autoimmuun cytopenie (AIC). Het is onbekend hoe deze complicatie ontstaat. In **hoofdstuk 7** wordt een retrospectieve studie beschreven waarin risicofactoren op het ontstaan van AIC zijn geanalyseerd. De resultaten van deze studie laten zien dat kinderen die niet voorbehandeld zijn met chemotherapie (voor HCT) een hogere kans hebben op het ontwikkelen van AIC na HCT. Ook blijkt uit deze studie dat acute GvHD en het gebruik van serotherapie een risicofactor zijn voor de ontwikkeling van AIC. In de periode voor AIC werden verhoogde immunoglobuline gehalten (zowel IgG, als IgM en IgA) in het bloed gemeten. Dit betekent dat men alert moet zijn op het ontwikkelen van AIC bij verhoogde immunoglobuline gehalten na HCT. Er werd geen stijging waargenomen van B-cellen. Dit neemt niet weg dat deze B-cellen auto-antilichamen kunnen produceren die mogelijk betrokken zijn bij de pathogenese van AIC.

In **hoofdstuk 8** wordt een vergelijkbare studie besproken waarin risicofactoren voor het ontstaan van allo-immuun gemedieerde longcomplicaties worden besproken. Er wordt gefocust op de twee meest voorkomende longcomplicaties: idiopathisch longontsteking syndroom (IPS) en bronchiolitis obliterans (BO). Het immuun herstel na HCT wordt onderzocht en vergeleken met patiënten zonder deze complicaties. De resultaten van deze studie laten zien dat, voorafgaand aan het ontwikkelen van IPS, patiënten een verhoogde endotheel activatie en stress index (EASIX) score hebben. Deze score is gebaseerd op een combinatie van creatinine-, lactaat dehydrogenase gehalte en trombocyten aantallen. Het is mogelijk dat schade aan endotheelcellen resulteert in de influx van donor T-lymfocyten, die vervolgens meespelen in de ontwikkeling van IPS. Daarnaast hebben kinderen die niet voorbehandeld zijn met chemotherapie (voor HCT) en/of een virale re-activatie van het adenovirus een verhoogd risico op het ontwikkelen van IPS of BO.

Deel 2 van dit proefschrift laat de potentie zien van het combineren van risicofactoren met de analyse van het immuun herstel om nieuwe hypotheses te genereren over de pathogenese van verschillende complicaties na HCT.

Concluderend laat dit proefschrift de potentie zien van immuunmonitoring in de context van HCT. Immuunmonitoring biedt de mogelijkheid om nieuwe hypotheses te genereren over verschillende ziektemechanismen. Daarnaast, kunnen geïdentificeerde voorspellers/markers mogelijk helpen om patiënten in te delen naargelang hun kans om te reageren op een bepaalde behandeling. Als immuunmonitoring protocollen gestandaardiseerd kunnen worden binnen klinische trials, dan kunnen resultaten hiervan gemakkelijker vergeleken worden. Immuunmonitoring kan in de toekomst bijdragen aan de ontwikkeling van een gepersonaliseerde behandeling zodat het maximale effect van de behandeling wordt bereikt met minimale toxiciteit.



## Dankwoord

Ken je dat gevoel van een achtbaan? Je stapt nieuwsgierig in zonder precies te weten waar je aan begint. Met pieken en dalen, af en toe een keertje over de kop, maar uiteindelijk heel trots, met beide benen weer op de grond en een ervaring rijker. Zonder een stevig fundament, pilaren, karretjes en veiligheidsgordels was deze rit nooit mogelijk geweest.

Allereerst wil ik mijn begeleidingsteam bedanken om mij aan boord te nemen!

Stefan, dank voor je enthousiasme, betrokkenheid en vele ideeën tijdens mijn promotieonderzoek de afgelopen 4.5 jaar. Ondanks je drukke agenda en onze wekelijkse meetings, maakte je tijd om 'even' in het lab naar ruwe data te kijken, een presentatie voor te bespreken of kwam je spontaan even binnen lopen in onze kamer voor een brainstormsessie met nieuwe ideeën. Geen vraag was te veel, altijd geïnteresseerd, en ten tijde van wat bureaucratische hordes bood je altijd steun!

Alwin, dank voor je steun en tijd die je hebt bijgedragen om dit werk tot een succes te maken. Altijd stipt op tijd, gestructureerd en geen enkele email onbeantwoord gelaten. Als mijn karretje van de baan dreigde te raken, zorgde jij dat we terug op het juiste pad kwamen. Overal had jij een oplossing voor, en na elk gesprek een duidelijke route.

Jaap Jan, dank voor je vertrouwen en het delen van je kennis en ervaring. De achtbaan kon voor jou niet snel genoeg gaan. Terwijl ik nog de ene na de andere foutmelding kreeg bij het inladen van de klinische data in R, zag jij de figuren en een voorlopige paper al voor je. Met je enthousiasme en kritische vraagstukken bewaakte jij de klinische relevantie van het werk.

Daarnaast wil ik Toine Egberts bedanken. In afwachting van de aanstelling van Alwin, voelde jij je verantwoordelijk als vervangende promotor. Maar ook daarna, gaf jij mij het gevoel gaf dat ik altijd bij je terecht kon.

Mijn eerste 'first author' publicatie was nooit gelukt zonder de hulp van Caroline Lindemans. Dank voor je hulp, tijd en kritische blik. Ik heb veel van je geleerd. Ook veel dank aan Birgitta Versluys om mijn werk tot een hoger niveau te tillen. Dank voor je input en tijd.

Binnen de solide tumoren wil ik Kathelijne Kraal, Lieve Tytgat, Max van Noesel en Miranda Dierselhuis bedanken. Jullie allen hebben waardevolle input geleverd tijdens mijn promotie en kritische vragen gesteld. Kathelijne, dank om me op weg te helpen en te begeleiden in de

wereld van wmo-plichtig onderzoek. Veel werk is nog niet zichtbaar in dit proefschrift, maar zal ongetwijfeld opgevolgd worden.

Gelukkig zat ik nooit alleen in de achtbaan. De meeste tijd heb ik doorgebracht met Coco. Als het niet op het werk was, dan was het vaak opgepropt samen in de bus, rennend op het station, in de trein (waar iedereen meeluisterende naar onze verhalen), in het vliegtuig, in de auto of zelfs op de ski's in Park City en de laatste tijd dicht bij huis in Brabant. Jij introduceerde mij in het labwerk, deelde graag je rijke immunologie kennis en bood altijd hulp en steun. Daarnaast leerde je me ook van alles over labradoodles. ;) Dank voor alle leuke momenten samen.

Ester en Vania, dankjewel om mij bij te staan voor en tijdens de promotie als paranimfen! En dank voor het nalezen van mijn proefschrift. Ester, je stond altijd klaar om mij te helpen, je leerde me veel in het lab en je was altijd geïnteresseerd. Vania, I admire your mindset and learned a lot from you. Thank you for being very helpful and caring. And of course, I also enjoyed all the time I spend with Ester and you when we were not wearing a labcoat (kwaak kwaak as frogs in Oeteldonk or as Pepper and Salt couple somewhere in Leersum).

Annelisa, dank voor je behulpzaamheid, samenwerking en alle gezellige koffiedates. Je bent een heel betrokken persoon met veel talenten. Ik ben ervan overtuigd dat jij heel ver gaat komen.

Denise, door jouw hulp in het lab staan er een aantal mooie figuren in dit proefschrift! Met jouw nauwkeurigheid en oplettendheid paste jij mijn protocollen aan zodat niets meer aan het toeval was overgelaten. Dank voor je hulp en de gezellige samenwerking!

Sara, dank voor je inzet tijdens je masterstage en gezellige (lange) dagen in het lab. Je hebt een grote bijdrage geleverd waar mooie resultaten uit voort zijn gekomen.

Bas, Brigitte, Shanice, Jurgen, Maud, Colin, Niek en studenten van de BoNi groep: ik heb wat minder tijd doorgebracht met jullie in het lab maar daardoor zijn jullie zeker niet minder belangrijk! Dank voor alles en alle leuke momenten samen. Brigitte, ik denk nog vaak terug aan onze mooie congres-roadtrip reis in Utah samen met Coco (het is me nog steeds een raadsel waarom we overal korting kregen en werden uitgenodigd voor BBQs en kaas-en-wijn avonden, maar who cares het was memorabel!).

Ook wil ik mijn 'voorganger' en 'opvolger' niet vergeten. Lotte, dank voor de wijze lessen die jij mij hebt geleerd en je vele tips en hulp! Linde, ik ben heel blij dat jij een gedeelte van het werk gaat opvolgen. Ik heb er alle vertrouwen in en kijk er naar uit wat je gaat ontdekken.

Ik ken weinig mensen die zo enthousiast zijn als Erik van Maarseveen. Deze positiviteit maakte een bezoekje aan de apotheek altijd erg prettig. Dank voor je vertrouwen en dank om mij te betrekken in het onderzoek binnen de apotheek. Een ander belangrijke persoon met veel talent is Mohsin El Amrani. Dank voor de samenwerking Mohsin!

De enige die weten wat ik met 'temptation office' bedoel zijn Simone, Anke, Coco, Jurgen en Niek. Zonder afleiding van zo'n leuke kamergenoten was mijn PhD een saaie bedoeling geweest. Van het bespreken van de meest "intellectuele (lees guilty pleasure)" tv programma's, het tijdig (=zomer) bepalen wanneer kerstboom Billy tevoorschijn mocht komen, tot het klagen over werk en afluisteren van iets te luide gesprekken in het aangrenzende ML-1 lab. Not to forget, Domenico and Bas for joining later in the new season of temptation office2.0. Thanks all!

Sabine, dank voor de gezellige treinritten en altijd ontspannende grappige gesprekken in de wandelgangen. Ik kijk uit naar de uitklapbare pop-up kافت die jij samen met Ester in gedachten hebt voor mijn proefschrift...het mag ook zonder glitters.

Als je op dezelfde dag aan je PhD begint, schept dat vaak een band. Als je dan ook nog de afgelopen 5 jaar in België hebt gestudeerd, beide uit Brabant komt en dezelfde opleiding hebt afgerond, raak je niet meer uitgepraat. Mitchell, dank voor de gezellige tijd en vele update momenten.

Anna V, de meest inspirerende persoon die ik ken, met een oneindige hoeveelheid doorzettingsvermogen en creatieve ideeën. Ik heb veel van je geleerd en vind het bijzonder knap hoe jij zo snel een nieuwe taal hebt geleerd, in combi met jouw vele hobby's en tijd die je vrij maakt om van kleine dingen te genieten. Dank voor de leuke momenten samen, zowel op het werk als daarbuiten.

Anne S, we zijn er beide over eens dat een uitgebreid promotiehandleiding en stappenplan voor de laatste PhD maanden wel zo efficiënt was geweest. Maar gelukkig hadden we steun aan elkaar. Dank ook voor de gezellige tijd tijdens de NVVI-BSI-congres in Liverpool, ook al lijkt dat nu wel erg lang geleden.

Collega's van de diagnostiek, dank voor jullie hulp en de mogelijkheid om altijd even langs te lopen met een 'paar' vragen. Speciale dank aan de dames van Cytomorfologie om mij keer op keer te bellen als er weer een sample klaar stond. Ook speciale dank aan de collega's van U-DAIR om mij te helpen met de patiënten-studie: Karin, Amelia, Lysette en Rowena bedankt! Eveline, dank om mee te denken met het neuroblastoom project en voor je last minute Olink hulp.

We blijven nog even bij de diagnostiek. Kirsten, ik ben blij dat jij me samen met Brigitte kwam vergezellen toen ik alle koekjes alleen op moest eten. Laten we de lunch-dates erin houden!

Daarnaast wil ik alle andere LTI-collega's bedanken voor alles! Dank om naar mijn presentaties te luisteren, samen te pauzeren, elkaar te helpen, en te leren dat om 11u30 lunchen helemaal niet vroeg is. Ook de PhD retreats, waar elkaar leren kennen centraal staat zal ik niet snel vergeten. 'Netwerken' werkt immers veel beter als je verkleed bent als 'kakker of kamper', in je pyjama of als Peper en Zout stel.

Wat voor de ene persoon als iets kleins voelt, kan voor de ander een grote betekenis hebben wat niet altijd 'ZICHTbaar' is. Kamil, grote dank voor je hulp!

Michelle en Lianne, jullie waren de eerste PhD's van het PMC die ik leerde kennen. Dank voor jullie hulp, tips, leerzame gesprekken en het uitleggen van de zoveelste klinische afkorting tijdens de MTB (toen deze nog in het WKZ was).

Tijdens het laatste jaar van mijn PhD versnelde de achtbaan. Geen tijd te verliezen want nieuwe achtbaanKarretjes uit het PMC waren in aantocht.

Jan, dank voor alle kansen die ik het afgelopen jaar heb gekregen om mezelf verder te ontplooiën binnen de kinderoncologie. Dank voor je flexibiliteit, steun en tijd die je me gegeven hebt om mijn proefschrift succesvol af te kunnen ronden. En voor de gezellige momenten tijdens de meetings: van serieuze zaken tot het bespreken wie de 'verloren mars' stiekem heeft opgegeten. Ik kan nog heel veel van je leren en kijk uit naar alle toekomstige projecten en plannen.

Daarnaast wil ik iedereen uit de Molenaar en Tytgat groep bedanken. Sommige van jullie heb ik al in het begin van de achtbaan rit leren kennen. Emmy dank voor de samenwerking en gezelligheid. Ook al zit je nu in Sidney, ik vind het heel leuk dat we nog steeds contact houden! Waleed, I admire your infinite enthusiasm! Kaylee, Lindy V, Nil, onze sunset picknick bij de Golden Gate Bridge zal ik niet snel vergeten! Bianca en Anke dank voor jullie hulp in de CSC!

Soms kom je iemand tegen waarbij je direct een unieke klik mee hebt. Karin, jij bent een groot voorbeeld voor mij en ik bewonder jouw rijke kennis en inzicht zoals je bij weinig mensen ziet. Dank voor je hulp, advies en tijd die je voor mij hebt vrijgemaakt in je drukke agenda.

Marli, Linda, Marlinde, Lindy A, Sander, Sabine, Michael, Kim, Jennemiek, Judith, Selma en studenten van de Molenaar groep: dank om mij samen met bovenstaande collega's vanaf dag één thuis te laten voelen in de gezelligste groep van het Máxima!

Naast top collega's stonden mijn lieve vrienden en familie altijd langs de zijlijn met raad en daad.

Linda en Eline, ook al wonen we niet in de buurt, toch voelt het alsof jullie dichtbij zijn. We hebben veel meegemaakt met elkaar, en het voelt altijd heel vertrouwt als we samen zijn. Dank voor alle ontelbare gezellige weekendjes in Leuven en Nederland. Ze zijn onvergetelijk, mede mogelijk gemaakt door jullie mannen Raphaël en Thomas. Mieke, we spreken en zien elkaar niet vaak, maar als we bij elkaar zijn voelt het heel vertrouwt. Ik kijk vol bewondering naar jouw talenten en passie voor de wetenschap. En hoe fijn is het om iemand te kennen die graag met mij om 6u opstaat voor een heerlijke ochtendwandeling. Kortom, ik hoop dat we hier in de toekomst meer tijd voor hebben.

Dank aan mijn lieve studievrienden en hun partners uit Leuven: Els & Karel, Maria & Daan, Jessica & Hans, Heleen, Daphne, Elise, Anne-Marijn. Van het vergelijken van PhD's tussen BE en NL, tot bruiloften en babyshowers: ik hoop dat we nog lang contact houden. Els, jou leerde ik als een van de eerste kennen in Leuven. En samen met Karel is daar een hechte vriendschap uit ontstaan met vele kilometers op en neer tussen Leuven en Den Bosch. Maria & Daan, ik vind het heel leuk dat jullie nu dichterbij wonen in jullie grote mensen huis. Zo kunnen we vaker samen kip eten en terugkijken op alle leuke feestjes en herinneringen van 'vroeger'.

Esther en Marjolein, in een paar jaar tijd zijn we hechte vrienden geworden! De zogenaamde 'bootcamp' vrienden hebben welgeteld minder dan 10x samen gesport vrees ik, maar wijntjes drinken, uiteten, en op z'n tijd een feestje kunnen we blijkbaar ook heel erg goed ;) Om niet het hockeyweekend te vergeten natuurlijk...kunnen we ook wel wegschrijven onder 'sport' denk ik. Dank voor alle ontspannende momenten!

Koen en Esther, dank om zo'n lieve burens en vrienden te zijn. Van het organiseren van onze bruiloft, samen hardlopen, een luisterend oor in moeilijkere tijden, borrelen, spelletjesavonden, carnavallen tot het vangen van spinnen. We hadden het niet beter kunnen treffen!

Daarnaast wil ik de Tour des Bières vriendengroep bedanken. Dank voor alle unieke oldtimer ritten en avonturen in binnen en buitenland. Ik ben blij dat we altijd heelhuids zijn thuisgekomen. Jos, zonder jouw comfortabele achterbank waren de ritten erg hobbelig geweest ;) en de trouwauto uit 1912 is onvergetelijk. Laurens dankzij jou kwamen we nooit bier, bubbels en eten tekort en genoten we van de Franse zon. Catherinus, jouw gevoel voor humor maakte de tour helemaal compleet.

Lubberta, als de auto's stilvielen hadden wij nog genoeg gespreksstof voor een hele week. Ik heb genoten van alle afterwork etentjes bij jou in Lunetten, ijsjes pauzes op de Uithof en de start-to-run lessen die we samen hebben gevolgd. En wie weet gaan we zelfs in dezelfde maand promoveren. Toen de dixi's door de lucht vlogen op die stormachtige dag, redde jij mij van het station en zorgde voor een heerlijke pasta. Kortom, met zo'n zorgzame vriendin met gemeenschappelijke interesses hoop ik nog erg lang contact te houden.

Lieve Corry en Leo, jullie zijn de beste schoonouders die ik me kan inbeelden. Altijd heel betrokken, zorgzaam en geïnteresseerd in mijn werk. Een voorbeeld voor velen.

Daarnaast voel ik me heel rijk met mijn schoonfamilie van Doremaele. Wat ben ik trots om onderdeel te mogen zijn van jullie liefdevolle en talentvolle familie: met 4 broers en 4 zussen rijker die altijd voor elkaar klaar staan. Marcel & Kassie, we don't see each other often, but I'm proud to have family in Sidney. Thanks for always being interested in my work. Eric en Marloes, dank voor jullie liefdevolle steun, jullie oprechte interesse en waardevolle adviezen. Marc en Gosia, dag en nacht, 365 dagen per jaar aan het werk als ondernemer van een champignonkwekerij en fruitteelt bedrijf. Maar voor belangrijke momenten maken jullie altijd tijd vrij. Dit vind ik heel bewonderenswaardig! Bas en Sanne, ook al zijn we aan de ene kant heel verschillend, we lijken ook weer veel op elkaar. Sanne, dank voor alle gezellige Picasso dates. Ik hoop dat er nog vele gaan volgen.

En natuurlijk mag ik mijn lieve neefjes en nichtjes niet vergeten: Max, Juliëtte, Cas, Niels, Elena, Milan en Anais. Ik geniet als jullie zorgeloos tussen de perenbomen spelen met Joey of vragen of ik even op de trampoline kom springen.

Dearest Mom and Dad, thank you for always supporting me in everything. Without your support and your advice to never compare yourself with others, I would have never come so far. You always showed lots of interest in my work and motivated me to continue to the end. If your Dad is interested in the lasers of the flow cytometer, and your Mom buys the newest Kuby

immunology book to learn more about immunotherapy and immune diseases (because my version is outdated) I think it is clear that a passion for science and lifelong learning runs in the family.

Justin, I'm very proud of you. You are the best brother ever. You are very talented, carrying and helpful. Thank you for saving my life when I 'lost' my presentation somewhere in an invisible folder, crashed my computer at 1am in the morning or when my computer got stuck in an update because the memory was full. You were always there to help me.

Grandma, thank you for always supporting me and being such a loving grandmother. I wished we would live closer and we could spend more time together. You remember me to always follow my hart and not to spend time on things you do not like. You have a very special place in my heart.

Lieve John, ik kon geen geschikte woorden vinden die omschrijven hoeveel ik van je hou. Je geeft me een heel bijzonder gevoel, dat niet uit te drukken is met woorden. Wij kunnen samen veel lachen. Ik hou van je humor, je gedreven karakter, je zorgzaamheid, je inlevingsvermogen en relativerende eigenschappen. Je geeft niet op, en denkt altijd in oplossingen. Geen enkele dag is hetzelfde. Je zorgt voor verrassingen en staat voor iedereen klaar. Zelfs als je moe bent en erdoorheen zit gebruik je je laatste energie om mij of iemand anders te helpen. Ik ken niemand die zo gedreven is als jij, die zijn eigen ding doet en zich niet druk maakt wat anderen van hem vinden. Dit vind ik zo leuk aan jou.

Een ding is duidelijk, zonder jou was deze PhD nooit gelukt. Al 12 jaar steun jij mij met alles. De laatste tijd was niet altijd even makkelijk, maar ik ben heel erg trots op alles wat wij samen hebben bereikt. Dank voor je onvoorwaardelijke steun en liefde! Ik hou heel veel van jou en ben samen met jou heel gelukkig. Ik kijk uit naar alles wat de toekomst ons gaat brengen!

## List of publications

Szanto CL, Cornel AM, Vijver SV, Nierkens S. Monitoring immune responses in neuroblastoma patients during therapy. *Cancers* 2020; 12(2), 519; doi:10.3390/cancers12020519

El Amrani M, Szanto CL, Hack E, Huitema ADR, Nierkens S, van Maarseveen EM. Quantification of total dinutuximab concentrations in neuroblastoma patients with liquid chromatography tandem mass-spectrometry. *Anal Bioanal Chem* 2018; 410(23):5849-5858.

Cornel AM, Szanto CL, van Til NP, van Velzen J, Boelens JJ, Nierkens S. A 'no-touch' antibody-staining method of adherent cells for high-throughput flow cytometry in 384-well microplate format for cell-based drug library screening. *Cytometry Part A* 2019. Epub ahead of print

Szanto CL, Langenhorst JB, de Koning CCH, Nierkens S, Bierings M, Huitema ADR, Lindemans CA, Boelens JJ. Predictors for autoimmune cytopenias after allogeneic hematopoietic cell transplantation in children. *BBMT* 2020; 26(1):114-122.

## In preparation

Szanto CL, Tamminga S, Delemarre EM, de Koning CCH, van den Beemt DAMH, Tas ML, Dierselhuis MP, Tytgat LGAM, van Noesel MM, Kraal KCJM, Huitema ADR, Nierkens S. Functional immune monitoring in patients with high-risk neuroblastoma during chemo- and immunotherapy reveals T cell unresponsiveness *Submitted 2020*

de Koning CCH, Szanto CL, Langenhorst JB, Lindemans CA, Nierkens S, Boelens JJ. Adequate CD4+ T-cell reconstitution enhances survival probability after acute graft-versus-host-disease. *Manuscript in preparation*

Szanto CL, Versluys B, Lindemans CA, de Koning CCH, Bierings M, Langenhorst JB, Huitema ADR, Boelens JJ, Nierkens S. Identifying early immune predictors for alloimmune-lung disease after hematopoietic cell transplantation in children. *Manuscript in preparation*



# **IMMUNE MONITORING IN THE CONTEXT OF HEMATOPOIETIC CELL TRANSPLANTATION IN CHILDREN**



**Celina Szanto**